THE DECAY OF THE NEUTRAL V-PARTICLE

Thesis by

Sylvan Dean Wanlass

In Partial Fulfillment of the Requirements

for the Degree of

Doctor of Philosophy

California Institute of Technology

Pasadena, California

1953

ACKNOWLEDGMENTS

Throughout these experiments Professor Carl D. Anderson and Professor Robert B. Leighton were a constant source of inspiration. For their enthusiasm, their patience and their active participation, and for their supervision of this thesis, I would like to express my sincere appreciation.

The cooperation of Mr. William Alford and Mr. Frank Shelton, with whom the operational phases of these experiments were shared, is likewise gratefully acknowledged. I would also like to express my appreciation to Professor Eugene W. Cowan for his many helpful suggestions.

ABSTRACT

In a set of 23,000 cloud chamber photographs taken in a study of penetrating showers, 134 examples of the decay of neutral V-particles were observed. These have been analyzed in an endeavor to determine the properties associated with this phenomenon.

It is apparent in the great majority of cases that the two charged decay-products are protons and negative π-mesons. There is, however, a significant number of data available to indicate the existence of other charged decay-products; the poor quality of these events has, unfortunately, prevented an interpretation in terms of a decay scheme.

No direct evidence has been observed which indicates the existence of neutral secondary particles, and the statistical data are consistent with a two-body decay scheme.

Q-values have been calculated under the assumption of a two-body decay into a negative π-meson and a proton; these values range from 10 ± 3 Mev to about 87 ± 15 Mev. It is exceedingly difficult to reconcile the observed results with any unique Q-value.

Other interesting events which were observed in these experiments included charged V-particles and heavy mesons. A brief analysis of these events has also been included.

TABLE OF CONTENTS

I. INTRODUCTION

In the few years since V-particles were first observed[1] in cosmic ray penetrating showers, their existence has become firmly established[2], and some of their properties have been determined[2-7]. This thesis represents a continuation of the study of these properties, in particular, a study of the mass of the neutral V-particle. Herein are reported the results of an analysis of 134 cases of the decay of these neutral V-particles which occurred in a set of 23,000 cloud chamber photographs. These results seem to indicate a rather great complexity in the phenomena associated with this decay, and do not provide complete answers even to such obvious questions as those concerning the number and identity of the decay products. It would seem that unambiguous answers to even the simplest questions will require the analysis of a great many more cases if new equipment and improved experimental techniques are not forthcoming.

II. APPARATUS

Cloud Chamber

The apparatus used in these experiments was a counter-controlled double cloud chamber operated in a magnetic field, the double cloud chamber consisting of two identical cloud chamber units placed one on top of the other. Figure 1 is a photograph of one of these assembled units. Each chamber was rectangular in shape, the interior being approximately 33 cm wide, 19 cm high and of 12 cm illuminated depth.

The actual construction of each chamber is shown in the series of diagrams in figure 2 and is described in the paragraph accompanying the figure. Each chamber body was fabricated out of flat plates of brass, the plates being held together by means of brass screws and all seams being made airtight with soft solder. The brass body was bright-chrome plated inside to improve the illumination of the cloud chamber. As indicated in figures 1 and 2, the front and one side of this chamber body were enclosed with ½" plate glass. The rear of the body was enclosed by a movable aluminum back plate. The expanded position of this plate, which was constantly being forced outward by the gas pressure within the chamber, was determined by fixed stops attached to the chamber body. With the expanded position thus fixed, the expansion ratio control was obtained by controlling the extent of the compression of the chamber. This was accomplished by means of a compressed-air piston assembly fixed in the magnet yoke; the expansion ratio was adjusted by varying the extent of this piston motion. It was found to be extremely important that each chamber have an independent expansion mechanism so that independent expansion ratio control could be maintained. An earlier double cloud chamber unit utilizing a single piston and expansion ratio mechanism to simultaneously control both

Fig. 1. Cloud Chamber Unit and Lead Absorber

Legend for Fig. 2.

A Needle valves.

B Brass chamber body.

C Glass window through which the interior of the chamber is illuminated. (1/2 inch plate glass)

D Aluminum back plate (movable).

E Neoprene section connecting movable back plate to the chamber body.

F Stops to limit the outward expansion of the back plate.

G Bakelite plate which insulates the compression piston (H) from the aluminum back plate.

H Aluminum compression piston.

I Front glass window (1/2 inch plate glass).

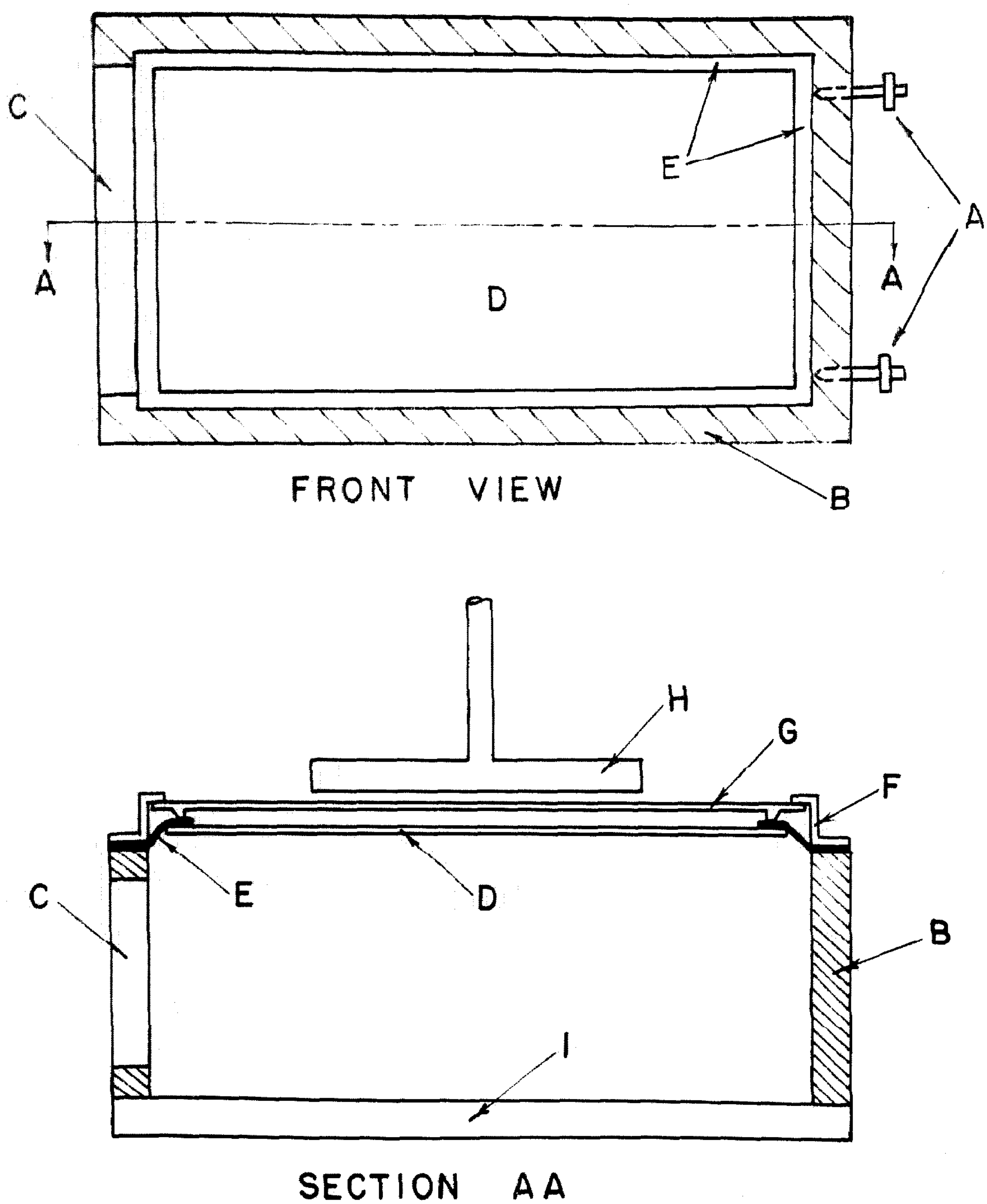

Fig. 2. Cloud Chamber Construction (Schematic)

chambers was found to be completely unsatisfactory.

Under operating conditions the chambers were filled with pure Argon gas and a saturated mixture of 65 percent ethyl alcohol and 35 percent water to a total gauge pressure of 20 cm of Hg. Under these conditions an expansion ratio of about 1.07 proved satisfactory.

Illumination

The illumination necessary for photographic purposes was provided by a single linear quartz flashtube situated to the left of the chambers, 500 joules of energy being used per exposure. Light from this source was first collimated into a uniform beam by a system of cylindrical lenses, and was then allowed to pass into the chambers. The above mentioned chrome plating on the interior of the chambers served a dual purpose: It increased the light intensity and at the same time made the illumination throughout the chamber more uniform. In this connection it was found that chrome plating was superior to silver plating in spite of the greater coefficient of reflectivity of the latter. This was due to the fact that the silver plating produced a mild poisoning of the chamber, probably because of the low photoelectric work function of silver oxide.

In order to keep light from scattering diffusely from the back plate of the chamber and thus from eventually fogging the film, a special treatment of this plate was necessary. The aluminum plate was first polished and was then treated to produce a black anodized surface. Finally, a thin layer of clear lacquer was applied. The resultant surface proved more satisfactory, photographically speaking, than did black velvet.

Photography

The anodized back plates of the two chambers provided the background against which the droplets were photographed by means of a single stereoscopic camera. Figure 3 is a photograph of this camera which was constructed to incorporate 3 lenses. Two of the lenses, mounted on the front of the camera box with lens centers 14 cm apart, were used to obtain stereoscopic photographs of the chambers. No shutters were provided for these lenses. Instead, the camera was fitted with a light tight box so that the film would be exposed only when the flashtube was energized. The third lens, placed on the side of the camera box, was used to photograph a data panel which exhibited such information as the frame number, the current flowing through the magnet windings, the time and the date. This lens was fitted with a shutter mechanism which operated in conjunction with the trigger unit of the electronics equipment as will be described later. The camera film advance also operated in conjuction with this trigger unit.

The data panel and the two stereoscopic views of the chambers were all photographed on the same roll of 70 mm Kodak Linagraph Pan film using a lens opening of f/11 and a film magnification of 6.3X from film to cloud chambers; this magnification corresponded to a distance of 93 cm as measured from the lens centers to the back plates of the chambers. The Linagraph Pan film, when developed in D-19 developer for about twice the recommended time, proved quite satisfactory.

Magnet

Figures 4 and 5 show the arrangement of the various physical components necessary for the automatic operation of the double cloud chamber. These photographs were taken inside of the trailer used to

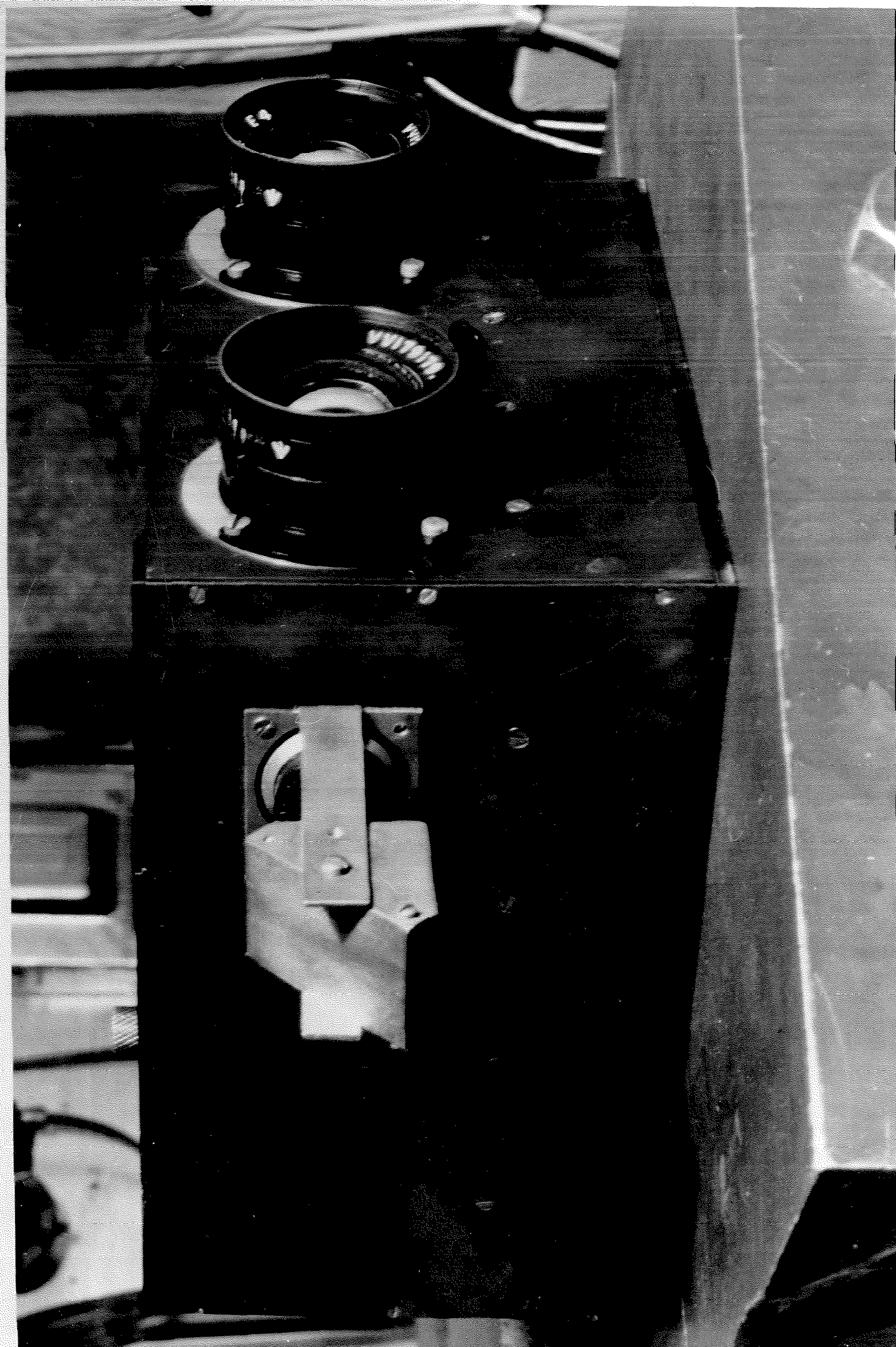

Fig. 3. Stereoscopic Camera

Legend for Fig. 4.

1. Stereoscopic camera.
2. Camera stand and light tight compartment connecting camera and magnet frame.
3. Hoses asscciated with thermostatting of camera well.
4. Magnet yoke.
5. Magnet coils and associated cooling pads.
6. Thermostatted copper-lined cellotex box enclosing magnet air gap.

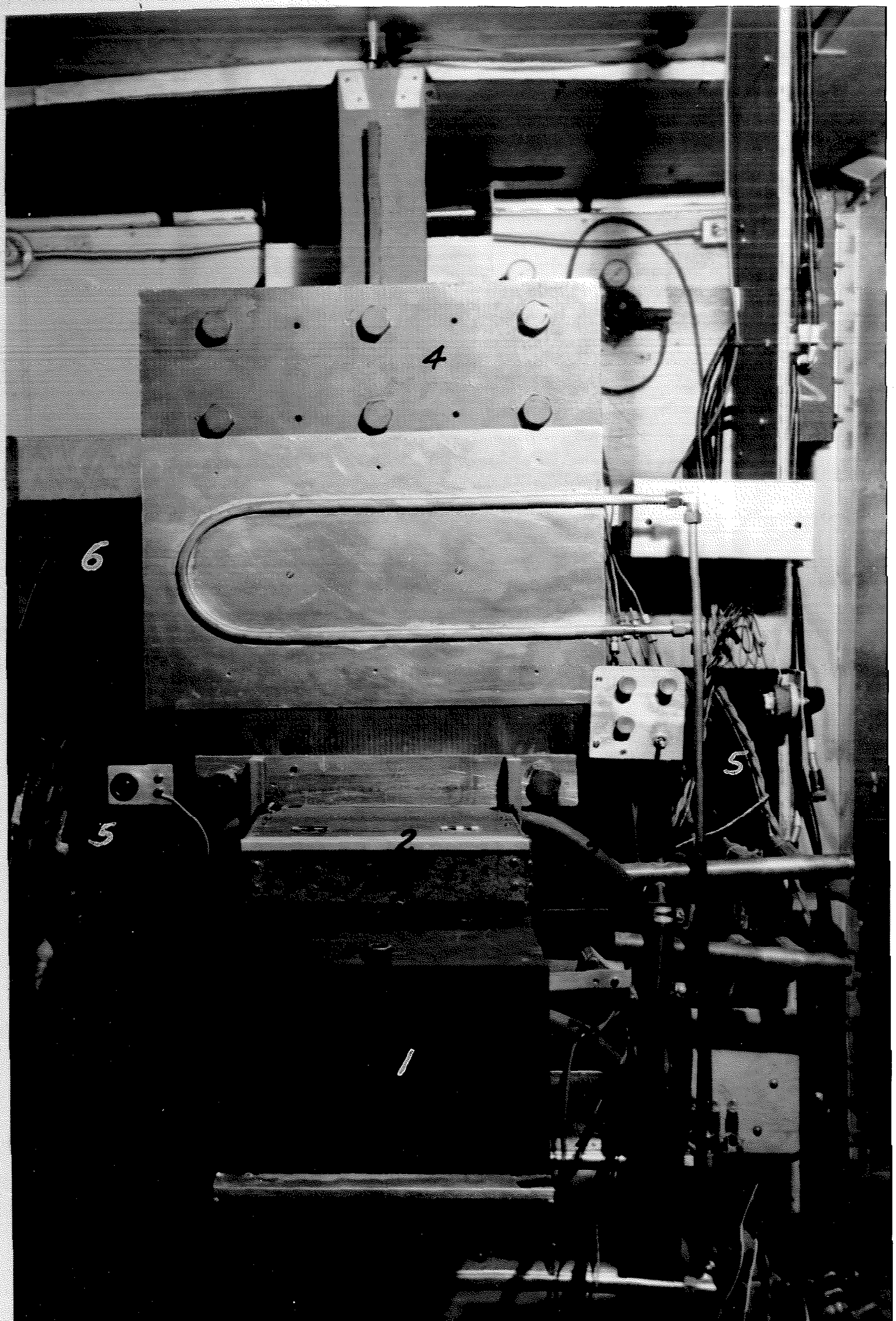

Fig. 4. Magnet Assembly

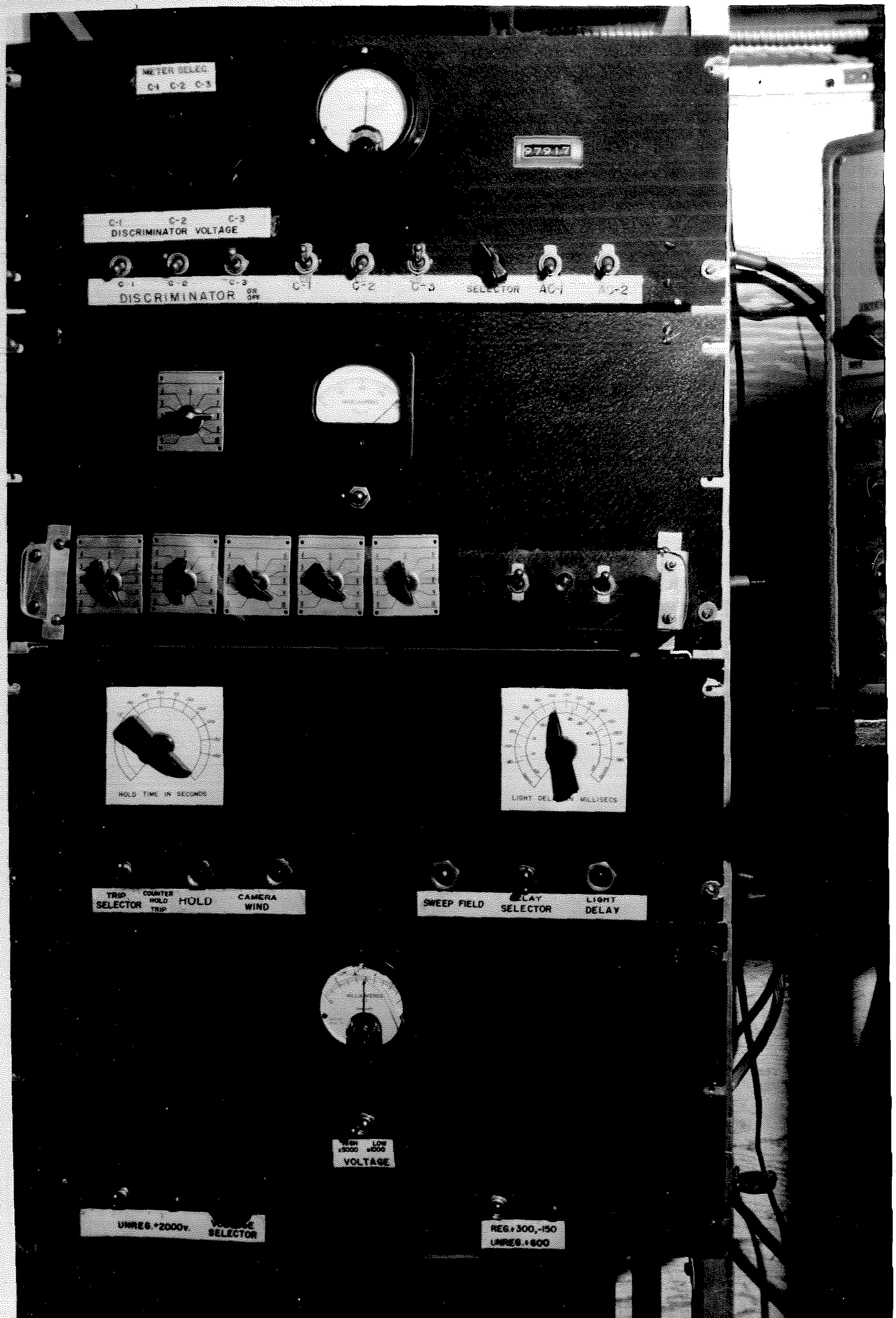

Fig. 5. Electronic Control Units

house the components.

The magnet is shown sketched in figure 6. The magnet yoke was fabricated out of a number of large rectangular pieces of iron which were bolted together to form the final configuration shown. Strips of copper were then wound onto the pole pieces to form the magnet coils. Under operating conditions, 13 kilowatts of power were fed into these coils with the result that an induction of about 5000 gauss was produced throughout the gap.

Thermostatting

The problem of temperature regulation was, of course, extremely important. The coils themselves were water-cooled, several stainless steel jackets, through which cold water was forced, being an integral part of the construction of the coils. The thermostatting of the chambers to eliminate track distortion was a considerably more difficult problem. For this purpose the magnet pole pieces were terminated in rectangular pole faces which were thermostatted to within $\pm 0.1^\circ$ C. This thermostatting was made more effective by insulating the pole pieces from the pole faces by means of small bakelite spacers as shown in figure 6. In addition a thermostatted copper-lined cellotex box, shown in figure 4, was added to enclose the chambers, the light source and the pole faces, and thus to further shield the chambers from outside temperature gradients. It was, of course, impossible to enclose the fronts of the chambers since photographs had to be taken here. Originally nothing was done to improve this particular phase of the thermostatting problem and resultant photographs showed distortions due to fluctuations in the temperatures of the glass plates on the fronts of the chambers. To improve this situation, a thermostatted copper-lining was fitted into the camera well; the input and exit

Legend for Fig. 6

A Yoke of the magnet.

B Rear pole piece of the magnet

C Front pole piece of the magnet.

D Magnet coils.

E Expansion mechanisms (including compression pistons).

F Stereoscopic camera.

G Field of view of the camera lens which photographs the data panel.

H Field of view of the stereoscopic lenses of camera.

I Double cloud chamber.

J Front pole face of the magnet

K Bakelite spacer to insulate the pole face from the pole piece.

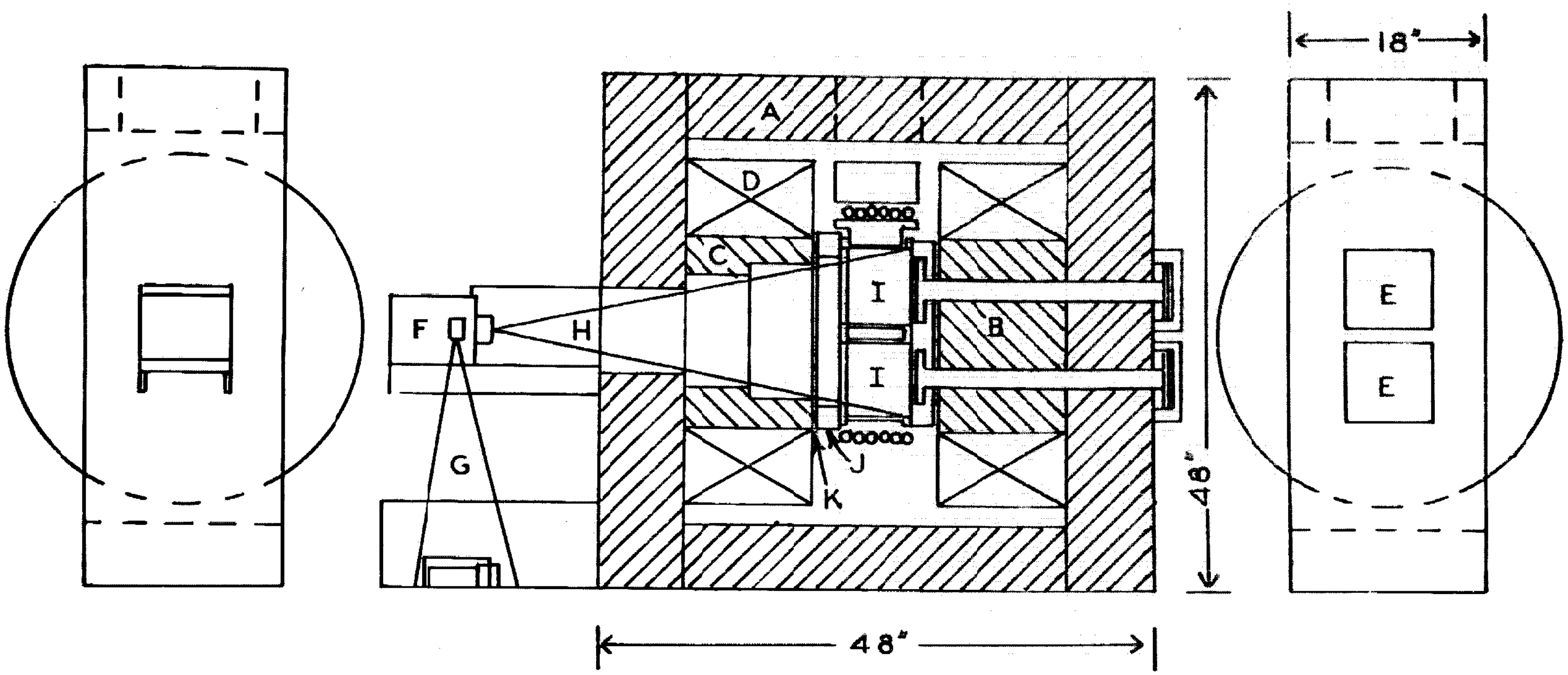

Fig. 6. Cloud Chamber Magnet Assembly

water hoses associated with this lining can be seen in figure 4.

In spite of these precautions, distortions were sometimes present, so that the maximum detectable momentum for long tracks varied from about 2 Bev/c to about 5 Bev/c.

Counters, Absorbers

The arrangement of the counters and the lead around the counters is shown in figure 7. This particular arrangement was adopted because a high percentage of penetrating-shower events was observed, and because the specific events of interest, V-particles, seemed to be closely associated with these penetrating showers. The top tray of six 1" x 12" counters was well shielded against soft radiation by 10 cm of lead above, 5 cm of lead below, and by the magnet windings at front and rear. The lower tray of six 1" x 12" counters was located immediately below the lower chamber and was shielded only by the chambers and the magnet windings. Such shielding was necessary to prevent the triggering of the cloud chambers on low energy events such as electron showers. Because of the extremely short lifetime of the V-particles, it was necessary that the lead absorber be placed as close as possible to the cloud chamber in order to minimize the loss of these particles through decay. The rectangular shape of the chambers was well suited to this purpose.

Electronics

The pulses from the two trays of counters were fed into a <u>pulse-height-discrimination coincidence unit</u> which was used to select events in which any n or more counters of the upper tray, and any m or more counters of the lower tray, were discharged simultaneously. Such an event is here called an n-m <u>coincidence</u>. When the prescribed coincidence had occurred, a pulse generated in this electronic

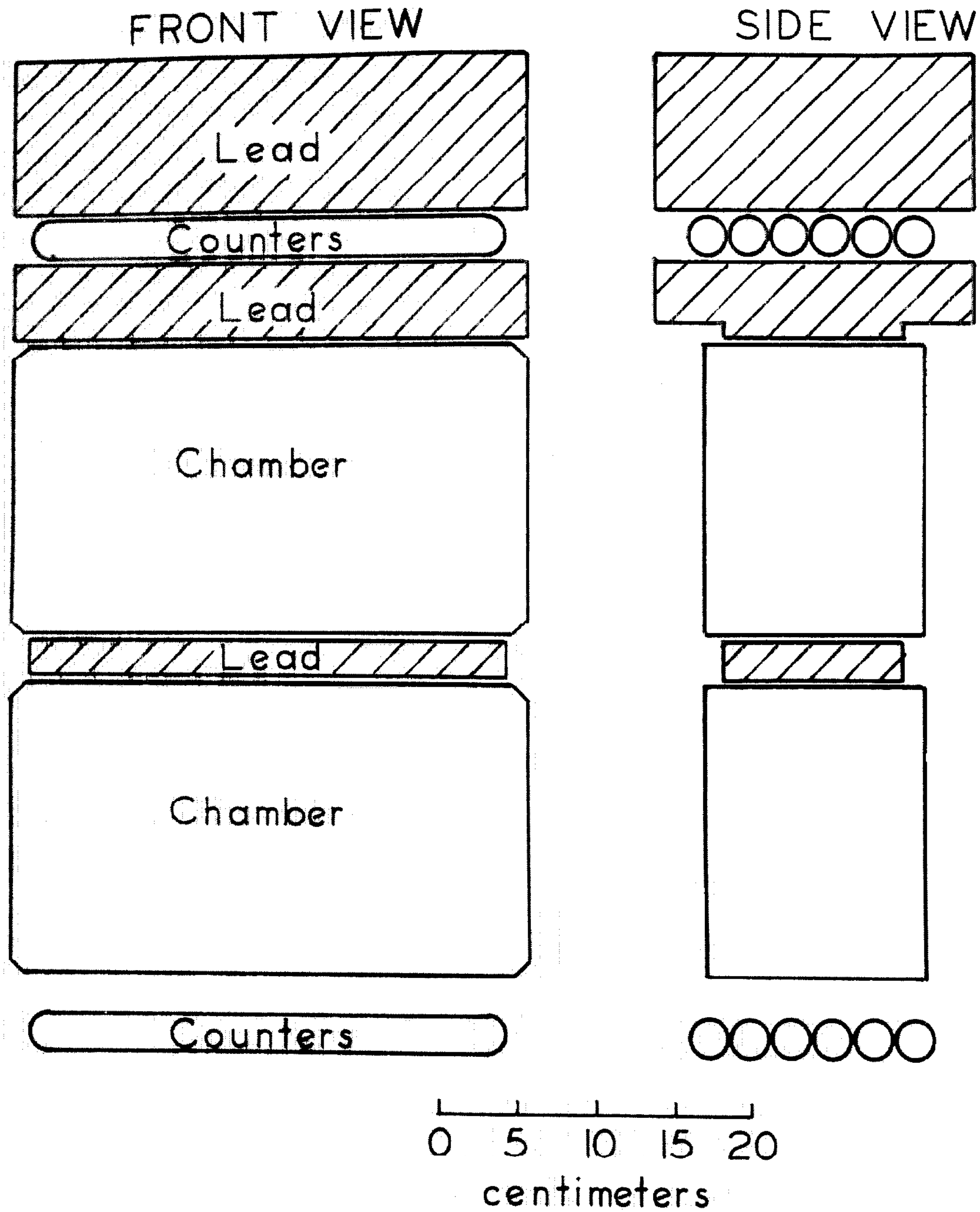

Fig. 7. The arrangement of counters and lead absorber around the cloud chambers. Only the inner walls of the chambers are indicated; the pole structure, yoke and magnet windings, which constituted additional absorber, are not shown.

coincidence unit was fed into the trigger unit and there it initiated the usual sequence of operations, including, (1) removal of the chamber sweep field, (2) expansion of the chamber, (3) triggering of the flash-tube, (4) operation and cycling of the camera, (5) cycling and recovery of the chambers.

The sweep field, which was alternately +150 volts and -150 volts with a period of approximately 15 seconds, was, of course, removed immediately. Likewise, each chamber was immediately expanded, the expansion being initiated by means of a condenser activated solenoidal valve. The expansion time of these chambers was approximately 16 milliseconds. The flashtube was triggered in a conventional manner; a condenser in the trigger unit was discharged into an automobile ignition coil, and the output of the coil was in turn applied to metallic electrodes placed next to the flashtube. A delay of approximately 100 milliseconds was introduced between the expansion of the chambers and this light flash in order to allow for adequate track growth. An additional delay or hold circuit was incorporated into the trigger unit to prevent any pulse from reaching this unit until a specified time, variable from 0 to 240 seconds, had elapsed since the activating pulse was received. This circuit provided a minimum period between chamber expansions, and allowance was thus made for suitable chamber recovery. The optimum length of time for this recovery was quite thoroughly investigated and a value of about two minutes was found to be most satisfactory.

Since the equipment was designed to operate automatically for relatively long periods of time, suitable safety devices were incorporated which would shut down the entire apparatus in the event of any marked deviation from normal operating conditions. Thus, protection was afforded against (1) electrical overloads, (2) excessive magnet current, (3) excessive magnet temperatures, and (4) inadequate flow of magnet coolant, etc.

III. OPERATION

Pasadena

The initial phases of the work were conducted on the Institute Campus in Pasadena, at 220 m elevation. Since the purpose of these studies was to continue the work on V-particles that had previously been conducted at the Institute[2], and inasmuch as previous experiments had indicated that V-particles were usually associated with penetrating showers, the coincidence unit was adjusted to trigger on such penetrating events. To accomplish this a 1-3 coincidence was adopted; the corresponding counting rate was about 4 hr^{-1}, but due to the fact that about two minutes recovery was allowed after each expansion, during which time a coincidence could not actuate the chamber, the actual picture taking rate was slightly smaller.

Mt. Wilson

After a period of successful operation had been concluded at Pasadena, it was decided that another location at greater elevation would be desirable. This decision was motivated by the fact that penetrating showers are highly altitude dependent and by the fact that the cosmic ray equipment was portable. The Mt. Wilson Observatory was selected as the new location because it was felt that year around operation at the moderate altitudes afforded by Mt. Wilson, 1750 m elevation, was more promising than summer expeditions to higher peaks.

There were, of course, special problems associated with the new location. Perhaps the most serious of these was the problem of cooling the magnet windings. In view of the critical water shortage on Mt. Wilson and in view of the fact that several gallons of water must be passed through the cooling jackets per minute, a closed circulating system was finally adopted. This system utilized a 50 gallon drum for storage, two large radiators with fans to control the temperature and a large centrifugal pump to continuously circulate the coolant. The coolant consisted of a mixture of distilled water and rust preventative. During the winter months an anti-freeze mixture was added.

Figures 8 and 9 are photographs showing the physical arrangement of the equipment at Mt. Wilson under actual operating conditions. As had been the case at Pasadena, a 1-3 coincidence was used to trigger the apparatus; this corresponded to a counting rate of 12 hr^{-1}, instead of 4 hr^{-1} as had been the case at Pasadena. Later a 2-3 coincidence requirement was adopted, corresponding to a counting rate of about 3.5 hr^{-1}. As was mentioned previously, a chamber recovery period followed each expansion and thus the actual picture taking rates were somewhat less than the above rates.

Legend for Fig. 8

This photograph was taken from one of the Observatory towers; a portion of this structure is visible in the photograph.

1. Trailer housing magnet used in these experiments. Figures 4 and 5 were taken inside this trailer.

2. Trailer housing smaller magnet.

3. Radiators used to cool magnet water.

4. Observatory reservoir.

5. Former telescope building. Now used to house motor-generator set.

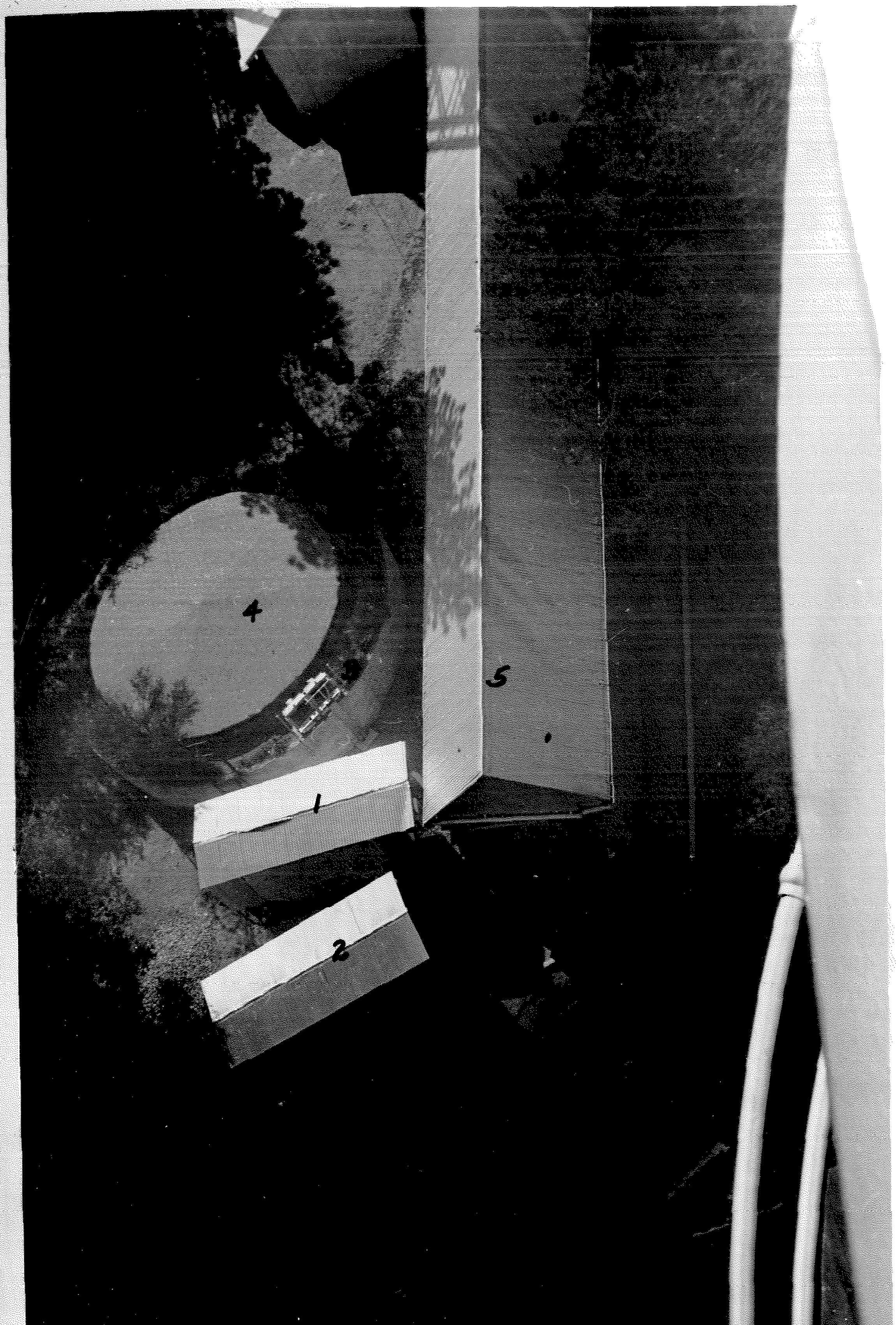

Fig. 8. Cosmic Ray Equipment at Mt. Wilson

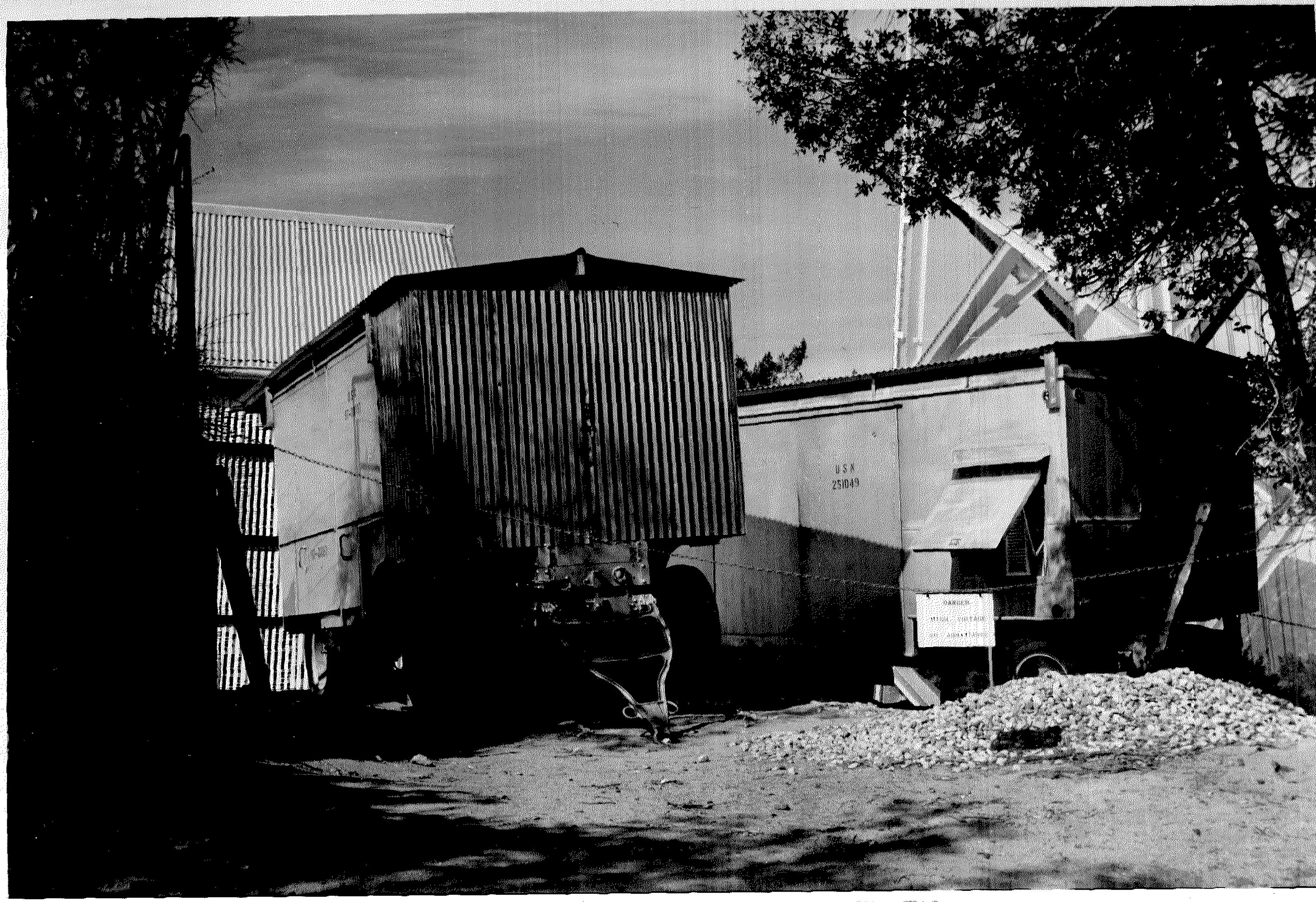

Fig. 9. Cosmic Ray Trailers at Mt. Wilson

IV. RESULTS

The results to be described are based upon a total of 23,000 photographs of which 14,000 were taken at 220 m elevation with 1-3 coincidences, 7000 at 1750 m with 1-3 coincidences and 2000 at 1750 m with 2-3 coincidences.

Penetrating Showers

Inasmuch as earlier experiments[2] had indicated that V-particles were closely associated with penetrating showers, coincidence requirements were selected which tended to trigger the apparatus whenever such events occurred. At 220 m, about 8 percent of the photographs, while at 1750 m, about 20 percent of the 1-3 photographs and about 40 percent of the 2-3 photographs showed penetrating showers (i.e. photographs showing two or more collimated, time associated, non-electronic particles). The figures here given represent lower limits to the percentage of cases in which the chamber was actuated by a penetrating shower, for many additional photographs showed slow protons and mesons, or other evidences of a penetrating shower. These, however, were not counted in the above statistics because they failed to meet the definition adopted above.

V-Particles

In this set of photographs, a total of 134 neutral V-particles and 18 charged V-particles were observed to decay. Figure 10 is a photograph of a typical neutral V-particle decay*, while figure 11 is a photograph of a typical charged V-particle decay. The association of these decays with penetrating shower events is quite obvious.

* The statistics associated with the neutral V-particle decays are summarized in Appendix I.

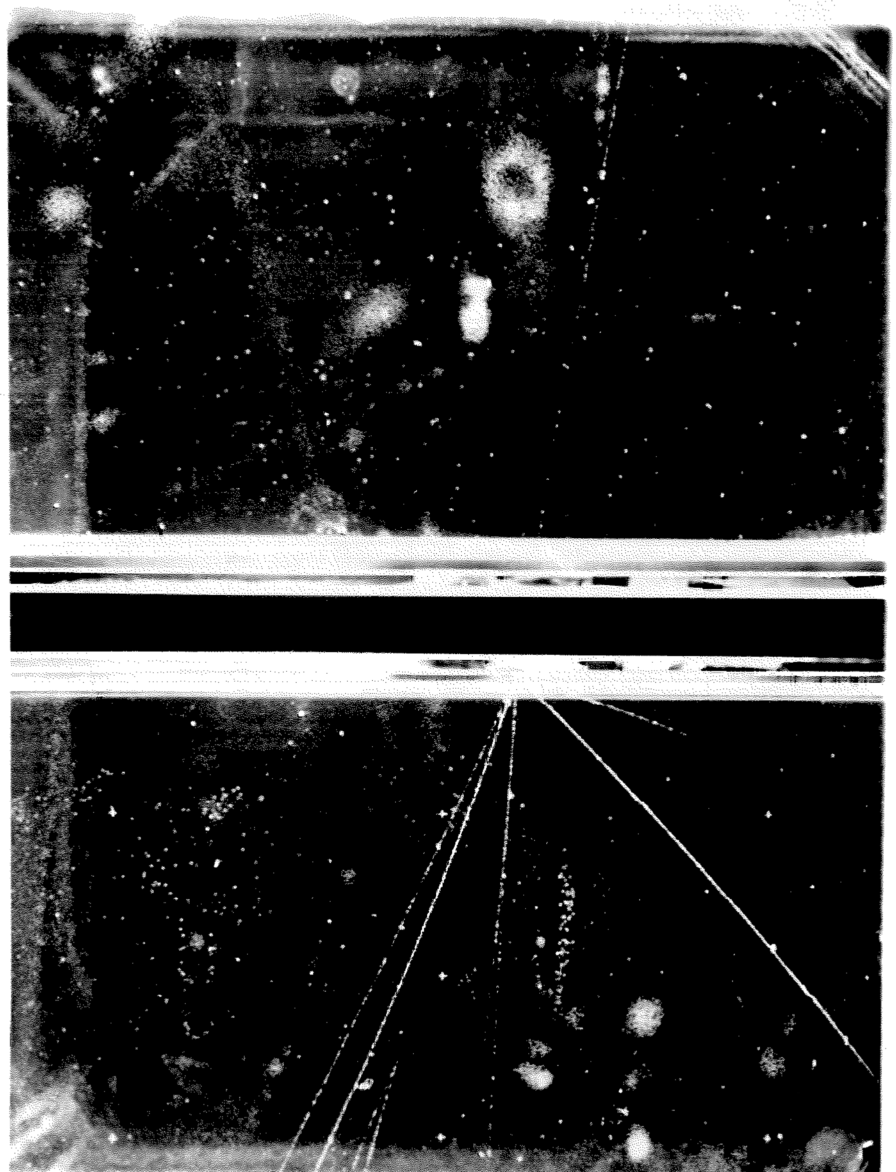

Fig. 10. (Case #17685) Example of the production of a neutral V-particle by a single charged particle. The statistics associated with this case are summarized in Appendix I.

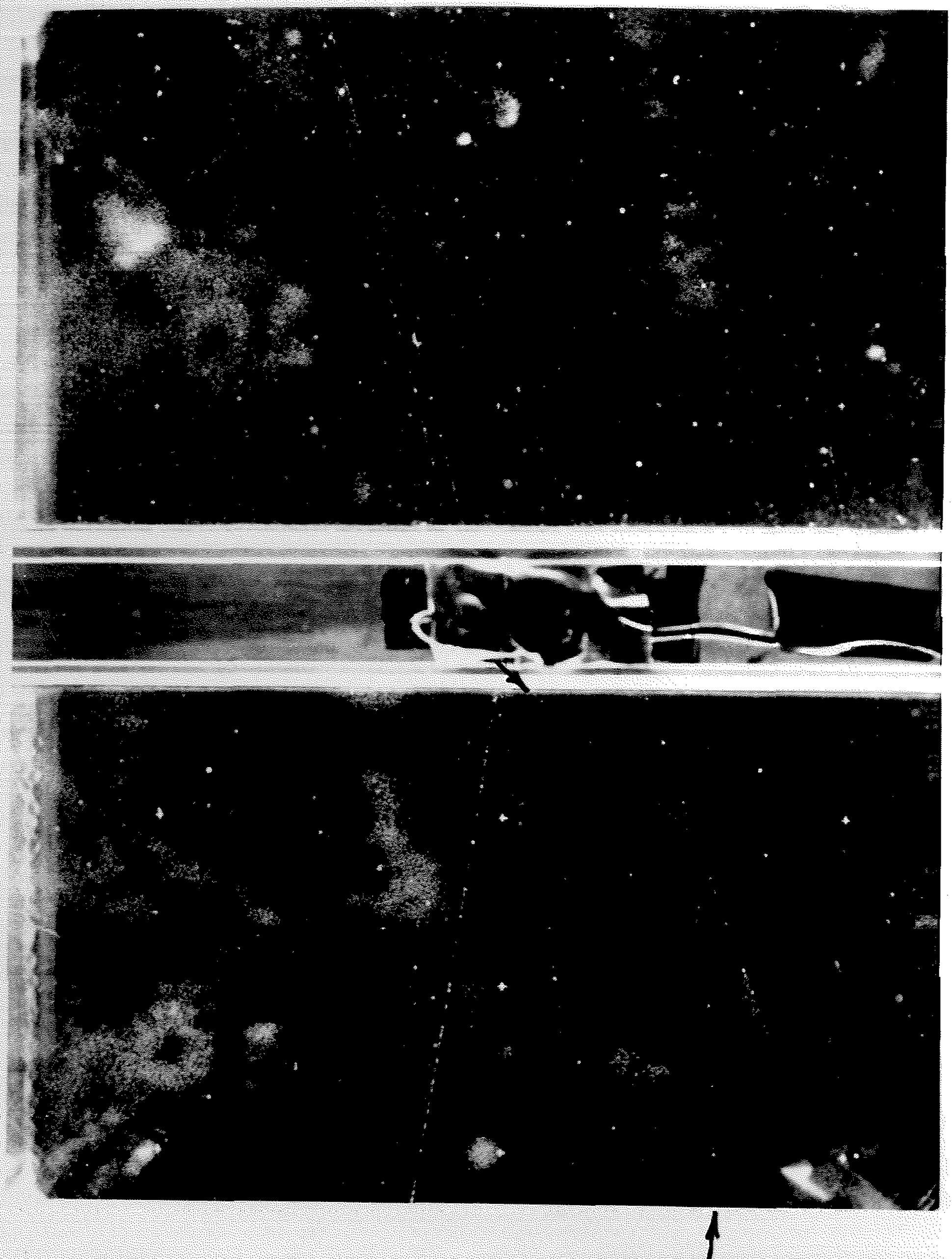

Fig. 11. (Case #13484) An example of the production and decay of a charged V-particle. The charged V-particle is indicated by an arrow. The other decay on this photograph is probably a charged V-particle.

As has previously been mentioned, the analysis of the neutral V-particles will be the primary effort of this paper. However, a similar, though less exhaustive, analysis of the charged V-particles has been included in Appendix II.

Heavy Mesons

Some of the secondary particles observed in penetrating shower events seemed to be less massive than protons and yet certainly more massive than π-mesons. In addition, further evidence for the existence of such particles exists in the form of observed characteristic decay phenomena. These particles are here grouped under the title of heavy mesons and will be considered in greater detail in Appendix III.

V. THE DECAY OF THE NEUTRAL V-PARTICLE

A. Introduction

Production Statistics

In the 23,000 cloud chamber pictures that were taken during these experiments, a total of 134 neutral V-particles, 7 positive V-particles, and 11 negative V-particles were observed to decay. Ten of these photographs showed more than one V-particle: in 3 cases, two neutral decays; in 1 case, three neutral decays; in 4 cases, one neutral and one charged decay; and in 2 cases, two charged decays. Only in three of these cases, however, did the V-particles appear to be produced in the same nuclear event. Examples of typical V-particle decays have previously been shown in figures 10 and 11. Additional examples are shown in figures 12, 13 and 14.

If the 134 cases of the decay of neutral V-particles are classified according to the circumstances of their occurrence, one finds that

72 occurred in penetrating showers whose origins were in the lead blocks above the chambers,

37 were produced in nuclear interactions (or stars) in the lead plate between the chambers, and

25 occurred in the chamber, or were not clearly associated with any nearby event.

Of the 37 stars in the lead plate from which neutral V-particles emerged,

27 were produced by charged particles which were themselves penetrating-shower secondaries from a nuclear collision somewhere above the chamber,*

* In order to be sure that an event was actually initiated by a charged

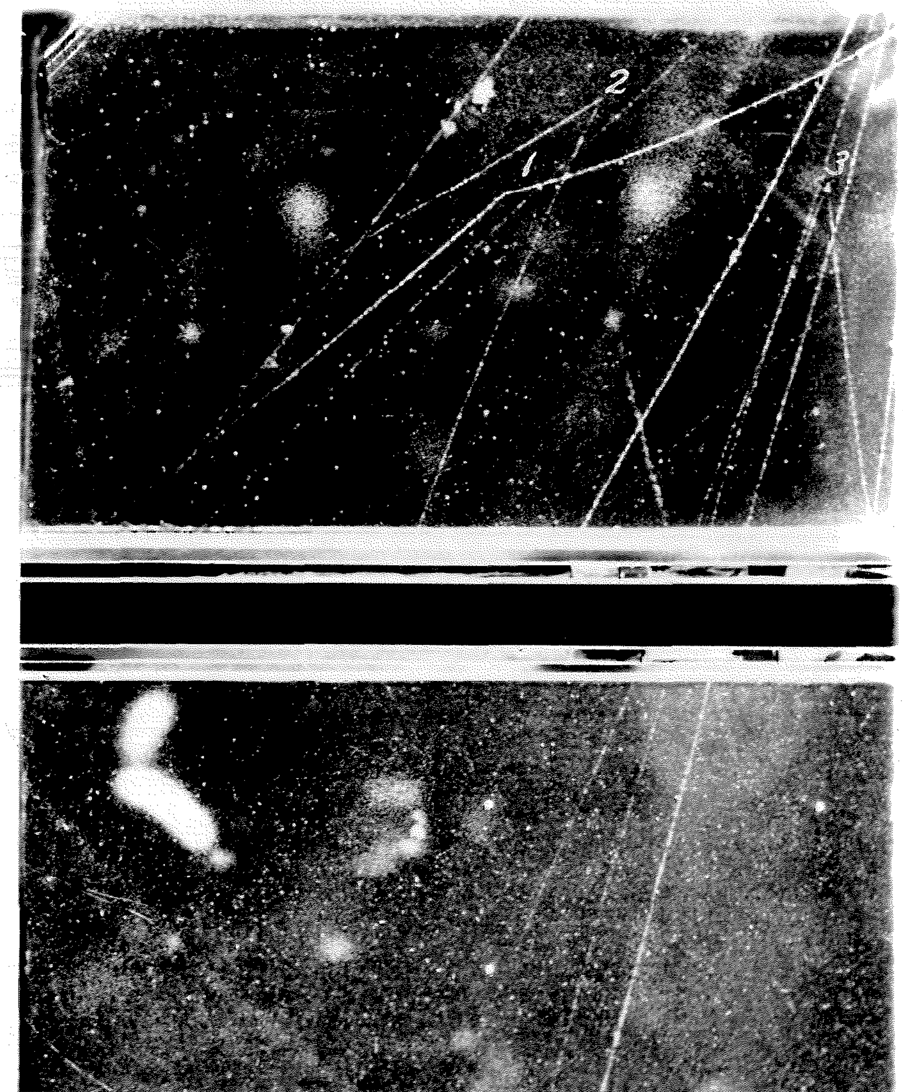

Fig. 12. (Case 19063) A rare example of three neutral V-particle decays. Two of the three decays (Nos. 2 and 3) are in excellent alignment with the origin of a nuclear event in the lead blocks above the chamber.

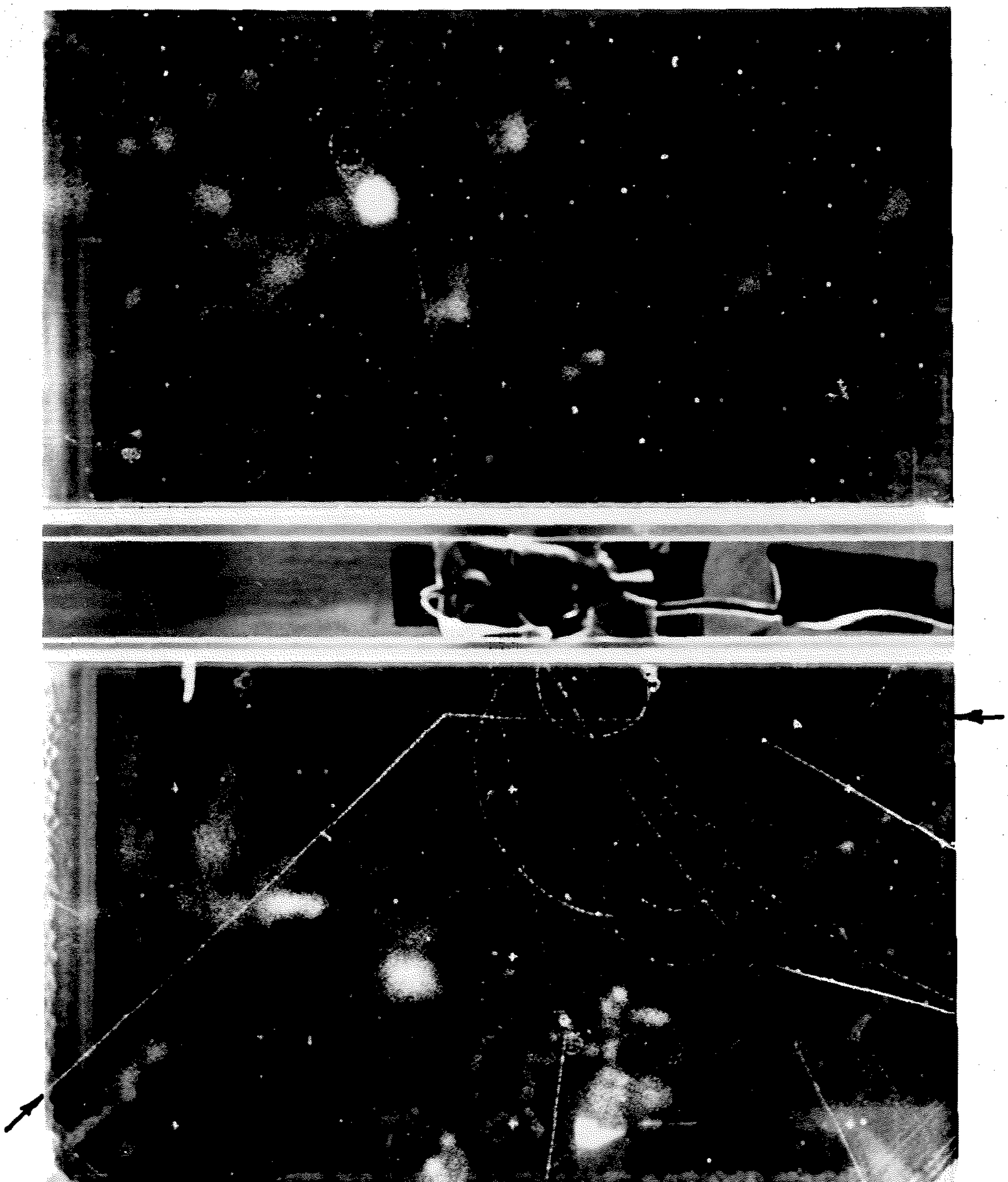

Fig. 13. (Case #11373) An example of a photogenic neutral V-particle decay.

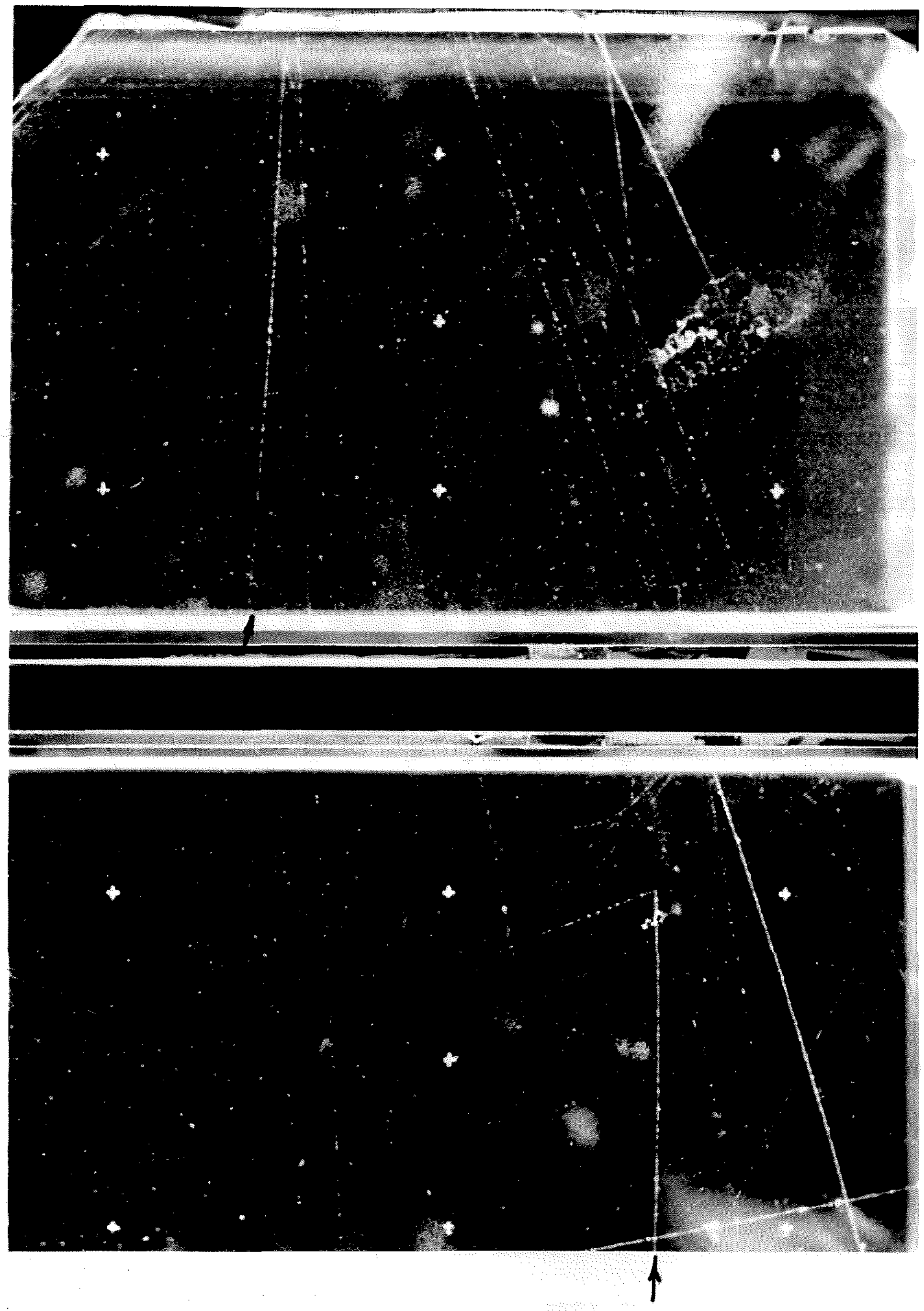

Fig. 14. (Case #23942) An example of two unrelated neutral V-particle decays, one near the top of the upper chamber with origin above the chambers, and the other in the lower chamber with origin in the lead plate between the chambers.

particle, it was required that this particle should have been visible in the lower chamber, had it traversed the plate without deflection, and that it actually be deflected by at least five degrees at a point coinciding, within accuracy of measurement, with the nuclear event in question.

---

6 were produced by single charged particles, unaccompanied by a shower or other indication of nearby nuclear events, and

4 were apparently produced by neutral particles.

A similar classification of the 18 charged V-particles showed that

9 occurred in penetrating showers whose origins were above the chamber, and

9 were produced in stars in the lead plate.

Of the 9 stars in the lead plate which yielded charged V-particles,

8 were initiated by charged penetrating-shower secondaries, and

1 was produced by a single charged particle.

None of these stars was produced by a neutral particle.

Preliminary Conclusions

It has been generally supposed that V-particles are produced in energetic nucleon-nucleon collisions, presumably with about equal cross-section in n-n, p-p, or n-p collisions. The above statistics indicate, however, either (1) that protons are many times more effective in producing both charged and neutral V-particles than are neutrons, (2) that energetic protons are many times more numerous than energetic neutrons, or (3) that meson-nucleon collisions can result in V-particle production. Of these alternatives, the last appears to be the most acceptable in view of the large body of experimental evidence in favor of charge independence of nuclear forces.

It would thus appear that in these experiments the great majority of both the neutral and charged V-particles were produced by mesons.

However, this result does not necessarily indicate a larger cross-section for V-particle production by mesons than for production by nucleons, since the number of high energy mesons present in a penetrating shower is known[8] to be much greater than the number of high energy nucleons. Also, V-particle production by mesons does not necessarily mean production by π-mesons, or by π-mesons alone, since it is now thought[9] that, at the very high energies prevailing in the original nuclear collisions with which we are here concerned, other heavier mesons may be produced about as copiously as are π-mesons.

A second conclusion regarding V-particle production, namely, that they are probably not always produced in pairs, can be deduced from the number of multiple V-particle decays that were observed in this series of photographs. For, if V-particles were always produced in pairs with comparable lifetimes, one would expect to have seen many more cases than were observed in which two V-particles decayed inside the cloud chamber; it is also perhaps significant to note that the number of double neutral decays, in which the origins of the two particles are different, actually exceeds the number in which both proceed from the same origin. This conclusion is, of course, based on the assumption that there is no competing neutral V-particle which decays into a neutron and a neutral π-meson; the existence of such a decay scheme would considerably weaken the above argument.

Division of Effort

To expedite the complete analysis of the 134 cases of neutral V-particle decay, an equitable division of effort, based upon the characteristic properties of this particle, was required. Inasmuch as a division into three parts was desired, this was accomplished by considering the three natural phases through which any unstable particle must pass, namely, creation, existence for a finite period of time, and finally, decay. An analysis of the creation of this particle ultimately results in the determination of a group of properties which may be called the production phenomena associated with the particle; these would include such obvious properties as cross-section, threshold energies, nature of incident particles, etc. An analysis of a neutral particle, based upon cloud chamber data and restricted to the period between creation and decay, would seem to be a fruitless undertaking. However, such an analysis, if properly executed, can result in the very important property of lifetime. Inasmuch as the production phenomena and the lifetime of the neutral V-particle are most ably considered elsewhere[10-11], only a discussion of the decay phenomena will be considered in the remainder of this paper.

Available Information

Before attempting to investigate these decay phenomena, it is well to pause for a moment and summarize the types of information that are available.

(1) Statistics: Statistics furnish one with the simplest and most fundamental types of information available, inasmuch as measurements are not required; classification and counting are the only operations involved. The value of this source lies in its very simplicity and in the fact that the mathematical laws governing such processes are quite well understood. The material presented in the earlier sections on

Production Statistics and Preliminary Conclusions provides an excellent example of the application of this source of information.

(2) Spatial Relationships: Having disposed of the category for which no measurements are required, the next simplest category would be that for which only the very simplest of measurements are required. This, it would seem, would be an investigation of the 3-dimensional geometry, the characteristic angles and distances, associated with the decay. However, before such measurements can be made, it is necessary that a means of reproducing the original spatial relationships from the stereoscopic photographs be found. Figure 15 illustrates schematically the reprojection system used. In this system, which was optically identical to the camera system, the surface of the viewing screen was made to correspond to the rearmost interior surface of the cloud chamber. Fiducial marks, scribed on this cloud chamber surface and present on each photograph, were brought into register on the screen- thus assuring the spatial correspondence of these surfaces. A point, P, in the interior of the cloud chamber thus appeared upon reprojection as two points, P_1 and P_2, separated by a distance Δx given by the formula,

$$\Delta x \approx z\, S/(D-Z) \qquad (1)$$

where the symbols are defined in figure 15. In the present experiment the quantities S and D were, respectively, 14 cm and 93 cm. The solution of this expression for z readily gives one of the desired 3-dimensional space coordinates. The two remaining coordinates were determined graphically with the aid of construction lines 1 and 2 drawn through P_1 and P_2 as shown. This ability to find the space

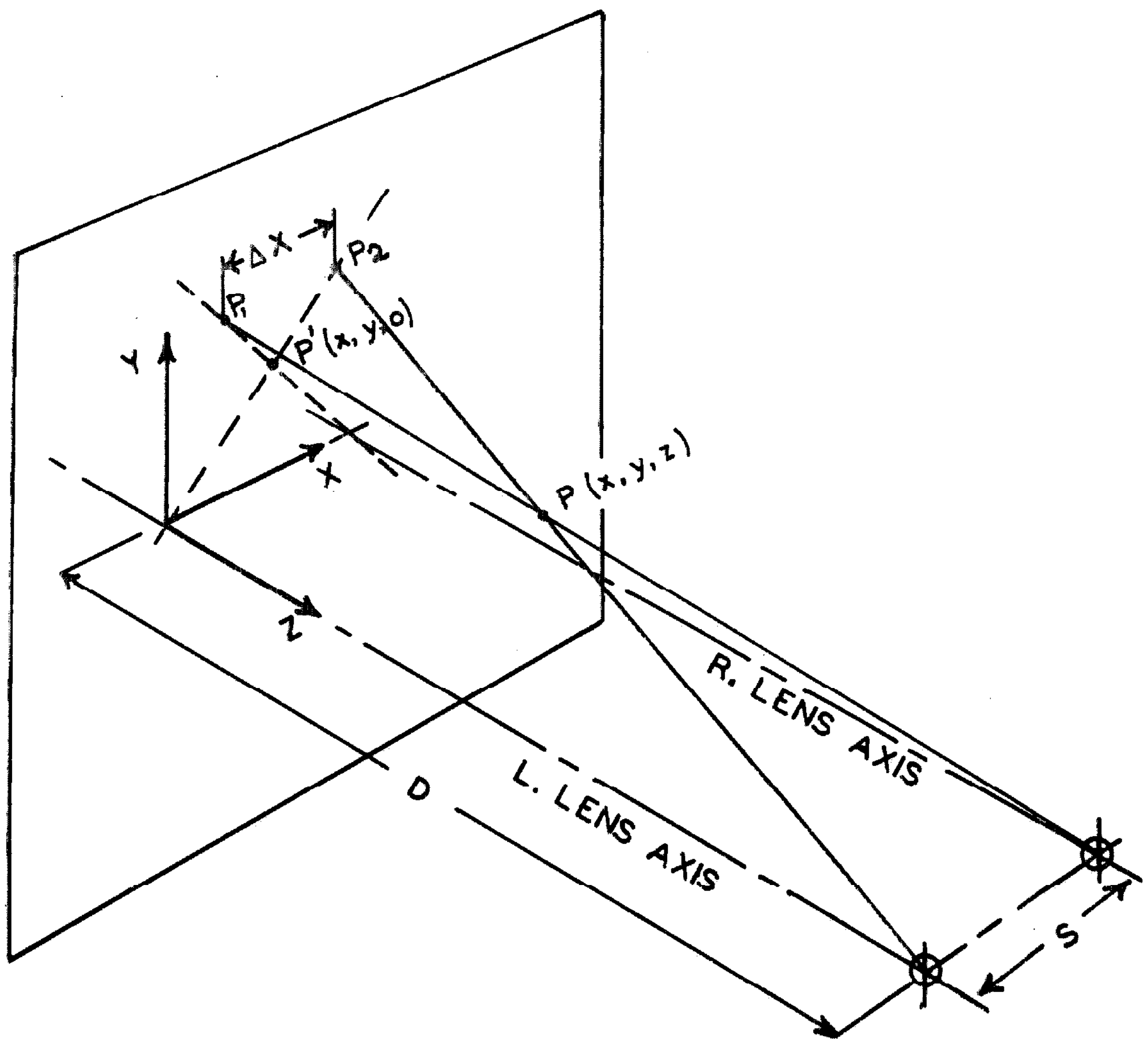

Fig. 15. Perspective diagram of the geometry of the reprojection system. The two stereoscopic views were reprojected through the same optical system as was used in the original camera, onto a screen perpendicular to the camera axes. A point P, which lay at the point (x,y,z) when photographed, thus projects into two points, P_1 and P_2, on the screen.

coordinates of any given point completely determines the original spatial relationship, inasmuch as two points will determine the vector representation of a line segment and the application of the vector concepts of cross product and scalar product will enable the angular relationships between two such segments to be found. To facilitate these graphical constructions, a sheet of tracing paper was customarily placed upon the viewing screen onto which the two sets of track images from the stereoscopic photographs were projected. Careful pencil traces were made of the two track images of the particles on the photographs. The required graphical constructions, more of which will be introduced later, were then made on this same sheet of paper.

(3) Curvature-Momenta: Another geometrical property available was the curvature of the track . The momenta of the charged particles were determined from the measurements of these curvatures and a knowledge of the magnetic field. In order to make these measurements sufficiently precise, it was necessary to incorporate certain refinements which have been neglected in previous cloud chamber work. It has usually been assumed that the magnetic field, although not constant in strength throughout the chamber, is at least unidirectional, and that the radius of curvature of a track on the film corresponds to the radius of curvature of a helix whose axis is parallel to the magnetic axis. Neither of these assumptions is strictly correct, for actually the field may have sizable components transverse to the magnetic axis, and also the track image on the film is not an orthogonal projection of a helix onto a plane, but is a projection through a point (i.e. through the lens aperature) onto a plane. An exact expression, which takes

both of these effects into account, has been derived relating the true momentum of a particle to the measured curvature of its track on the film. To make use of this exact relationship, it was necessary to measure the three rectangular components of the magnetic field throughout the chamber, and thus to make allowance for the direction of the magnetic field as well as for the variation in its axial component. In the application of this formula to the track measurements, the only assumption involved is that the measured average radius of curvature over the length of the track is equal to the true radius of curvature at the center of the track. The correction arising from the use of this more exact formula was found usually to be about 5-10 percent, but in some cases was as great as 20 percent.

The curvature of a track was measured on each stereoscopic view, and a value of the momentum was calculated from each measurement. In each case an uncertainty was assigned whose size was appropriate to the length and quality of the track. These two values of the momentum were then combined to obtain the final measured momentum. The final uncertainty was taken to be somewhat less than that of either of the individual uncertainties, but was always large enough to include both measured values, and was never taken to be less than the error to be expected from multiple scattering or less than P/40 percent (P in Mev/c).

(4) <u>Specific Ionization</u>: Further information as to the character of particles is provided by a determination of their specific ionization. The accurate measurement of ionization is exceedingly difficult, even in cases where the droplets along the track are actually resolved. Fortunately, a considerably larger error can be tolerated

in the ionization than in the momentum (for ionizations greater than twice minimum) to obtain a mass measurement of given accuracy. In the present experiment, the specific ionizations for individual tracks were estimated independently by two or more observers, and were evaluated a second time by the same observers several weeks later. The estimates were made by visual comparison with other tracks on the same photographs whose ionizations were considered known. For example, a straight penetrating shower-particle track (> 1000 Mev/c) was taken to be at minimum ionization, while an electron track (50-100 Mev/c) was assumed to be 1.3 times minimum. If a track appeared indistinguishable from such comparison tracks, it was assigned an ionization less than 1.5 times the minimum value. In some cases a track appeared definitely heavier than a track of minimum ionization, and yet not as heavy as one of twice minimum; in such a case a value of 1.1-1.8 times minimum might be assigned. A track whose ionization was above twice minimum could often be compared with heavily ionizing mesons or protons of known momenta and therefore of known specific ionizations. In all cases a range of ionization was determined within which all observers could agree that the actual value almost surely lay, and outside of which it was very unlikely to lie. This range of values thus does not represent a "probable error" or "standard deviation" in the usual sense.

Inasmuch as the mass of a particle of unit charge is determined from the momentum and the ionization by an equation of the form

$$M = P \cdot F(I) \qquad (2)$$

where P is the momentum and F(I) is a function of the specific ionization only, it follows that the error in the mass value that arises from errors in momentum and ionization is approximately

$$\frac{\Delta M}{M} = \frac{\Delta P}{P} + \frac{F'(I)}{F(I)} \quad \Delta I \qquad (3)$$

Thus it can be assumed that the errors in the estimate of ionization, while perhaps rather large and not subject to direct statistical treatment, are at least independent of the identity of the particle. This being the case, it was possible to evaluate the accuracy with which specific ionization can be estimated by calibrating on heavily ionizing π-mesons, for which the momenta could be measured very accurately; this calibration also made it possible to investigate, and possibly to eliminate, any systematic errors which might have been present.

(5) Change in Curvature or Specific Ionization: Additional information may be provided by observed changes in the curvatures and the specific ionizations of particles under investigation. In the present work such changes were occasionally observed when the same particle could be identified in both the upper and lower chambers. If one attributed these changes solely to ionization losses in the absorber, deductions as to the particle identity could be made even if possible systematic errors were assumed to exist.

(6) Interactions: Observed interactions in the lead absorber separating the chambers, or in the chamber gas, were very useful. For instance, the presence of electrons could be established by their characteristic multiplication on passing through the lead absorber. On the other hand, the absence of this phenomenon served to indicate the presence of a penetrating particle. Similarly, in identifying

mesons, interactions in the lead plate made it possible for one to distinguish between π- and μ-mesons, a feat that would have been extremely difficult if mass measurements alone had been utilized. Finally, interactions in the chamber gas and in the absorber might serve to make known the presence, and possibly the identity, of neutral particles or rays associated with the decay of these neutral V-particles.

Objectives

The investigation of the decay phenomena associated with the neutral V-particle can only be considered as completely successful when the identity of all secondary particles, including possible neutral particles or rays, has been established, and when the mass of the incident V-particle has likewise been determined. In the sections that follow, the available information, as outlined above, will be used in conjunction with the basic relativistic principles of conservation of momentum and conservation of mass-energy in an endeavor to determine these properties.

B. Nature of Decay Products--Charged Secondaries

Geometrical Considerations

A statistical analysis based solely upon the geometrical properties of the neutral V-particle decay and upon the assumption that one is here dealing with a two-body decay phenomenon will now be undertaken. This will be based solely upon the size of θ_+ relative to θ_- (see figure 16).

Consider a two-body decay of a neutral V-particle of mass M_o into charged particles of mass M_+ and M_- as shown in figure 16. In the center of mass system (henceforth denoted by CM) each particle has a momentum P', and the positive particle is emitted at an angle θ' with respect to the direction of travel of the neutral V-particle. In the laboratory system, moving with speed $-\beta c$ along the x-axis relative to the CM system, the momenta are P_+ and P_-, at angles θ_+ and θ_- with the path of the V-particle. The transformation equations between the laboratory system and CM system can be written in the form

$$\begin{aligned}
&(a)\quad P_{+_x} = \frac{P_o P' \cos\theta'}{M_o\beta} + \frac{P_o}{2M_o^2}\left[M_o^2 + (M_+^2 - M_-^2)\right] \\
&(b)\quad P_{+_y} = P' \sin\theta' \\
&(c)\quad P_{+_z} = 0 \\
&(d)\quad P_{-_x} = -\frac{P_o P' \cos\theta'}{M_o\beta} + \frac{P_o}{2M_o^2}\left[M_o^2 - (M_+^2 - M_-^2)\right] \\
&(e)\quad P_{-_y} = -P' \sin\theta' \\
&(f)\quad P_{-_z} = 0
\end{aligned} \tag{4}$$

where

$$P' = \frac{\left[M_o^2 - (M_+ - M_-)^2\right]^{\frac{1}{2}}\left[M_o^2 - (M_+ + M_-)^2\right]^{\frac{1}{2}}}{2\,M_o} \tag{5}$$

and where all momenta, masses, and energies have been written in

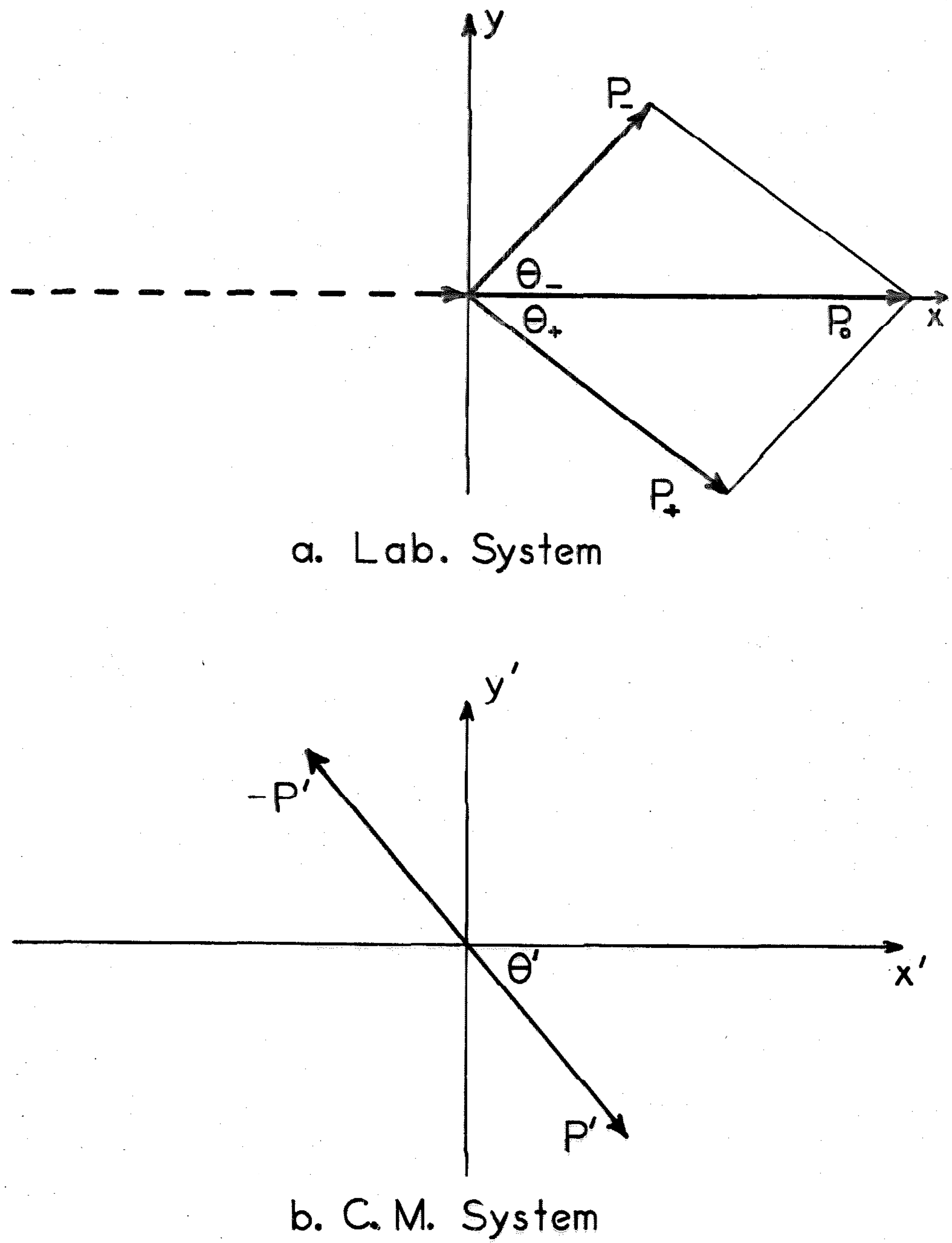

Fig. 16. Momentum diagrams of the two-body decay of a neutral V-particle as seen in the laboratory system (cloud chamber) and in the center-of-mass system moving with the V-particle.

energy units. Application of the law of cosines to figure 16 gives,

$$\text{(a)} \quad P_{+_x} = P_+ \cos \theta_+ = \frac{P_o^2 + P_+^2 - P_-^2}{2P_o} \tag{6}$$

$$\text{(b)} \quad P_{-_x} = P_- \cos \theta_- = \frac{P_o^2 + P_-^2 - P_+^2}{2P_o}$$

Inserting these expressions into Eq. 4(a) and 4(d), subtracting 4(d) from 4(a), and dividing by P_o, one obtains:

$$\frac{P_+^2 - P_-^2}{P_o^2} = \frac{M_+^2 - M_-^2}{M_o^2} + \frac{2P' \cos \theta'}{M_o \beta}$$

$$= \frac{\sin^2\theta_- - \sin^2\theta_+}{\sin^2\theta_T} = \frac{\sin(\theta_- - \theta_+)}{\sin(\theta_- + \theta_+)} \tag{7}$$

where the second equality follows from the law of sines applied to the momentum parallelogram of figure 16, and where θ_T is the total angle between the secondary tracks in the laboratory system.

The value of the quantity on the left of Eq. (7) has been used by the Manchester workers[7] as a criterion for the classification of neutral V-particles into two groups, into which they assume that all neutral V-particles must fall. Their notation, α , for this quantity will be adopted here. Thus

$$\alpha = \frac{P_+^2 - P_-^2}{P_o^2} = \frac{\sin(\theta_- - \theta_+)}{\sin(\theta_- + \theta_+)} \tag{8}$$

Eq. (7) indicates that, for a given mode of two-body decay, a given speed βc, and an isotropic distribution in the CM system, the quantity α has an average value equal to $(M_+^2 - M_-^2)/M_o^2$, and is uniformly distributed, with amplitude $2P'/M_o\beta$, on either side of the average. The actual distribution of α for a given two-body decay scheme is the result of a number of such uniform distributions, each having the same average value but a different amplitude, because of the different speeds, βc, involved in the various cases. The total distribution thus should have a maximum at the value $(M_+^2 - M_-^2)/M_o^2$ and should be symmetrical about this maximum. Thus by evaluating α for those cases in which θ_+ and θ_- can be measured, one can hope to gain some information as to the relative masses of the decay products.

The values of α were computed for the 60 cases for which the origin of the neutral V-particle could be found. The distribution of those values is shown in group I of Fig. 17. On the figure are drawn several vertical lines, which correspond to the expected average values of α for the various decay schemes indicated in Table I.

TABLE I

Central values of α and minimum amplitudes of the α-distribution for various decay products.

No.	Decay Products M_+ (m_e)	M_- (m_e)	Q Mev	Central Value $(M_+^2 - M_-^2)/M_o^2$	Amplitude $2P'/M_o$
1	276	276	120	0	.71
2	276	210	120	.06	.73
3	500	276	50	.22	.44
4	1000	276	50	.49	.32
5	1837	276	35	.69	.17
6	1837	210	35	.74	.19

The energy release or Q-value was assumed to correspond roughly to those obtained by direct analysis of the data*. The great preponderance of positive values of α indicates that at least a large majority of these decays, if not all of them, yielded a relatively heavy positive

* Q-values will be discussed in Section V-D.

Legend for Fig. 17.

The distribution of α for 92 cases of neutral V-particle decay is shown in Fig. 17. The quantity α is defined in the text.

Group I is the distribution of those values of α that were derived from the angles θ_+ and θ_-.

Group II is a similar distribution, but in this case the values of α were evaluated from the measured momenta only.

Group III is a composite distribution.

The cross-hatched portion of each distribution indicates the contribution made by cases whose positive particles, being heavily ionizing, were known to be much heavier than π-mesons. The numbered vertical lines identify the average values of α to be expected for the decay of a neutral V-particle into particles whose masses are indicated in Table I.

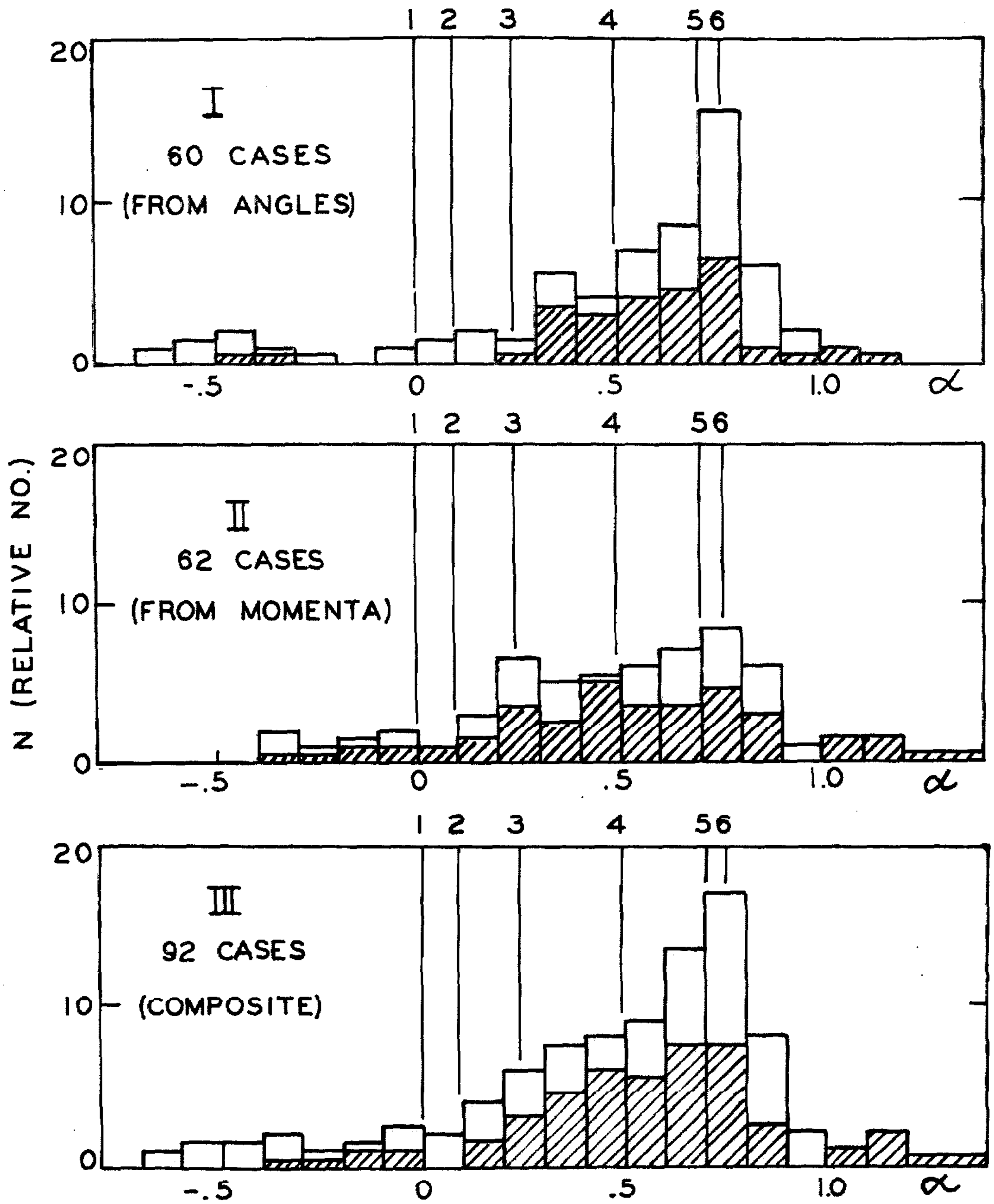

Fig. 17. Distribution of α for neutral V-particle decay.

particle and a relatively light negative one. It will be noted that the data are certainly consistent with, and the peak in figure 17 would tend to indicate the presence of, a neutral V-particle which decays into a proton and a π^- or μ-meson. Further, the distribution strongly suggests the existence of at least one other type of decay, but it does not serve to identify clearly the nature of this latter scheme.

As indicated by Eq. (8), a distribution of α-values can also be arrived at if the values of P_+ and P_- are known from measurements. In group II of figure 17 are plotted the values of α for 62 cases for which these momenta were measurable. This distribution is seen to be somewhat similar to that of group I and consequently would result in similar conclusions.

The difference in the shapes of the α-distributions of groups I and II can be explained in part by the difference in the selection criterion involved. The sole criterion for the inclusion of a case in group I was that it possess an origin so that the angles θ_+ and θ_- could be measured. This distribution is, therefore, unbiased, since the value of α depends only upon the speed of the V-particle and upon the orientation of the decay in the CM system. On the other hand, the criterion for the inclusion of a case in group II was that both of the decay particles have measurable momenta. This criterion tends to exclude decays in which the V-particle, and hence at least one of its decay particles, possesses a very high momentum. These excluded decays, for the most part, will be those for which the momentum of the heavier particle would have been unmeasurable no matter in what direction it might have been ejected in the CM system, but some borderline cases will also be excluded in which the momentum of the heavy particle was unmeasurable only because it was ejected in the forward direction in the CM system. Thus the sharp peak would be less pronounced, and the center of gravity of the distribution would be shifted toward the smaller values of α.

A composite α-distribution is shown in figure 17, group III. This distribution was constructed by combining groups I and II. In the 30 cases in which α was known both from angle division and from momenta, that value was used that was considered to be the more accurate.

The cross-hatched portions of the three α-distributions represent the contribution of those cases whose positive particle was identifiable as being much more massive than a π- or μ-meson. The selection of this sub-division is of course statistically biased since it will tend to favor those cases in which the positive particle is ejected backward in the CM system. These cases correspond to negative values of cos θ' and hence to smaller than average values of α.

Measured Masses

Unfortunately the conclusions of the previous section are based upon the assumption of a two-body decay, and must for that reason be held in abeyance pending confirmation. Thus it is useful at this time to undertake an analysis that is not subject to similar limitations; such an analysis is the direct determination of the masses of the secondary particles from a knowledge of their momenta and specific ionizations.

In 87 of the 134 neutral V-decays, it was possible to measure the momentum of at least one of the decay particles. Some of these particles were also heavily ionizing so that estimates of their masses could be made. Many of the particles, on the other hand, were essentially at minimum ionization so that only upper limits could be placed on their masses. These limits often served to distinguish between "heavy" and "light" particles, and thus permitted a rough classification of decays according to the relative masses of their secondaries, as shown in Table II; in this table, 700 m_e represents a useful, but nevertheless quite arbitrary, dividing point. In each of the 42 cases of group 1b

TABLE II

Classification of Secondary Particles in V^o -decay

M_+ \ M_-	1 $M_- < 700\ m_e$	2 $M_- > 700\ m_e$	3 M_- Indeterminate	Total
a $M_+ < 700\ m_e$	2	1	4	7
b $M_+ > 700\ m_e$	42	0	3	45
c M_+ Indeterminate	29	0	6	35
Total	73	1	13	

the positive particle, because of its ionization and momentum, is definitely known to be heavier than the negative particle. One can conclude in addition that the majority of the 29 positive particles in group 1c, which are at minimum ionization, must also be more massive than their companion negative particles. This conclusion follows from the relative populations of groups 3a and 1c, which would be expected to be equal for any decays which yield positive and negative particles of equal mass. Thus the direct mass determinations would indicate that not over 10 percent of these decays could yield particles of equal mass.

Three of the cases appearing in Table II are of special interest. Group 1a seems to indicate the existence of decays of the type postulated by the Manchester Group in which the two products have equal mass, while the single case in group 2a seems to indicate the existence of decays leading to a light positive particle and a heavy negative one. These three interesting cases will be considered in some detail later in this section.

The measured masses of the secondary particles, as determined by their measured momenta and estimated ionizations, are shown in figure 18; only those cases in which a particle was heavily ionizing are represented. All cases represented in the diagram are plotted as rectangles of the same area, whose widths correspond to the mass ranges derived from the central values of the measured momenta and the extreme limits of the ionization estimates.

The most striking feature of the diagram is the peak corresponding to the mass of a π-meson. As was previously pointed out, the error in the mass measurement of a light particle is determined almost entirely by the error in the ionization estimate. The sharpness of this peak thus indicates, not only that the negative particles are most probably π-mesons, but also that the estimates of ionization were sufficiently reliable, statistically, to distinguish π-mesons from μ-mesons.

It is also to be noted that the mass distribution reaches a maximum at a value somewhat lower than a proton mass; after considerable study of the measurement technique that was used, it was concluded that this does not necessarily indicate a mass lower than that of a proton for all these particles. In fact, it is believed that the great

Legend for Fig. 18

The measured masses of the neutral V-particle secondaries are exhibited in figure 18. In this diagram each particle is represented by a rectangular area whose width corresponds to the mass limits determined by the limits of the estimated ionization and by the central value of the measured momentum, and whose height is adjusted to give equal area to each rectangle.

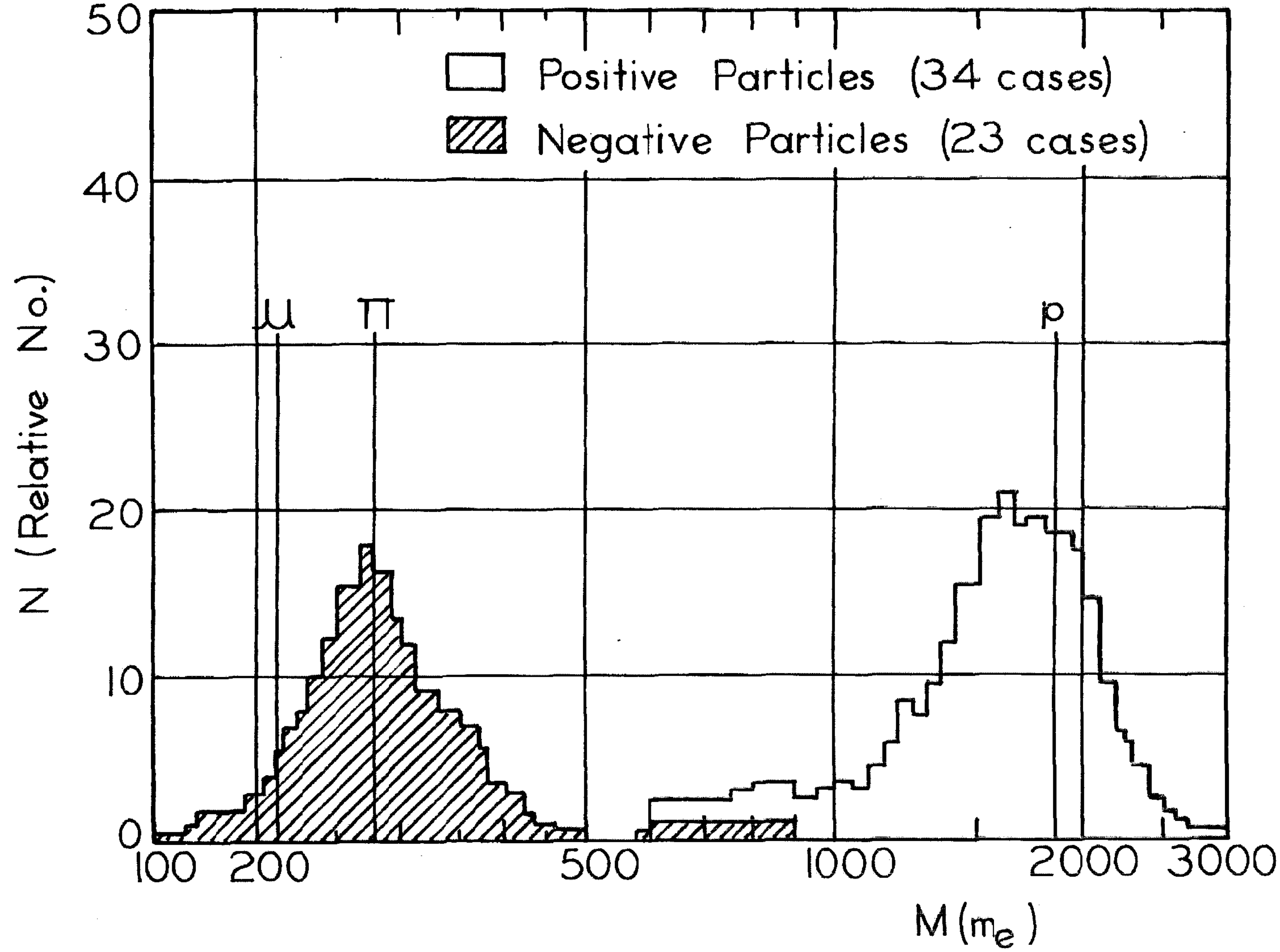

Fig. 18. Mass distribution of the secondary particles

majority of these positive particles were indeed protons but that a few τ- or κ-mesons could have been present. The spread in the measured masses of these positive particles is broader than that of the negative particles because of the greater difficulty of measuring the higher momenta here involved; that these positive particles do have larger values of momenta is clearly shown in figure 19.

Individual Cases

The previous paragraphs of this section have been primarily statistical in nature. An attempt will now be made to utilize the added information that is made available if the individual cases are considered. Before proceeding, however, it is important to stress the fact that some of the following observations may merely represent extreme statistical fluctuations due to experimental errors, and thus that they may lead to erroneous conclusions.

(1) π-mesons: It is certainly apparent from figure 18 that the great majority of the negatively charged secondary particles are π-mesons. There are, in addition, other evidences that tend to support this conclusion. For instance, figure 20 is an example of a neutral V-decay in which the negative secondary particle apparently decays. Presumably this is a π-μ decay; at least it is consistent with the properties of such a decay. In the 134 cases of neutral V-decays, only two such phenomena were observed, but this is entirely consistent with the relatively long lifetime of the π-meson.

Figure 21 is an example of a neutral V-decay which occurred in the upper chamber. The interesting feature of this case is the fact that the negative secondary undergoes an interaction as it passes through the lead plate, thus indicating a π-meson rather than a

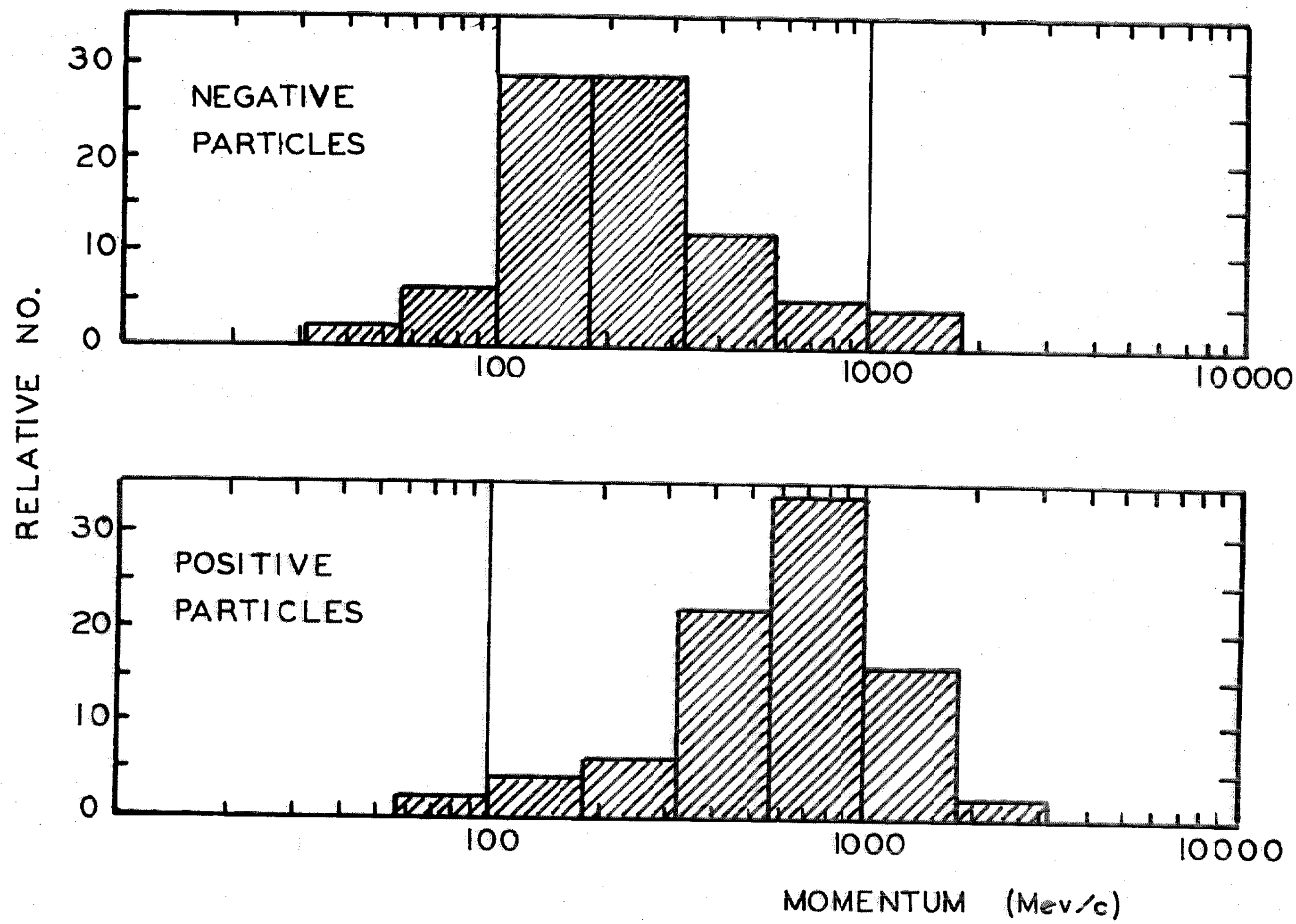

Fig. 19. Distribution of momentum of the neutral V-particle secondaries. 79 positive particles and 86 negative particles are represented in these histograms.

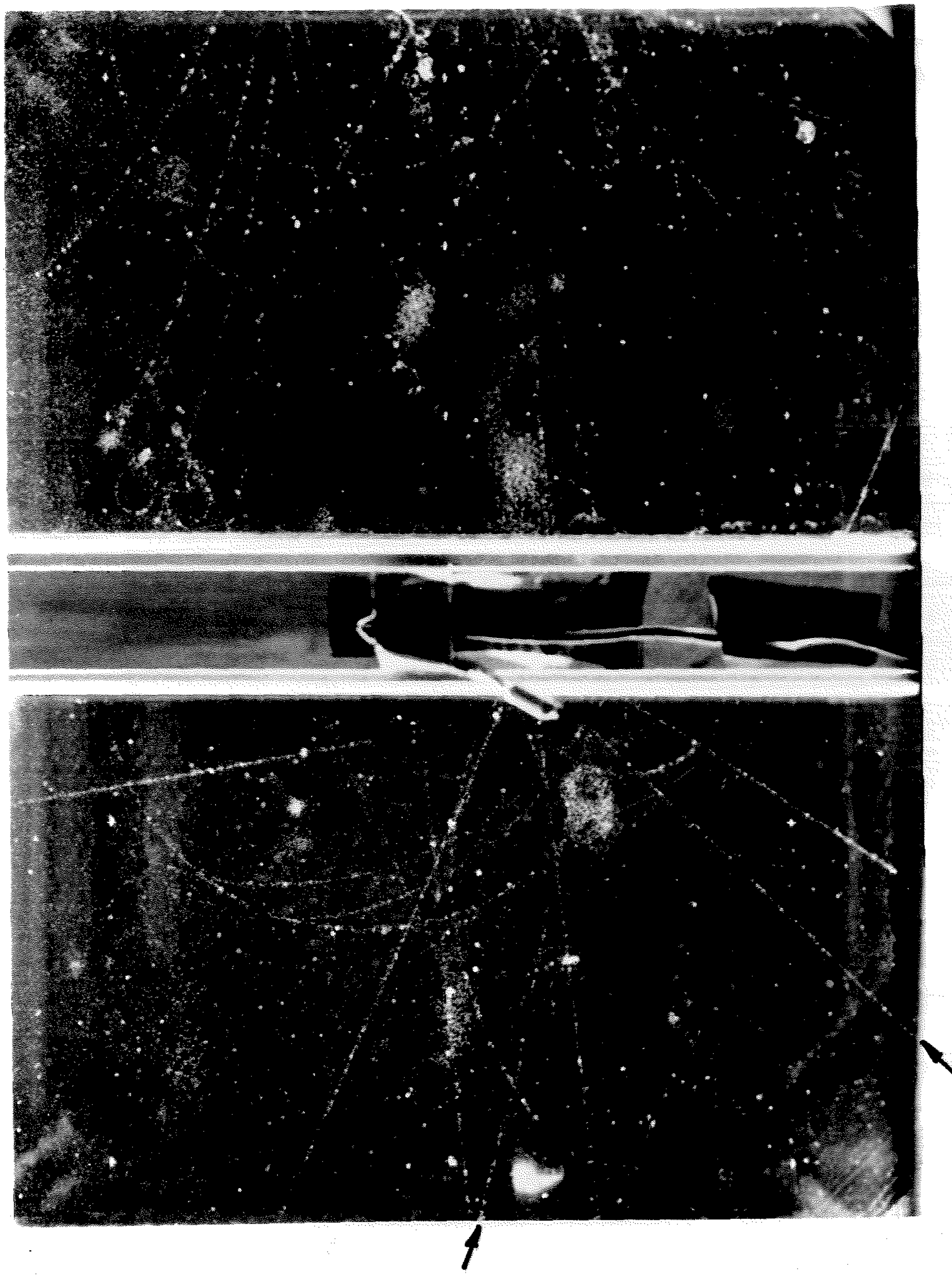

Fig. 20. (Case #09489) An example of a neutral V-particle decay (see arrows) in which the negative secondary particle (left) decays. Presumably this is a π-μ decay.

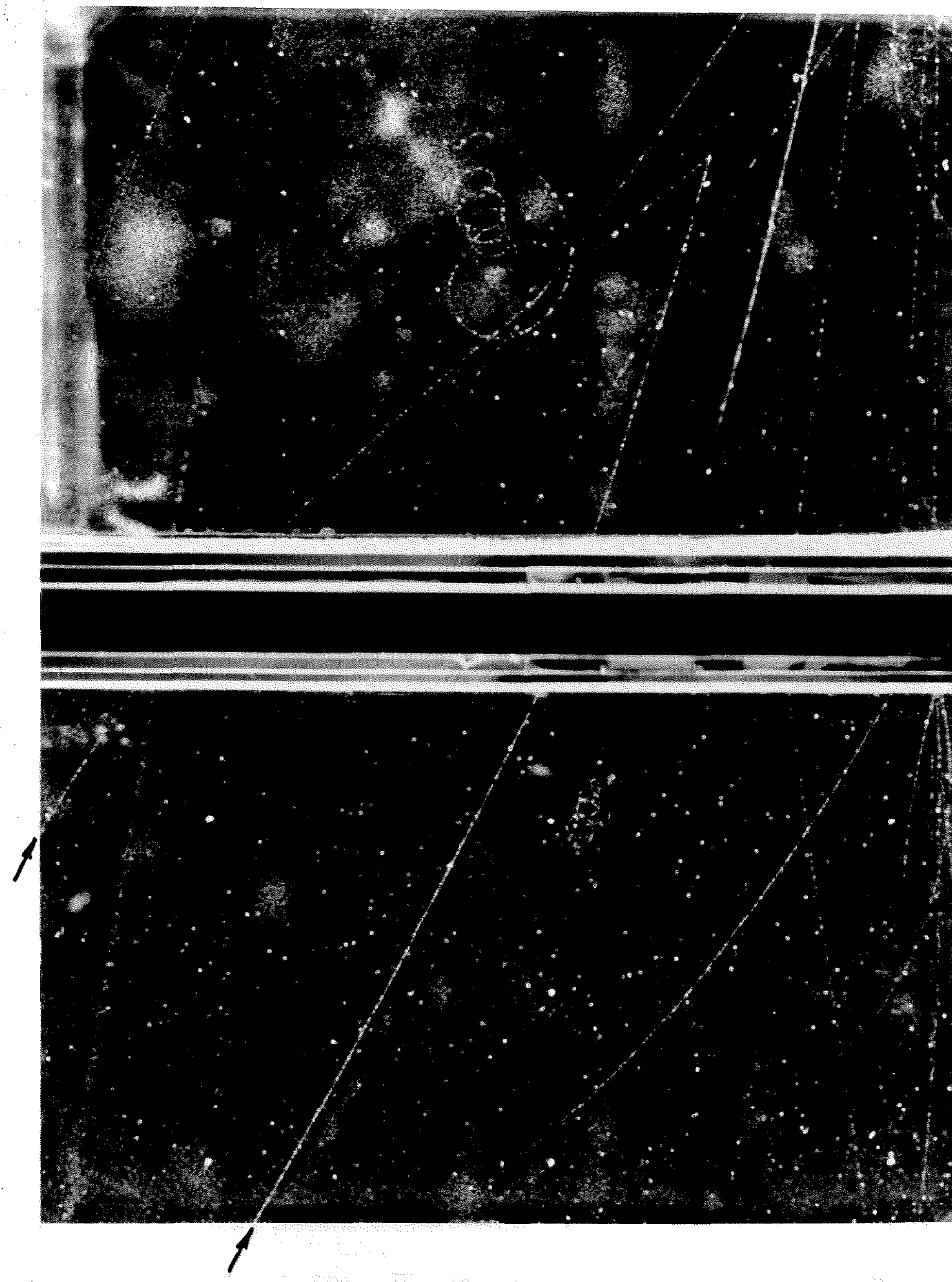

Fig. 21. (Case #23159) An example of a neutral V-particle decay in which both of the secondary particles interact in the lead plate. The interaction of the negative secondary particle (left) is particularly interesting.

μ-meson, a deduction which would have been extremely difficult if based only upon the mass measurement of this particle.

In addition to the existence of negative π-mesons, the three cases comprising groups 1a and 2a in Table II indicate the possible existence of positive π- or μ-mesons. Of these, the best example is the single case comprising group 2a. A photograph of this case is shown in figure 22. The momentum of the positive particle is 190 ± 20 Mev/c and its specific ionization is less than 1.5 times minimum. This restricts its mass to be less than about 350 m_e. There is, of course, the question of whether this is indeed an example of a neutral V-decay. The decay is in general alignment with the two high momentum tracks that traverse both chambers, but there is no identifiable origin with which it is associated. On the other hand, this can also be said of many of the neutral V-decays. If it were to be interpreted as a charged V-decay or a K-meson decay, the particle would have been traveling upward, and would similarly not have been proceeding from an identifiable origin. Of the 18 charged V-particles observed in the present experiment, none were traveling upward, and all were clearly associated either with a penetrating shower or with a nuclear interaction origin in the lead plate between the cloud chambers. Furthermore, the kinetic energy of the π- or μ-meson in the CM system of an assumed charged V- or K-decay is greater than 200 Mev, a value considerably higher than is now thought to be associated with either of these types of decay. Thus, this case most probably represents a neutral V-decay, and thus, positive π- or μ-mesons are indicated as charged secondary particles.

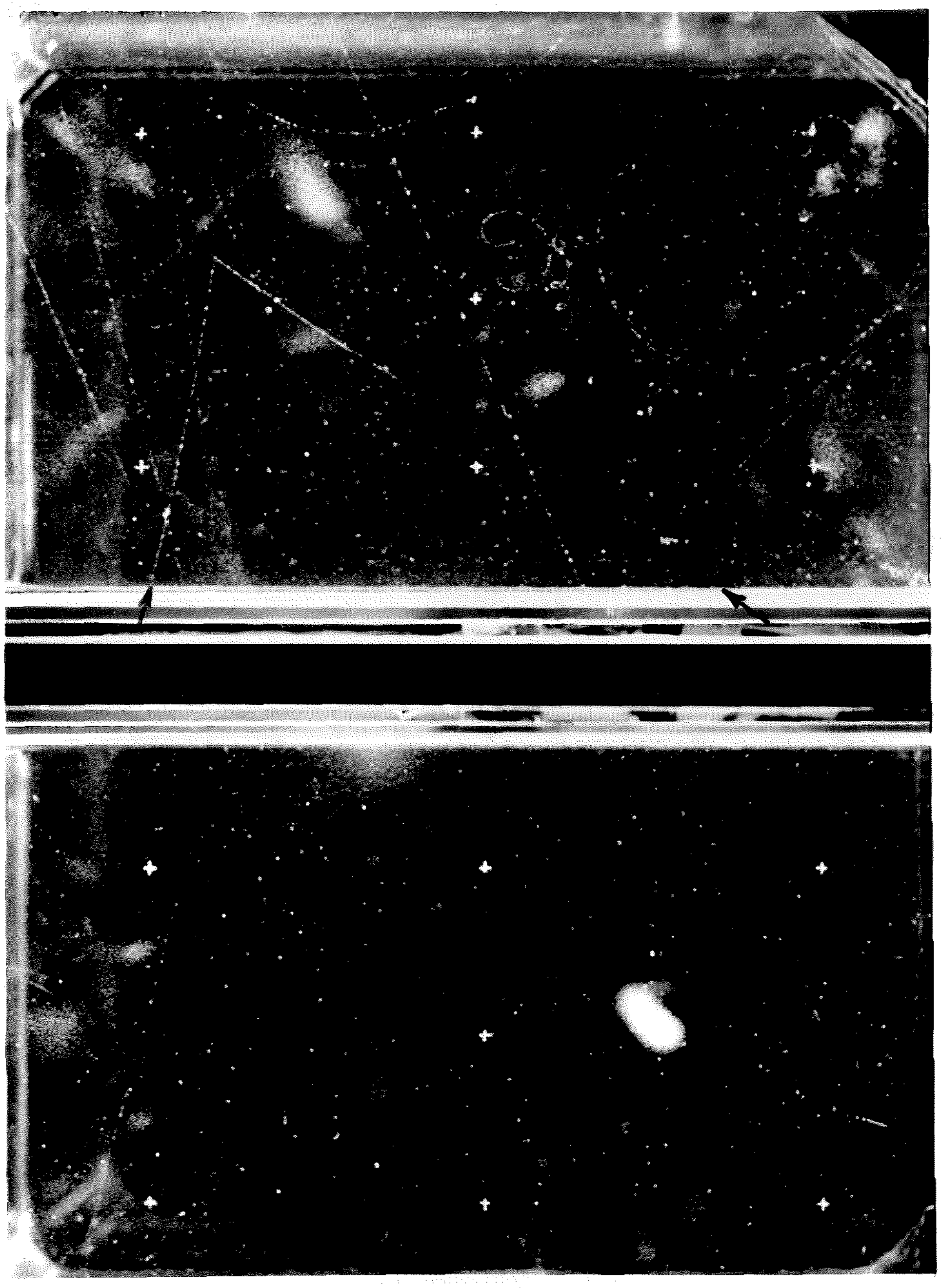

Fig. 22. (Case #24692) An Example of a neutral V-particle decay leading to a positive meson (presumably a π-meson) and a negative particle whose mass is considerably greater than that of a π-meson.

(2) μ-mesons: Although the mass distribution of figure 18 indicates that almost all of the light particles were π-mesons, there were five cases, two heavily ionizing and three at minimum ionization, whose measured masses or upper mass limits were too low to reconcile with the mass of a π-meson. This number of cases suggests that μ-mesons may sometimes be produced in neutral V-decays, but is surely too small to permit any strong conclusions as to decay schemes with which they may be associated. The statistics for these five cases are summarized in Table III. Of the five cases,

TABLE III

μ-mesons in Neutral V-particle Decays

Quantity / Case No.	P_- (Mev/c)	I_- (x Min.)	M_- (m_e)	P_+ (Mev/c)	I_+ (x Min.)	M_+ (m_e)
24141	117±15	<1.5	<220	(360±50)*	3-6	1200-2000
25686 (figure 23)	67±7	1.5-3.0	130-230	375±100	4-8	1600-2400
25890	122±4	1.2-1.5	170-230	153±11	>15	>1500
26867	140±50	<1.3	<200	(400±200)	>1.3	>600
30129	110±5	<1.5	<200	(500±35)	<1.5	<1000

* The parentheses indicate momentum found by momentum balance techniques.

#25686 is the most interesting; this case is shown in figure 23. It seems fairly certain in this case that the negative secondary particle is a μ-meson, but it is much less certain that the observed phenomenon is indeed a neutral V-decay. It might, for instance, be an example of a negative K-meson traveling upward. If it were a K-meson decay, the energy of the μ-meson in the CM system would be about 44 Mev, a value not inconsistent with other observed cases[12-13]. On the other

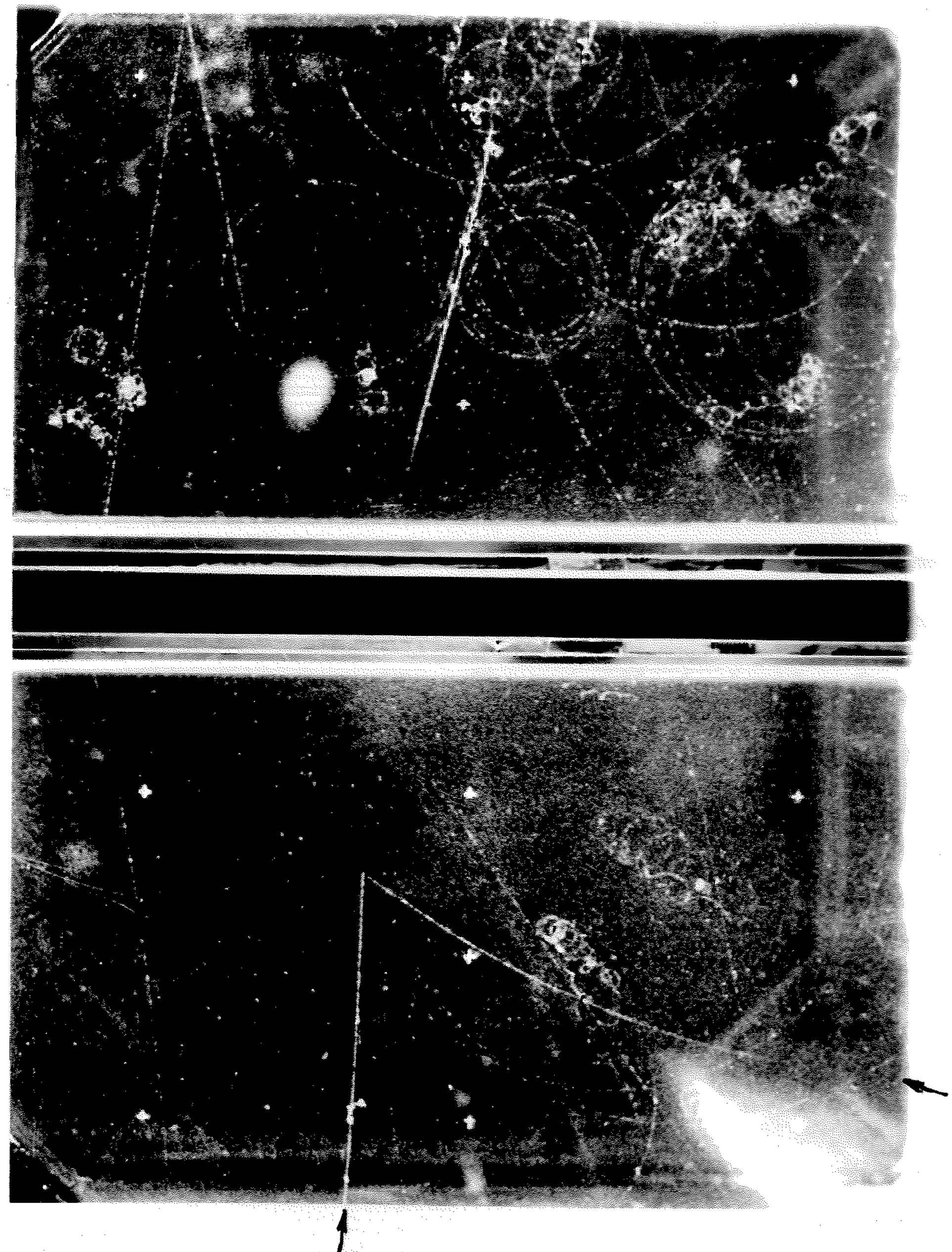

Fig. 23. (Case #25686) A probable neutral V-particle decay that has a very low Q-value. In addition, the negative secondary particle (right) is apparently a μ -meson.

hand, the direct mass measurement of the associated positive particle would seem to indicate a mass somewhat heavier than that of the κ-meson.

(3) Protons: From the mass distribution of figure 18 it is apparent that the positive secondary particles were predominately protons. The positive particle associated with the decay shown in figure 23 is one of the many individual examples that tend to confirm this conclusion. Fortunately, the momentum of this particle, 375 ± 100 Mev/c, is in that range wherein the mass measurements of heavy particles are most reliable; for smaller momenta, the specific ionizations become too large to estimate accurately, and for larger momenta, the uncertainties associated with these momenta become excessive. The specific ionization for this case was estimated to be 4-8 times minimum, resulting in a measured mass of 1600-2400 m_e.

(4) τ- and κ-mesons*: As was previously noted, the mass distribution of figure 18 seems to indicate the existence of positive particles of lighter-than-protonic mass, possibly τ- or κ-mesons. There is, of course, no particular reason why such secondary particles, if they do exist, should not be negatively as well as positively charged. In this connection, it is interesting that one such case of a neutral V-decay has been observed. This is the single case comprising group 2a of Table II; it is shown in figure 22. The momentum of the negative secondary particle is 210 ± 40 Mev/c and its specific ionization is estimated to be 2 - 4 times minimum. This would indicate that its mass lies in the range 450 - 1000 m_e. Thus, even if one allows for

---

* The general properties of τ- and κ-mesons are discussed in Appendix III.

extreme errors in the determination of both the curvature and the ionization, it is extremely difficult to interpret this particle as either a π-meson or a proton (which would in any case be a negative proton). In addition to this case, a few examples of slow heavy positive secondary particles were found whose measured masses seemed to lie in the range 600 - 1200 m_e. A few cases were also found whose upper mass limits were sufficiently low to exclude protons, and whose accompanying particles were apparently π-mesons. However, none of these was of sufficiently high quality to yield a reliable mass determination.

Decay-Schemes

(1) Protons and Negative π-mesons: By now it has become quite apparent that the neutral V-decays observed in these experiments were predominately of the type whose charged decay-products were positive protons and negative π-mesons. In fact, the information presented in figure 17 (α-plots), in Table II (classification of secondaries according to mass limits), and in figure 18 (mass distribution), would indicate that perhaps more than 85 percent of all decays were of this type.

(2) Positive π-mesons and Negative π-mesons: A decay scheme has been postulated by the Manchester workers[7] in which the charged decay-products were both π-mesons. It will be of interest to examine the data presented in the preceding paragraphs with regard to this decay scheme.

As was mentioned earlier, the α-plots of figure 17, and particularly the asymmetry in the plot of group I which represents an unbiased selection criterion, strongly suggest that more than one decay process is here involved. Assuming that two decay processes are represented and that they are decays into two π-mesons and into a proton and a π-meson, respectively, it is possible to place an upper limit upon the percentage of the cases which could be of the two π-meson variety. For these cases the α-plots would be expected to be symmetrical about α equal to zero, and thus if one takes all of the negative values of α (some of which are definitely known to correspond to a decay into a heavy and a light particle) and a corresponding number of positive values of α as representing this decay process, one obtains only about 20 percent which could possibly be of this type.

The question naturally arises as to what direct evidence exists for such a decay into two mesons. The two cases in group 1a of Table II seem to be of this variety. The first of these cases, however, may not be a neutral V-decay at all. The apex of the decay, while in the gas of the cloud chamber, was just outside the visible region, so that it may actually represent a chance coincidence of two unrelated tracks. In addition, the momentum and ionization of the positive particle restrict its mass to be less than 700 - 800 m_e, and thus a π-meson is not necessarily indicated. The second case is almost certainly a neutral V-decay. In this case, the momentum of the positive particle was about 295 Mev/c and its ionization was less than 1.5 times minimum, and thus its mass was less than about 500 m_e. The track of the negative particle, however, was so short that its curvature could not be measured. The momentum of this particle was evaluated from transverse momentum balance with respect to an assumed line of flight from a clearly defined nearby origin, a method of analysis that is subject to some question. In addition to these two cases, the single case in group 2a of Table II, which has previously been considered in connection with figure 22, may possibly be of the variety that decays into two π-mesons. However, the mass limits on the negative decay-product, 450 - 1000 m_e, indicate that it is extremely doubtful if this particle is a π-meson.

In view of these data, one concludes that there is little direct evidence that indicates the existance of a decay into equal particles, but that a few decays (groups 1a and 3a, 4 or 5 of group 1c and possibly group 2a) might be so interpreted. In any case not over about 10 percent of the decays could possibly be of this type.

(3) Anomalies: There is sufficient evidence that indicates the existence of a μ-meson secondary particle, that such a decay must be considered. In Table III, the characteristics of the five cases which seemed to involve negative μ-mesons were listed. It is to be noted that four of the associated positive secondaries were heavy particles, presumably protons, but possibly τ- or K-mesons. In the remaining decay, the mass of the positive particle was indeterminate. Thus if μ-mesons are really present, they are most probably associated with heavy positive particles and would not, therefore, explain the shape of the α-plots, unless heavy negative particles are postulated.

The single case in group 2a has already received considerable attention, but it is recalled once more since it definitely indicates a neutral V-decay in which a light positive and a heavy negative particle are produced. If such a decay were really a decay into a μ-meson and a τ- or K-meson, with the signs arbitrarily distributed, then there is additional evidence for this decay. For then the μ-mesons, the positive particles of lighter-than-protonic mass, the shape of the mass distribution of the positive particles, the existence of a number of heavy negative particles and the shape of the α-plots could, possibly, all be explained.

C. Nature of Decay-Products--Neutral Secondaries

A careful analysis of the 134 pictures in which neutral V-particles were observed, has failed to yield any direct evidence indicating the existence of neutral secondary particles. As a result, the present discussion of the possible existence of such neutral particles must necessarily be restricted to statistical considerations.

Coplanarity

It is possible to derive some information concerning the existence of neutral secondary particles by making use of certain purely geometrical properties of the decay. One such property is the so-called "coplanarity" of the decay, i.e., the angular relationship between the line of travel of the V-particle and the "decay-plane" defined by the tracks of its two charged decay products.

To measure the angular deviation from coplanarity for a given decay, one must know the path of the neutral V-particle as well as the paths of its two charged decay products. This information is available in those cases where the event in which the V-particle originated also yielded a number of charged particles whose tracks appear in the chamber. The path of the V-particle is then taken to be along the straight line connecting this origin (located by the backward extrapolation of the charged particle tracks) with the point at which the decay occurred.

In these experiments the numerical data required for calculating the orientations of the decay-plane and the path of the V-particle were obtained from a graphical construction. A sheet of tracing paper was placed on the viewing screen, upon which the two sets of track images from the stereoscopic photographs were projected, and careful pencil traces were then made of the two track-images of the V-particle and of the other particles on the photographs. The construction by which the deviation from coplanarity was then measured is shown schematically in figure 24. In this figure the rectangle represents the boundaries of the visible region of the cloud chamber. The two sets of track images resulting from projection through the left and right lenses are shown dashed and solid, respectively. In the case of V-particle secondaries, tangents to the tracks at the apex of the decay were used instead of the tracks themselves. Auxiliary lines are shown dotted and are numbered in the order of their construction. First, the tracks radiating from the origin of the V-particle are projected backward to their intersection point (O,O'). Next, the path of the neutral V-particle (OD,O'D') is constructed and extended beyond the decay point (D,D'). The problem now consists in determining the angle that this extended line makes with the decay-plane, namely, the plane formed by the two lines (DA,D'A') and (DB,D'B'). To accomplish this, an arbitrarily chosen sloping line (AB,A'B'), lying in the decay-plane is drawn as indicated. (Note how points A' and B' are found by construction lines 4 drawn parallel to DD'.) Upon completion of lines 5 and 6, two points appear which are of particular importance, i.e., a point (C,C') on the extended V-path, and a point (C,E') in the decay-plane. The horizontal distance E'C' on the diagram can readily be converted with the aid of Eq. (1) into a difference in depth of these two points. This in turn is then readily converted into an angle δ between the line (DC,D'E') and the neutral V-path (DC,D'C') and thence to the angle δ_1 between the V-path and the decay-plane. The last step was rarely taken, since δ is always larger than δ_1 and thus provides a sharper test of coplanarity.

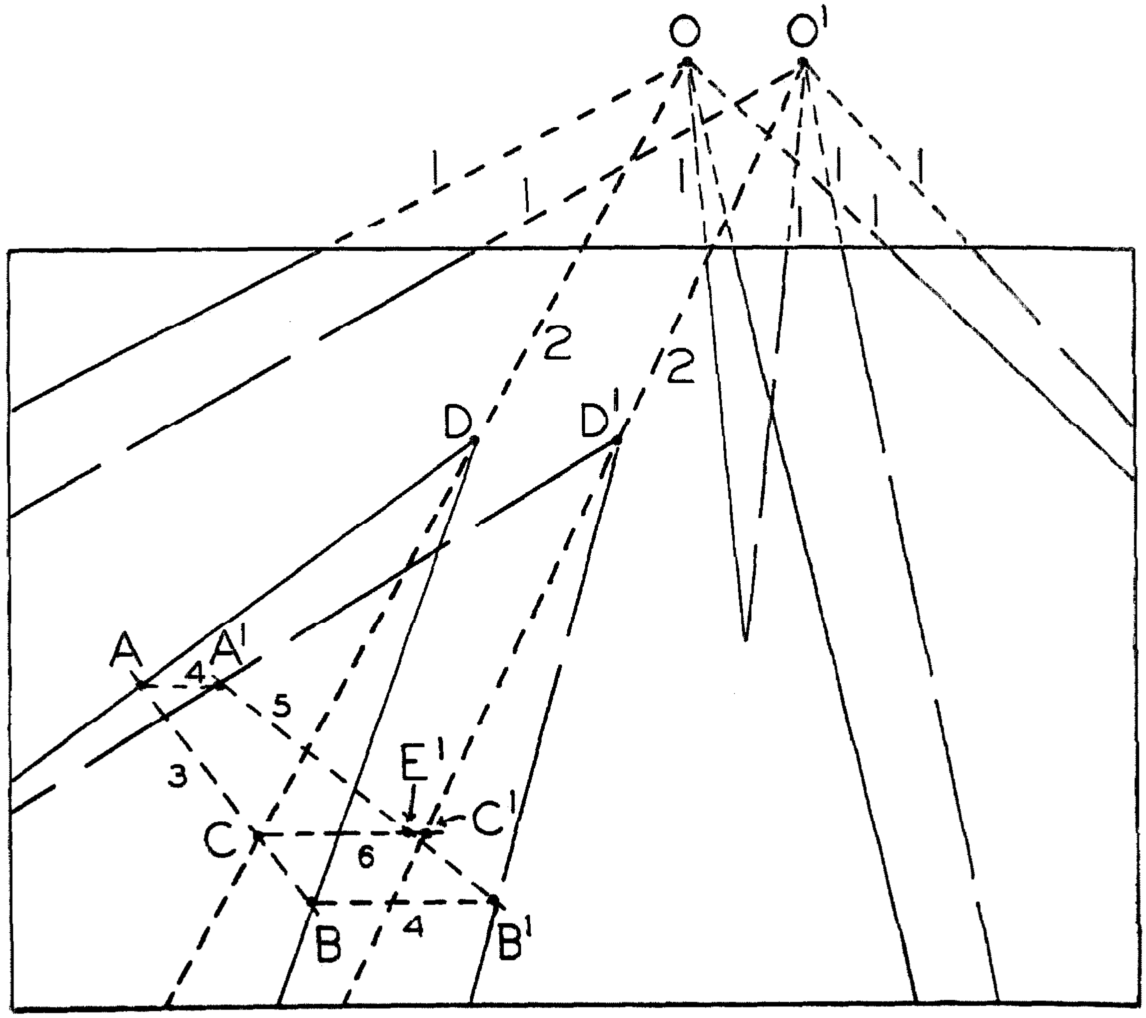

Fig. 24. Schematic diagram of the coplanarity test. The rectangle represents the boundaries of the visible region of the cloud chamber. The two sets of tracks resulting from projection through the left and right lenses are shown dashed and solid, respectively. If the extended neutral V-path (DC, D'C') lay in the decay-plane (ADB, A'D'B'), the two points E' and C' would coincide.

The accuracy with which it is possible to carry out the above construction varies from case to case for several reasons: The accuracy with which an origin can be located depends upon the number of tracks available for the backward extrapolation, and the distance of the extrapolation (sometimes as great as 20 cm); the angular accuracy with which the V-path can be drawn depends upon the distance from the V-particle decay-point to the origin; the angular accuracy with which tangents to the decay-tracks can be drawn depends upon the length of the tracks; and the sensitivity of the coplanarity test depends upon the orientation of the neutral V-decay, it being most sensitive when the decay-plane is seen edgwise in one camera view. The overall accuracy with which the coplanarity could be measured thus varied from about 1° to about 10°, but was usually in the range 2° - 4°.

Sixty of the 134 neutral V-decays exhibited origins and thus could be analyzed for coplanarity. Of these, 37 had origins in the lead plate between the chambers, and the remaining 23 had origins in the lead blocks above the chambers. The distribution of δ for these 60 cases is shown in figure 25. The cross-hatched portion of the diagram represents the 28 most accurate cases obtained by eliminating all those whose estimated error of measurement is greater than 2°. It appears from this distribution that almost all of the decays could have been exactly coplanar, and hence could have been two-body decays.

Perhaps a more meaningful test of coplanarity is a comparison of the measured deviation δ with the smaller of the two angles, θ_+ or θ_-, between the charged particle tracks and the neutral V-path, since in any case δ cannot exceed the smaller of these angles. The ratio $\sin\delta\ /\sin\theta_s$ (where θ_s denotes the smaller of the two angles) is a

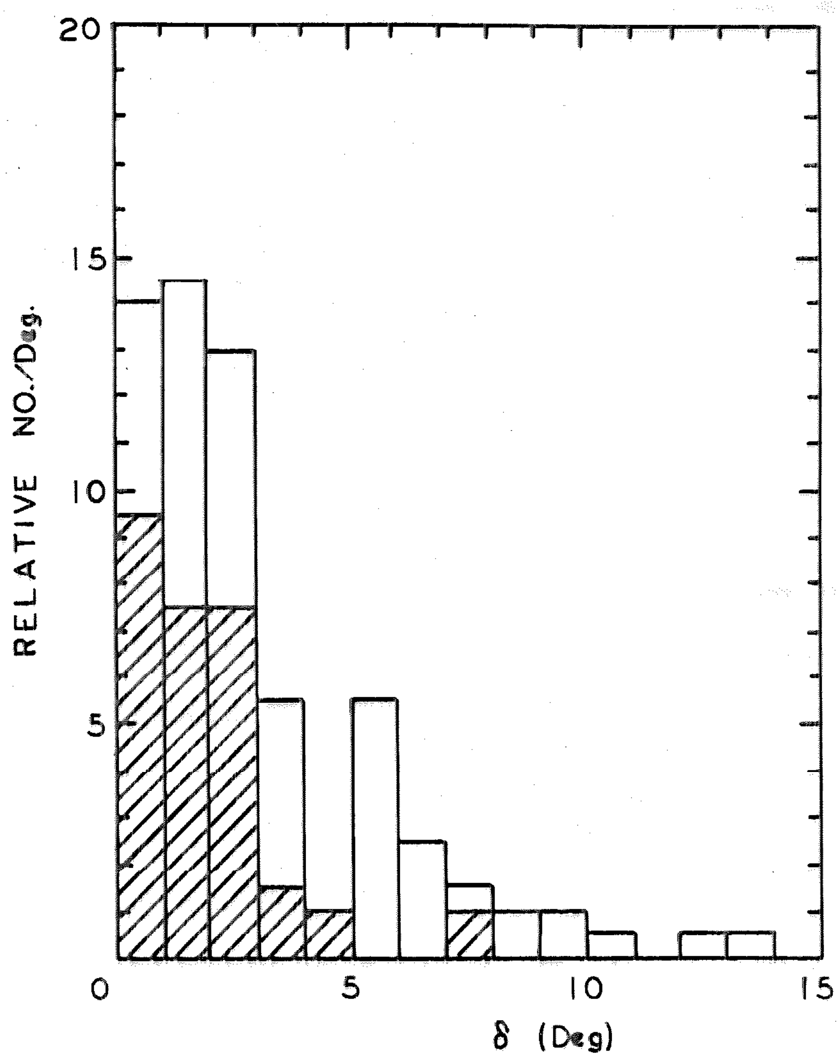

Fig. 25. Distribution of angular deviation δ from coplanarity for 60 cases. The cross-hatched portion of the distribution represents the contribution of the 28 cases whose estimated errors of measurement were 2° or less.

quantity which compares approximately the component, perpendicular to the decay-plane, of the momentum of the neutral V-particle, with the component, perpendicular to the neutral V-path, of the momentum of one of the charged particles. The distribution of sin δ/sin θ_s is shown in figure 26. Again almost all of the decays could have been coplanar, and hence could have been two-body decays. However, we cannot rule out any type of decay in which the transverse momentum carried by a third decay particle is on the average less than about 50 percent of that carried by one of the charged particles.

Momentum Balance

Some additional evidence as to the number of particles resulting from the decay of a neutral V-particle can be obtained by testing the balance of the components of momentum transverse to the neutral V-path in those cases where θ_+ and θ_- and also P_+ and P_- are known independently. The difference $\Delta P_T = |P_+ \sin \theta_+ - P_- \sin \theta_-|$ is a measure of this balance, and should have the value zero, if momentum transverse to the direction of the V-particle is conserved. The distribution of this quantity is shown in figure 27. It is apparent that almost all of the decays could have satisfied the condition of momentum balance, but, as in the discussion of coplanarity, one cannot exclude certain types of multi-body decay in which the transverse momentum of an unseen particle is small on the average compared to the transverse momenta of the visible particles. The restriction that can be placed upon this "missing" transverse momentum is about the same as in the case of the coplanarity test--namely that it be less than about 50 percent of the transverse momentum of the visible particles. This conclusion follows as a result of a comparison of the distribution of the transverse momentum of the

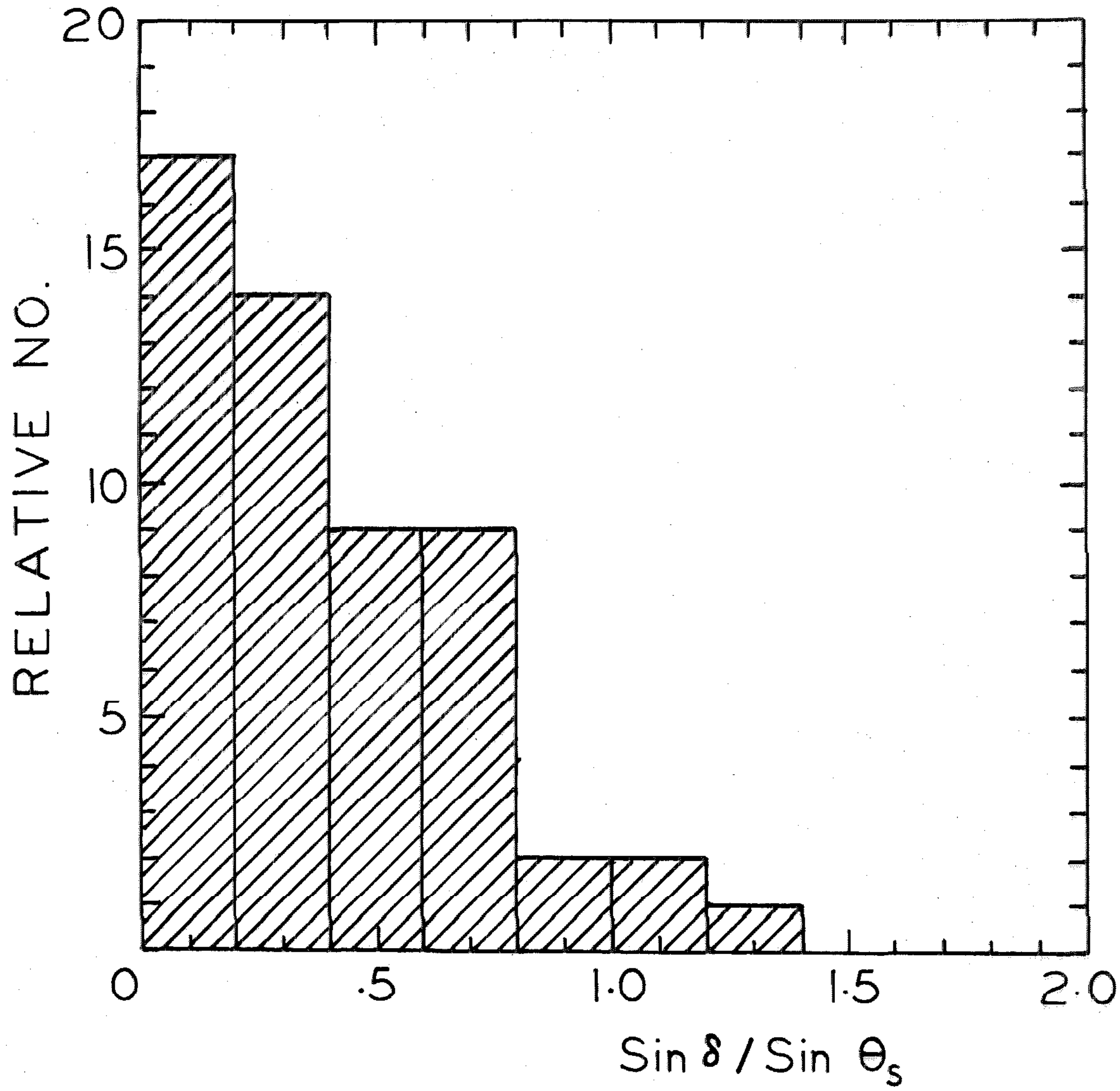

Fig. 26. The distribution of sin δ/sin θ_s for 54 cases. The entire width of this distribution could have been due to errors of measurement or to scattering of the V-particle before decay.

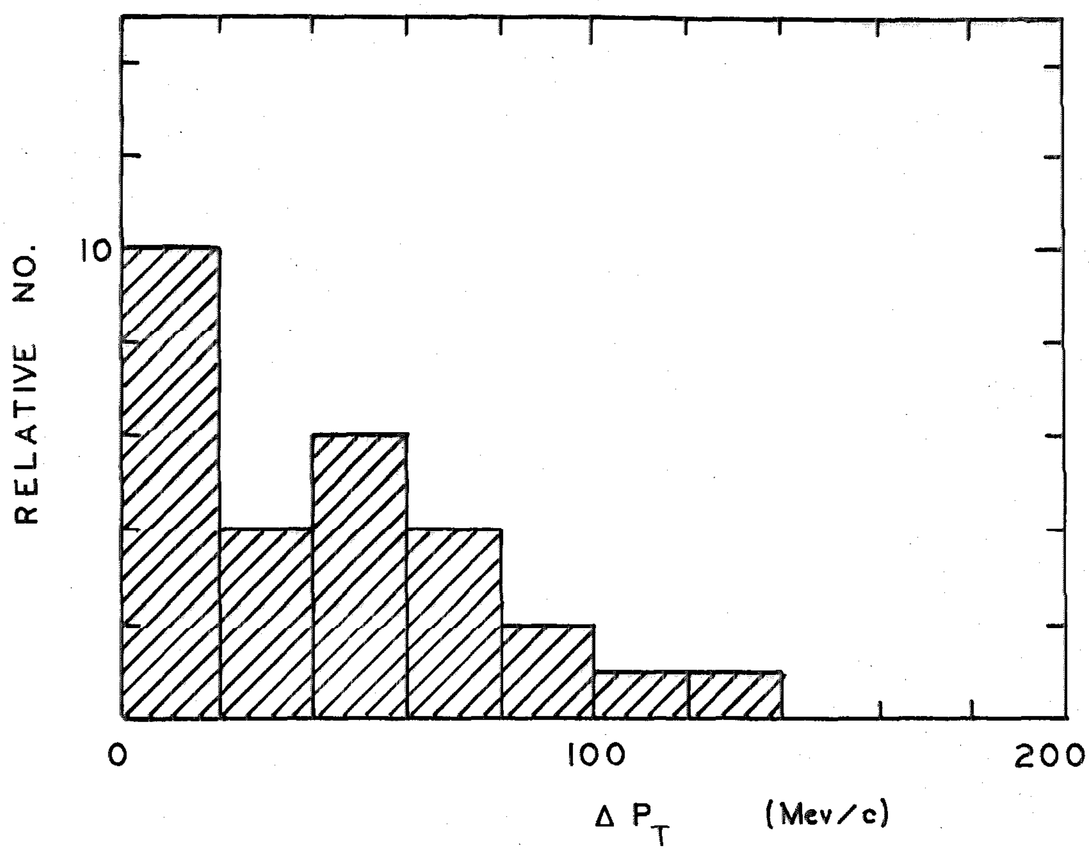

Fig. 27. The distribution of $\Delta P_T = |P_+ \sin \theta_+ - P_- \sin \theta_-|$ for 28 cases. This quantity represents the "missing" transverse momentum in the plane of the decay.

negative particles, $P_- \sin \theta_-$, as given in figure 28, with the distribution previously presented in figure 27.

Conclusions

The present experiments have thus far provided no information that would indicate the existence of neutral secondary particles in the decay of the neutral V-particle. However, it will be recalled that earlier in this paper, in the discussion on the nature of the charged secondary particles, several different neutral V-particles, or at least several different modes of decay of a unique V-particle, were indicated. It was estimated at that time that at least 85 percent of the cases seemed to be of a common type which apparently yielded a π-meson and a proton as charged secondary particles. In view of this fact, and in view of the statistical nature of the evidence presented in the prededing paragraphs, any conclusions drawn at this time should probably be restricted to this predominant mode of decay.

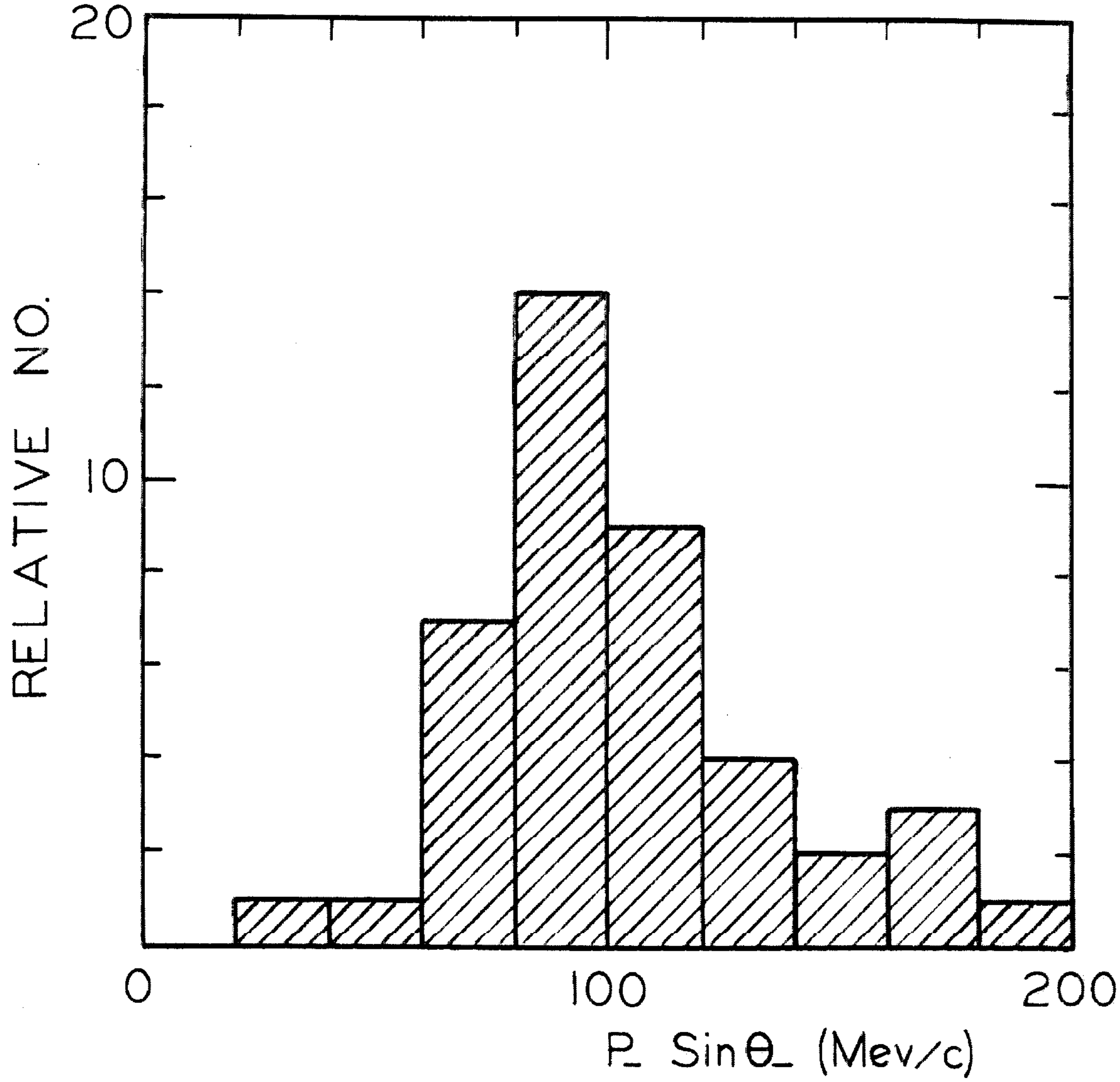

Fig. 28. The distribution of P_- sin θ_- for 42 cases. This quantity is equal to the transverse momentum P' sin θ' if the decay is a two-body decay. The sharp peak in this distribution falls at about 95 Mev/c, the limiting value to be expected for a two-body decay into a proton and a π-meson with an energy release of 35 Mev. The presence of transverse momenta substantially greater than this limiting value strongly suggests the presence either of two-body decays, or of multibody decays, with energy releases greater than 35 Mev.

D. Energy Release

The results of the previous section indicate that the great majority of the observed cases of neutral V-particles are consistent with two-body decay schemes. Therefore, this section will be developed under the assumption that all of the observed cases are two-body decays.

α-distribution

It will be recalled that the discussion of α-values was also based upon the assumption of a two-body decay, and it is interesting to note that one can estimate an energy release, or Q-value, from the half-width of the α-distribution peak as given in figure 17. This follows if one notes that from Eqs. (5) and (7), one can obtain

$$\text{half-width} = \frac{2P'}{M_o \beta} \qquad (9)$$

and

$$Q \approx (P')^2 M_o / 2M_+ M_- \qquad (10)$$

if one assumes that $Q \ll M_+ + M_-$. Now assuming a decay into a proton and a π-meson as suggested by the study of the charged secondary particles, and taking $\beta = 1$, $M_o = M_p + M_\pi + Q \approx M_p + M_\pi$, and the half-width of the α-distribution peak equal to 0.15, one obtains

$$Q \approx 26 \text{ Mev.}$$

It will be noted later in this section that this value agrees surprisingly well with the actual measurements of the energy release.

Q-Values

The energy release, or Q-value, of the two-body decay of a neutral V-particle can be determined from the momenta of the two decay-particles and the included angle between their paths, if the masses of the decay-particles are known. In the two-body decay described by figure 16, we have, in the laboratory system,

$$E_0 = E_+ + E_- = (P_+^2 + M_+^2)^{\frac{1}{2}} + (P_-^2 + M_-^2)^{\frac{1}{2}}$$

and

$$P_0^2 = P_+^2 + P_-^2 + 2P_+P_- \cos\theta_T$$

so that

$$\begin{aligned} M_0^2 = E_0^2 - P_0^2 &= M_+^2 + M_-^2 + 2E_+E_- - 2P_+P_- \cos\theta_T \\ &= (M_+ + M_-)^2 + 2E_+E_- - 2M_+M_- - 2P_+P_- \cos\theta_T \;; \end{aligned} \tag{11}$$

we therefore have for the energy release that

$$\begin{aligned} Q &= M_0 - (M_+ + M_-) \\ &= (M_+ + M_-)\left[\left(1 + \frac{2\,Q_1}{M_+ + M_-}\right)^{\frac{1}{2}} - 1\right] \\ &= Q_1 - \frac{Q_1^2}{2\,(M_+ + M_-)} + \cdots\cdots \end{aligned} \tag{12}$$

where

$$Q_1 = \frac{E_+E_- - M_+M_- - P_+P_- \cos\theta_T}{M_+ + M_-} = \frac{M_+T_- + E_-T_+ - P_+P_- \cos\theta_T}{M_+ + M_-}\;, \tag{13}$$

and E_+, T_+ and E_-, T_- are the total and kinetic energies, respectively, of the product particles in the laboratory system, the remaining quantities having the same significance as in Eq. (4)-(8). The quantity Q_1 was introduced in order to simplify the computation of Q; it will be noted that $Q \approx Q_1$ for small values of Q.

Of the decays for which sufficient data were available to permit the calculation of a Q-value, 38 clearly yielded a light negative and a heavy positive particle; these constituted practically the entirety of group 1b of Table II. It will be recalled that the previous study of the identities of these particles strongly indicated that they were π- mesons and protons, and thus a Q-value was calculated for each of these cases assuming a two-body decay yielding a negative π-meson and a proton. The Q-values so obtained ranged from 10±3 Mev to 87±15 Mev, and were distributed within this range as indicated by the cross-hatched portion of the histogram of figure 29.

In addition to these 38 decays, there were another 25 cases in which there was no evidence against the assumption of decay into π-mesons and protons, and in which the α-values, in being greater than +0.5, actually gave some support for this assumption; these 25 decays constitute practically the entirety of group 1c of Table II. Q-values were calculated for these decays assuming two-body decay into a π-meson and a proton. The Q-values so obtained ranged from 10± 5 Mev to 97±30 Mev, and were distributed within this range as indicated by the unshaded portion of the histogram of figure 29.

The histogram of figure 29 was constructed by counting the number of Q-values within each 5 Mev range, without regard to the errors involved in the individual measurements. This histogram strongly suggests the existence of at least two Q-values, one at about 35±3 Mev, another at about 75±5 Mev, and possibly a third near 45 Mev, although a continuous distribution with or without one or more discrete values would also be consistent with the observed distribution. Armenteros et al[7] obtained Q-values for twelve cases which were distributed in excellent agreement with the above histogram. These authors concluded, however, that their data indicated a single Q-value at 46±6 Mev. In order to determine whether the present results will support such a conclusion, it is necessary to investigate the errors involved in the Q-value determination.

The accuracy with which the Q-value may be determined from the measured momenta and the angle depends upon the accuracy with which

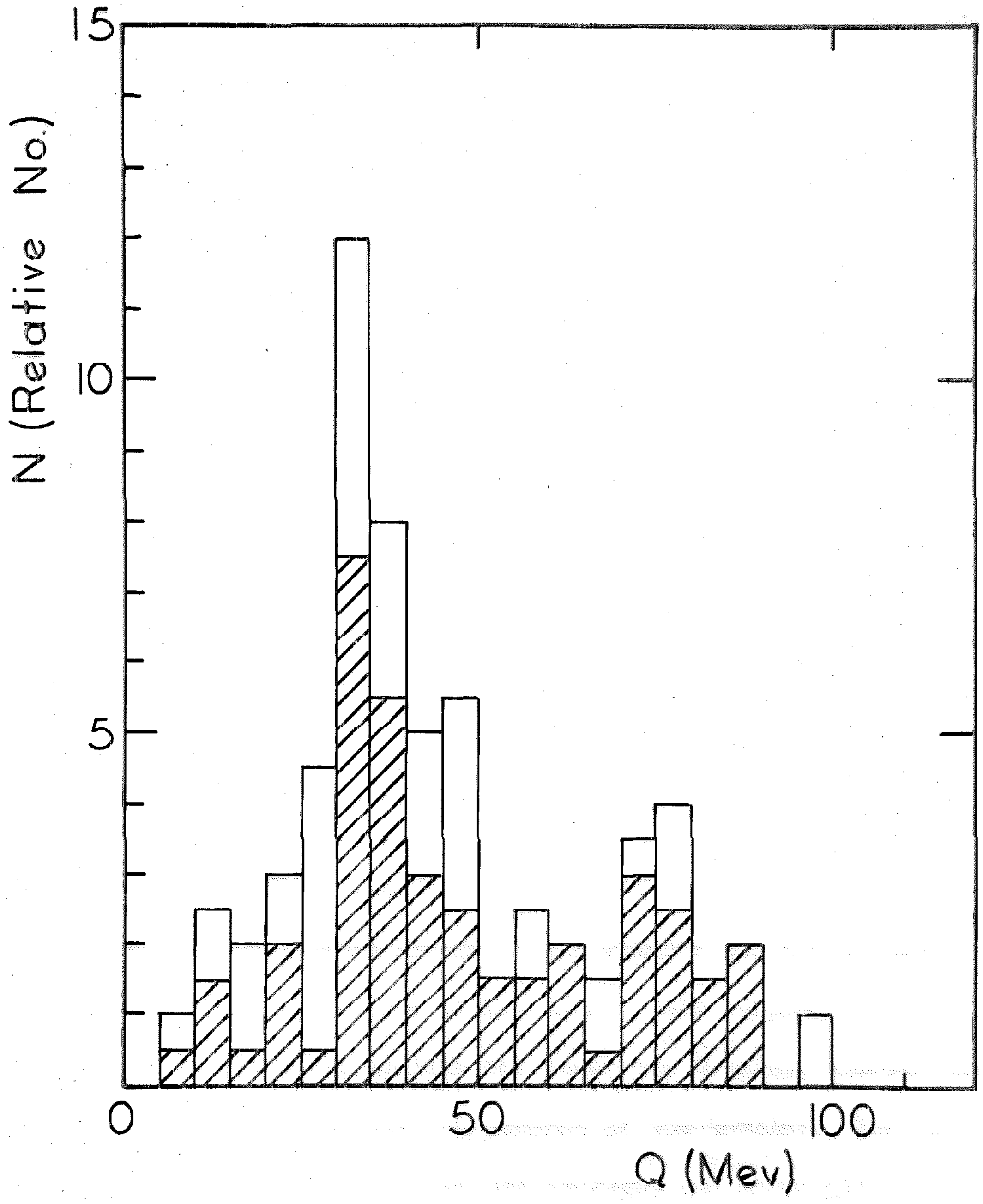

Fig. 29. The distribution of measured Q-values for 63 cases in which the decay into a proton and a π-meson was indicated. The cross-hatched portion of this histogram represents those cases in which the positive particle was surely much heavier than a π-meson.

these three quantities are known. The error in Q-value is often much more sensitive to the error in a certain one of the quantities, usually the momentum of the lighter particle, than to errors in the other quantities. This can be seen by evaluating the derivatives

$$\text{a)} \quad \frac{\partial Q}{\partial P_+} = \left(\frac{E_- P_+}{E_+} - P_- \cos \theta_T \right) / (M_+ + M_- + Q)$$

$$\text{b)} \quad \frac{\partial Q}{\partial P_-} = \left(\frac{E_+ P_-}{E_-} - P_+ \cos \theta_T \right) / (M_+ + M_- + Q) \qquad (14)$$

$$\text{c)} \quad \frac{\partial Q}{\partial \theta_T} = (P_+ P_- \sin \theta_T) / 57.3 \ (M_+ + M_- + Q) (\text{Mev.deg}^{-1})$$

The numerical values that were commonly found for these derivatives were, for the π-meson and proton decay,

$$\text{a)} \quad \frac{\partial Q}{\partial P_+} = -0.1 \text{ to } +0.2 \text{ (usually about } +0.07)$$

$$\text{b)} \quad \frac{\partial Q}{\partial P_-} = 0.3 \text{ to } 1.0 \text{ (usually about } 0.6)$$

$$\text{c)} \quad \frac{\partial Q}{\partial \theta_T} = 0.5 \text{ to } 3.0 \text{ Mev/deg (usually about } 1.5)$$

To each Q-value an uncertainty was assigned whose magnitude was derived from the estimated errors in the momenta and the included angle, using the partial derivatives of Eq. 14 for this purpose. The absolute uncertainty tended to be smaller the lower the Q-value, whereas the percentage error was roughly independent of the Q-value. The estimated errors were about ± 30 percent on the average, and about ± 15 percent in several of the best cases. Thus the average estimated uncertainty in the Q-value might be large enough to permit an interpretation in terms of a single Q-value at 46 ± 6 Mev. However, if this were the case one would expect that the distribution would, within reasonable statistical fluctuation, shown a maximum near 46 Mev; also, those Q-values having small estimated uncertainties should be distributed more closely about this value than are those of large estimated uncertainty so that the few best cases should give Q-values very close to 46 Mev. That this is not the case will be demonstrated in the following paragraph wherein individual cases are treated.

Individual Cases

Although the 38 cases represented by the shaded portion of the histogram of figure 29 were cases for which a light negative and a heavy positive secondary particle were observed, all of these secondary particles were not necessarily consistent with the assumption of a decay into a π-meson and a proton. In three of these decays the lighter particle seemed too light to be a π-meson, and in five other decays the heavier particle seemed too light to be a proton. Q-values were, therefore, recalculated for these eight decays assuming in the first three cases a two-body decay yielding a μ-meson and a proton, and in the latter five cases a two-body decay yielding a π-meson, and a τ-meson of mass 975 m_e or a κ-meson of mass 1250 m_e. These alternative Q-values were approximately equal to the Q-values calculated for π-meson and proton decay, and were spread over a comparable range. In view of the small number of these "anomalous" cases and the large inherent errors in an individual mass measurement, particularly in the case of a massive positive particle, these cases, calculated for the π-meson and proton decay, were included in the histogram along with the other cases.

An additional seven decays, not included in figure 29, were observed that seemed to exhibit properties which would preclude an interpretation in terms of a decay into a negative π-meson and a proton. These decays were those of groups 1a, 2a and 3a of Table II.

Q-values were calculated for various possible two-body decay schemes chosen to fit the observed properties of each individual case, with the following results:

1) Three of the decays, which could have yielded a positive and a negative π-meson, gave Q-values of about 110 Mev for this decay scheme.

2) Two of the above three decays might alternatively have yielded a negative π-meson and a positive τ- or κ-meson. One of the other decays seemed to yield a positive π-meson and a negative τ- or κ-meson. These three decays interpreted in terms of a decay into a π-meson and a τ-meson, all gave Q-values of about 60 Mev.

3) The remaining three decays were of much poorer quality and could be interpreted in terms of either of the above decay schemes, but the Q-values did not seem to agree with those indicated above or with one another.

It is clear that more of these "anomalous" decays will be required before any definite conclusions can be drawn.

Consideration will now be given to the best individual cases of neutral V-particle decay that were observed and analyzed during the present study. These cases are shown in figures 12 and 23, and in figures 30-35; the results of the analysis of these cases, based upon the assumption of two-body decay into π-mesons and protons, are shown in Table IV. It is perhaps worthwhile to note that the Q-values of these eight cases would be difficult to reconcile with a single Q-value.

Summary

A complete summary of the statistics associated with the analysis of the 134 observed cases of the decay of neutral V-particles has been included in Appendix I.

TABLE IV

Q-values for eight examples of V^{o} -decay that yield a proton and a meson.

Quantity \ Case No.	25686 (Fig. 23)	14539 (Fig. 30)	31044 (Fig. 31)	31817 (Fig. 32)	19063 (1) (Fig. 12)	30514 (Fig. 33)	19955 (Fig. 34)	28167 (Fig. 35)
P_+ (Mev/c)	375±100	390±50	660±100	72±20	400±50	510±50	500±50	800±150
L_+ (x min.)	4-8	3-4	1.5-3	> 15	3-6	2.5-4	2-4	1.5-2
M_+ (m_e)	1600-2400	1350-1650	1200-2300	> 700	1400-2200	1500-2100	1300-2200	1500-1900
P_- (Mev/c)	67±7	150±10	205±10	125±5	60±5	130±5	300±25	77±7
L_- (x min.)	1.5-3	1-2	< 1.5	1.5-3	3-6	1.5-2.5	< 1.5	3-4
M_- (m_e)	130-230	< 370	< 380	230-430	205-330	240-380	< 550	265-310
θ_+ (deg.)	-	-	8	-	-	14	-	9.5
θ_- (deg.)	-	-	24	-	-	56	-	104.5
θ_T (deg.)	53±1	45±1	32±1	52±1	151±2	70±1	19±1	114±1
$\partial Q/\partial P_+$	.015	-.025	-.027	.061	.10	.043	-.11	.11
$\partial Q/\partial P_-$	.19	.42	.35	.51	.68	.50	.42	.77
$\partial Q/\partial \theta_T$	.29	.65	1.1	.11	.19	.97	.20	.82
Q(Mev)	10±3	33±5	36±5	37±3	41±7	46±4	72±10	79±15

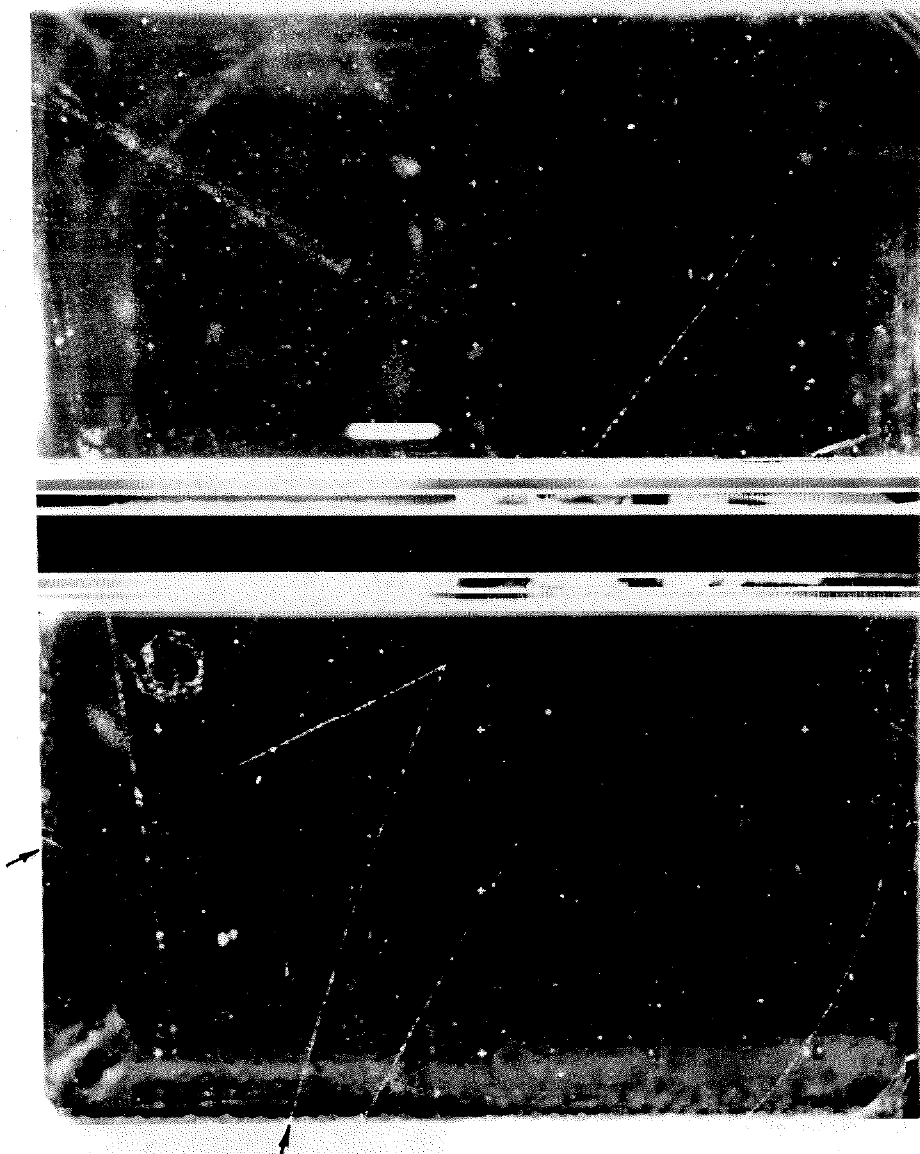

Fig. 30. (Case #14539) One of the eight outstanding neutral V-decays which were observed in this study. Assuming that the positive particle (left) is a proton and that the negative particle is a π-meson, the Q-value for this decay is 33±5 Mev.

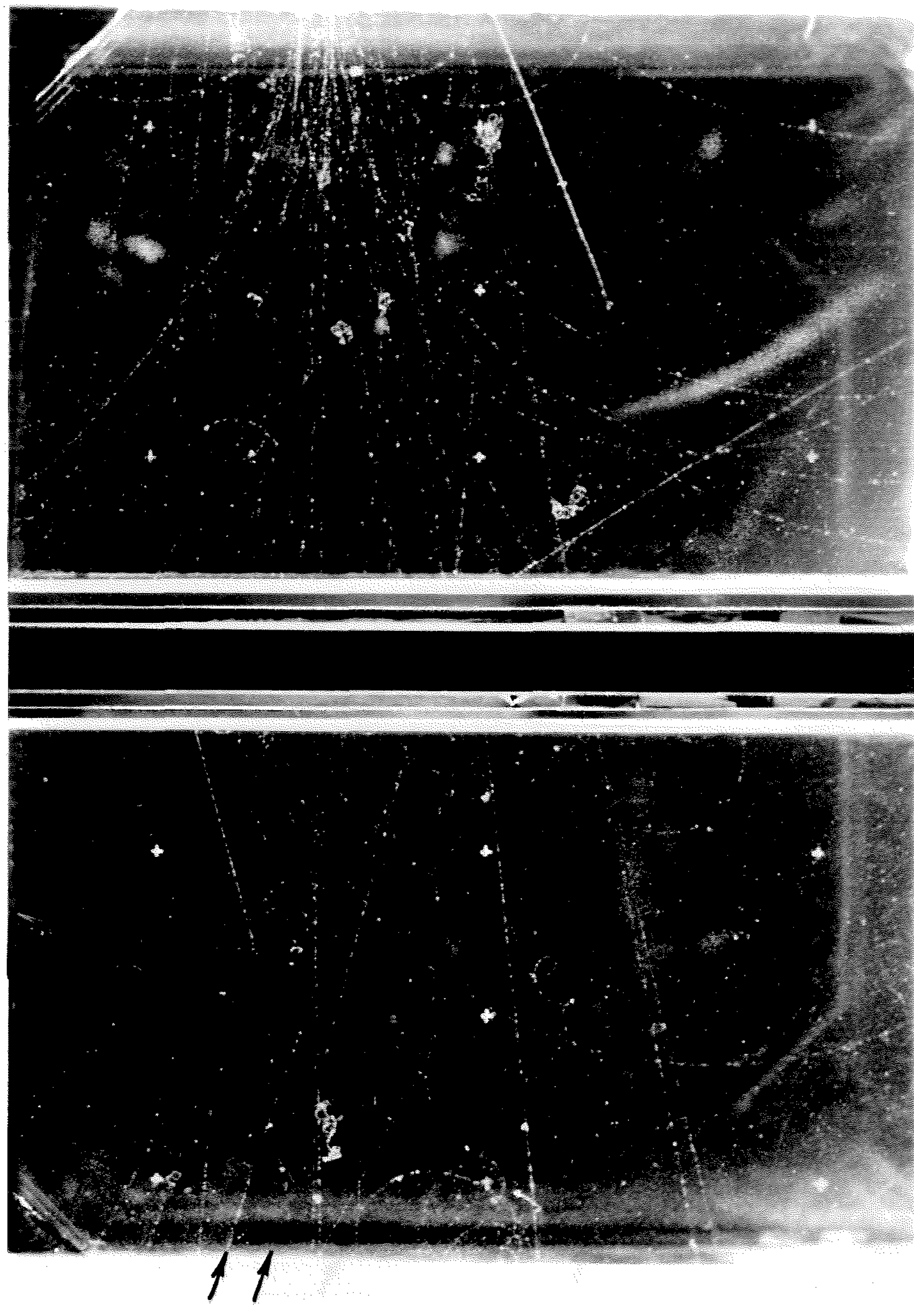

Fig. 31. (Case #31044) One of the eight outstanding neutral V-decays which were observed in this study. Assuming that the positive particle (right) is a proton and that the negative particle is a π-meson, the Q-value for this decay is 36 ± 5 Mev.

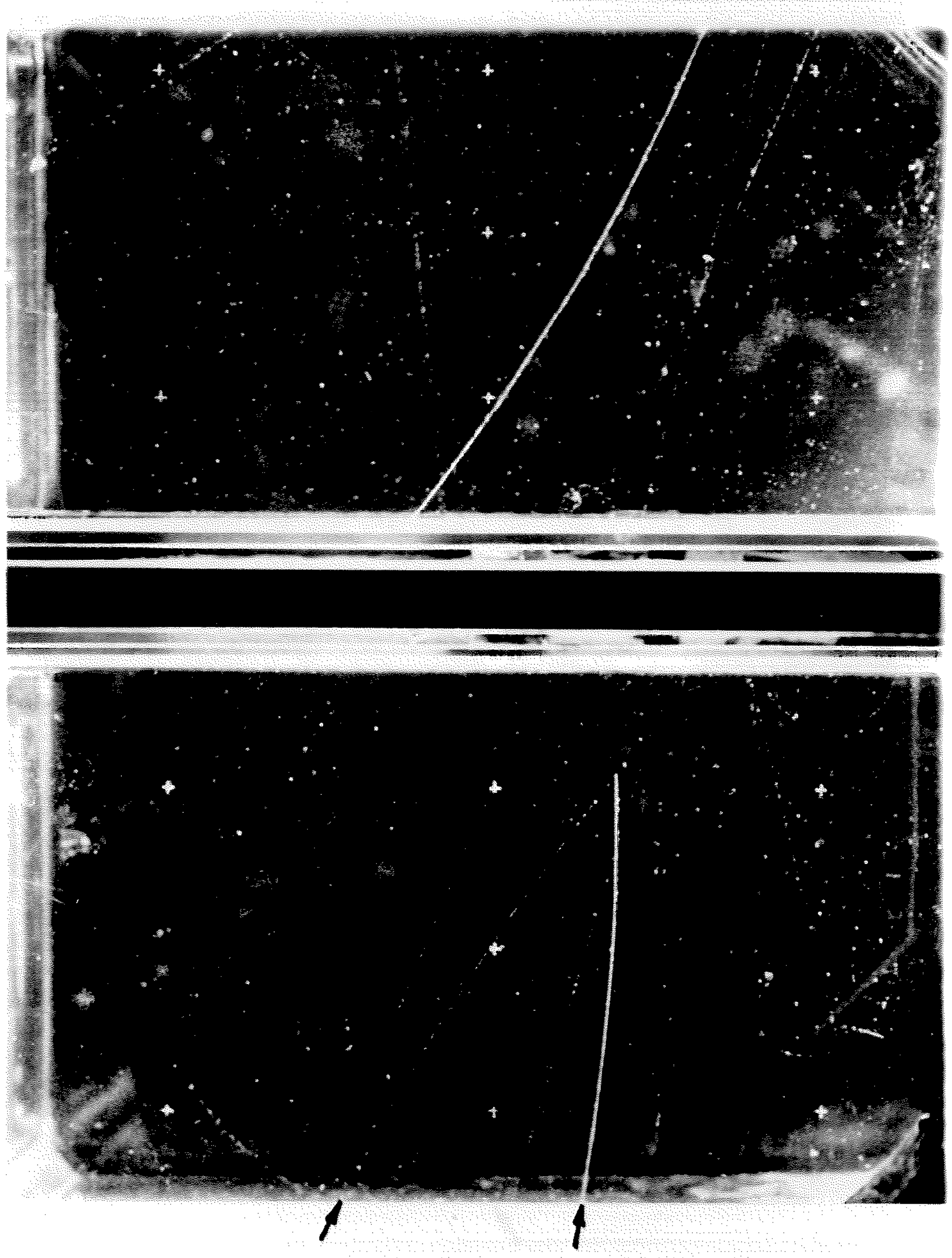

Fig. 32. (Case #31817) The finest example of a neutral V-decay observed in this study. Assuming that the positive particle (right) is a proton and that the negative particle is a π-meson, the Q-value for this decay is 37 ± 3 Mev.

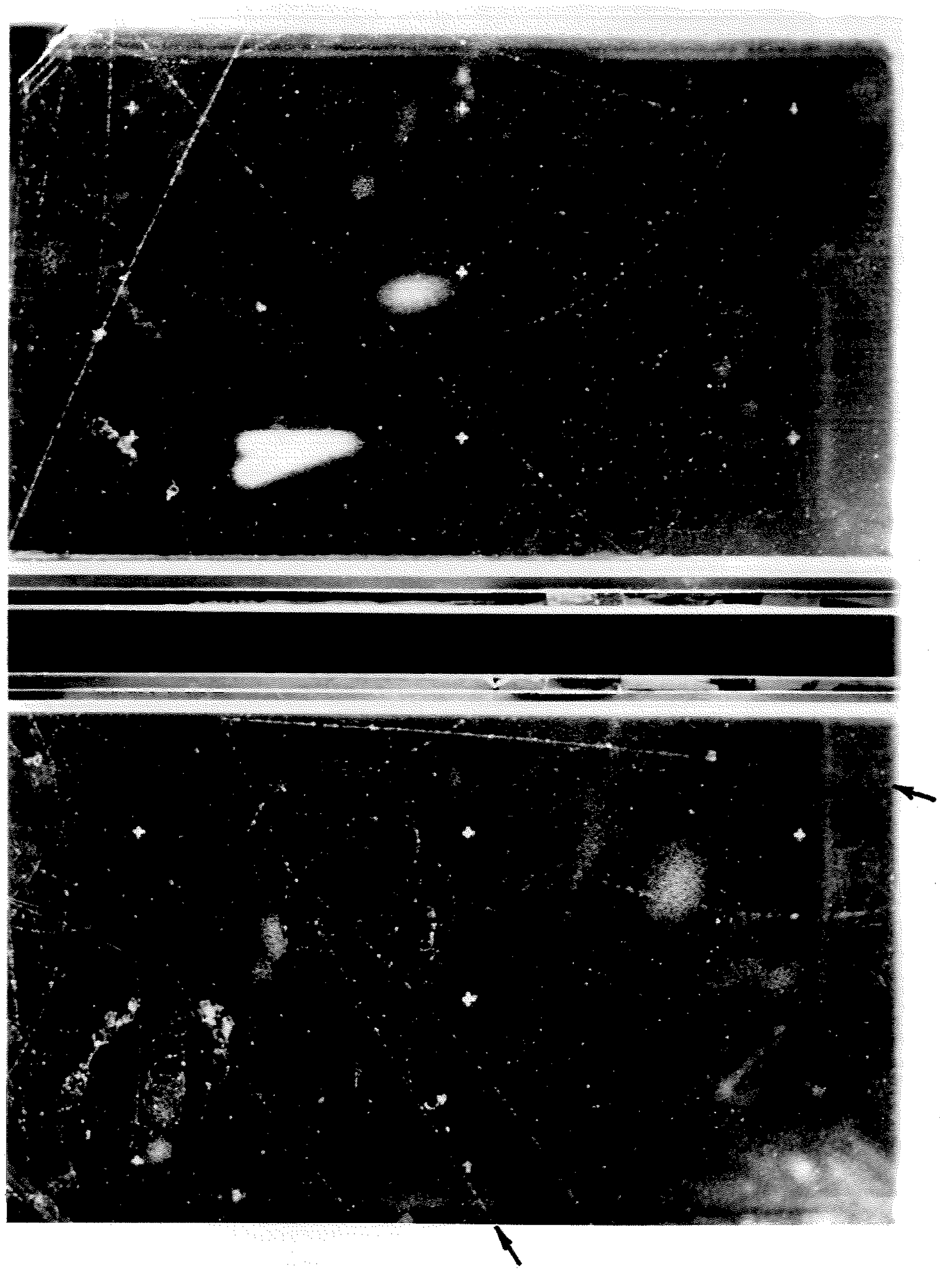

Fig. 33. (Case #30514) One of the eight outstanding neutral V-decays which were observed in this study. Assuming that the positive particle (upper) is a proton and that the negative particle is a π-meson, the Q-value for this decay is 46$\pm$4 Mev.

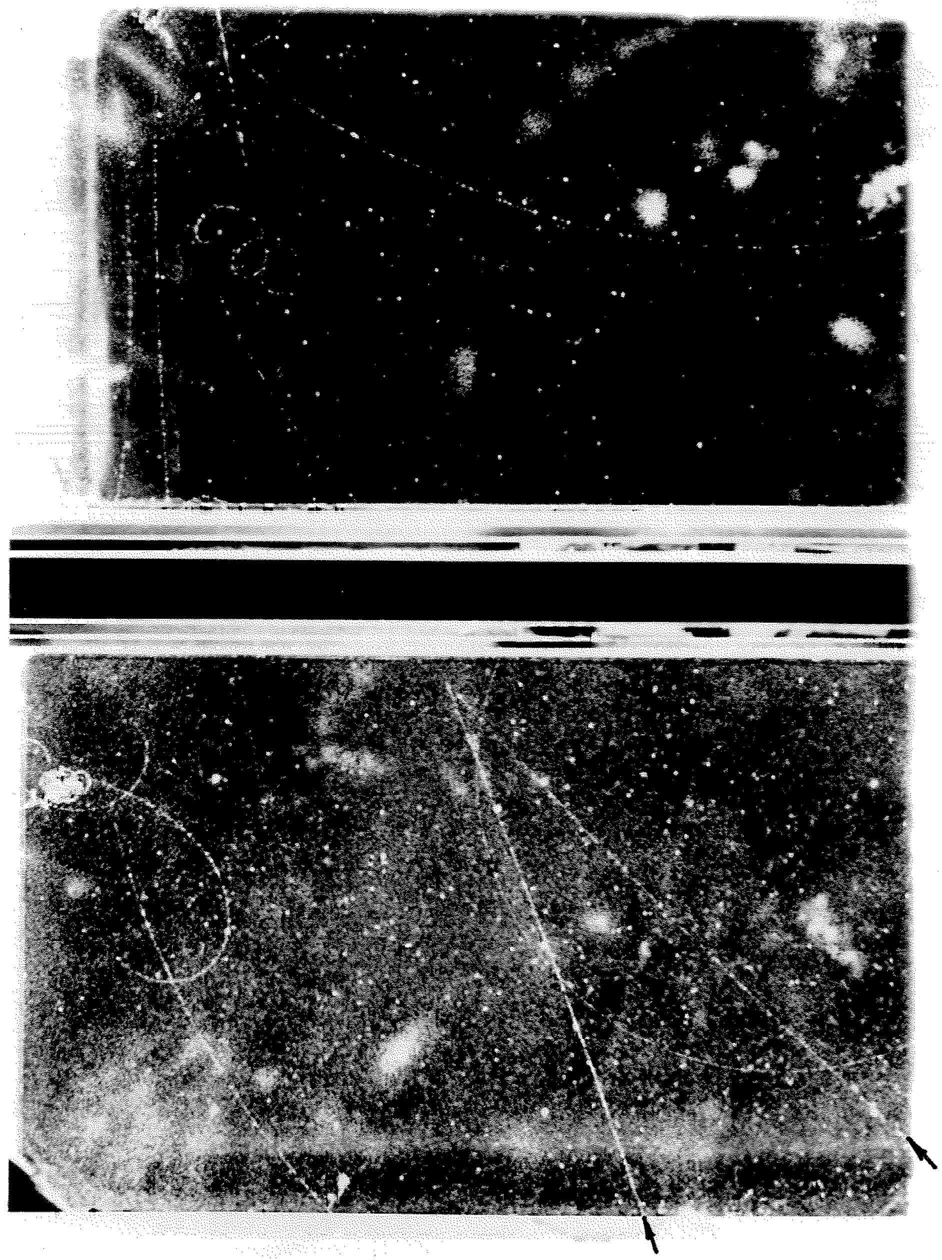

Fig. 34. (Case #19955) One of the eight outstanding neutral V-decays which were observed in this study. Assuming that the positive particle (left) is a proton and that the negative particle is a π-meson, the Q-value for this decay is 72$\pm$10 Mev.

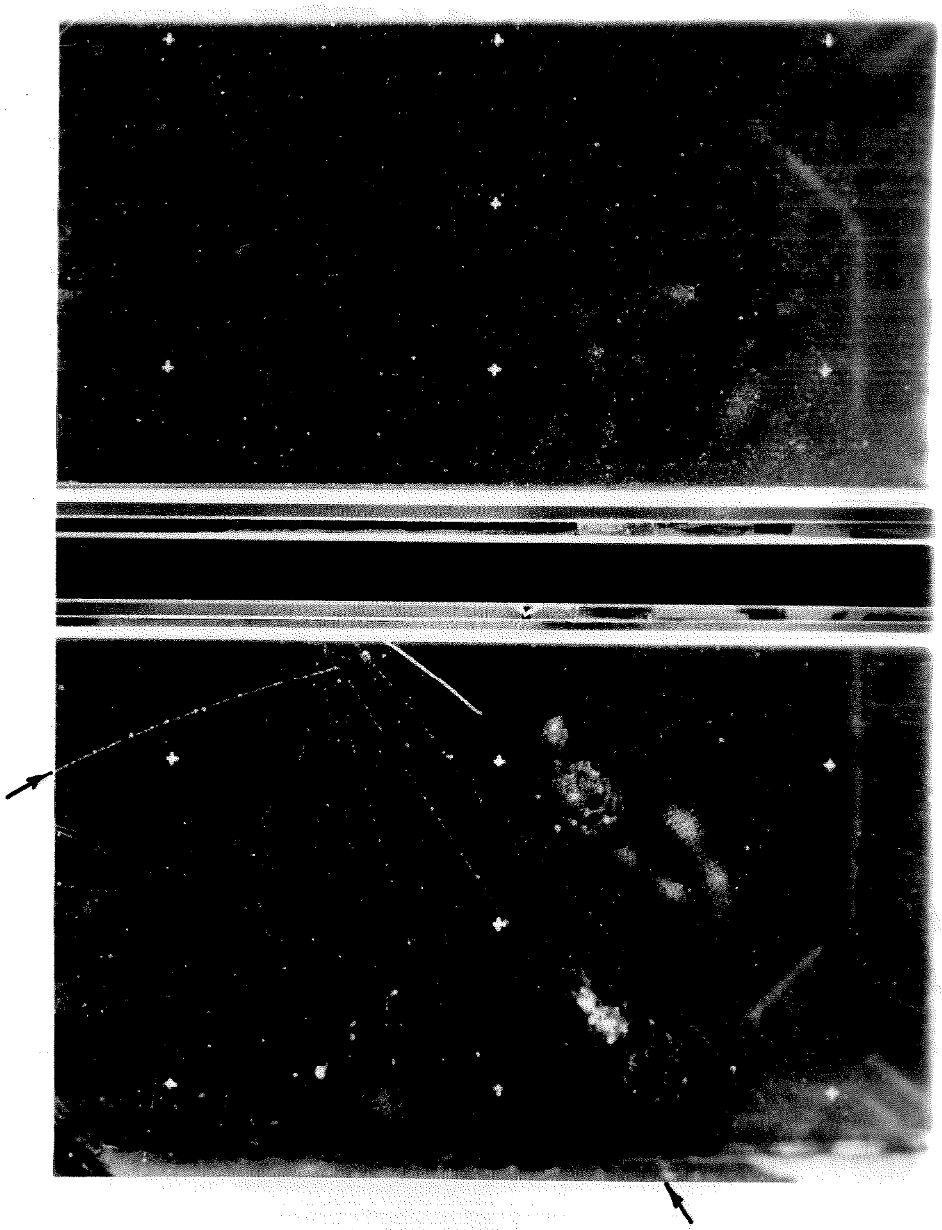

Fig. 35. (Case #28167) One of the eight outstanding neutral V-decays which were observed in this study. Assuming that the positive particle (right) is a proton and that the negative particle is a π-meson, the Q-value for this decay is 79 ± 15 Mev.

E. Discussion

In the preceding sections it was shown that the great majority of the neutral V-particle decays yield a heavy positive and a light negative particle as decay-products. In most instances these events are best interpreted in terms of a two-body decay yielding a proton and a negative π-meson; in fact, perhaps 80 percent of all of the observed decays are consistent with this scheme. The disturbing feature of this interpretation is a lack of agreement with regard to energy release, or Q-value. It is apparent from figure 29 that the measured Q-values are not consistent with a single value. In this regard it is especially interesting to recall the observed properties associated with the eight most outstanding decays obtained in these experiments; these cases are summarized in Table IV and are shown in figures 12 and 23, and in figures 30-35. Without exception these cases are of the type which yields a heavy positive and a light negative particle as decay-products. In almost every case, these particles are best interpreted as protons and π-mesons, respectively, but even in this select group the identification is not completely satisfactory inasmuch as negative μ-mesons and positive K-mesons are suggested as possible decay-products in several of the decays. In addition, in view of the select nature of these eight cases, it is important to note the significant spread in the measured Q-values, which seems to indicate the existence of at least two distinct values. (In this regard it will be recalled that this same conclusion was suggested by the Q-value histogram of figure 29. In fact, the distribution in figure 29 is very nearly the same as the distribution exhibited by these eight outstanding examples.) The possibility that the entire spread in Q-values can be attributed to errors of measurement is considered to be exceedingly unlikely in view of the high quality of the cases, but cannot of course be excluded. Alternative explanations are, of course, available. These range from an interpretation in terms of special multi-body or multi-mode decay schemes, to an interpretation in terms of excitation levels for the V-particle or the secondary particles. It is possible that the neutral V-particle decay phenomenon is as complex as some of these models would indicate, but if such is the case considerably more data of much higher quality will be required to establish this fact. For the present all that can be said is that perhaps 65 percent of all of the observed cases of neutral V-particle decay can be interpreted satisfactorily in terms of a two-body decay into a proton and a negative π-meson, with an energy release of approximately 37 Mev.

It is exceedingly difficult to arrive at any general conclusions regarding those cases which were not consistent with a decay yielding a heavy positive and a light negative particle as decay-products; about 20 percent of all of the observed cases were of this type. The identity of these particles was considered in appropriate detail in the section on the nature of the charged secondary particles (Section V. B) and significant number of data were presented indicating the possible existence of negative μ-mesons, positive π-mesons, and τ- or κ-mesons. The possibility of a neutral V-decay yielding two π-mesons was of considerable interest inasmuch as this decay had been postulated by the Manchester workers[7]. A number of cases were found to be consistent with this scheme, but no case was found which had the high quality necessary to establish the existence of such a decay. Recently, the existence of this decay has been established by R. W. Thompson's group at Indiana University (paper to appear in Physical Review, April 15, 1953). The Q-values obtained by this group were of the order of 200 Mev. It is interesting to note that this value is not inconsistent with the Q-values obtained in this study (see Appendix I).

APPENDIX I

Neutral V-Particle Statistics

The statistics for 96 of the 134 cases of neutral V-particle decay are presented below. These cases may be identified by their case number; this number has also been included in the caption of all photographs used in the text of this paper. The angle between the secondary particles was the only information available in the 38 cases which have not been included in this summary.

List of Symbols

1) Angles

θ_+, θ_- The angles between the extended V-particle path and the paths of the secondary particles.

θ_T The angle between the two secondary particles.

All angles are measured in degrees.

2) Momenta

P_+, P_- The momenta of the secondary particles expressed in Mev/c. Those momenta included in parentheses have been determined by means of transverse momentum balance.

3) Ionization

I_+, I_- The specific ionizations of the secondary particles.

4) Masses

M_+, M_- The masses of the secondary particles.

5) Decay Scheme

A - decay into a proton and a negative π-meson.

B - decay into two π-mesons.

C - decay into a negative proton and a positive π-meson.

D - decay into a proton and a negative μ-meson.

E - decay into negative 750 m_e particle and a positive π-meson.

6) Q-value

The energy release of the V-particle decay assuming a two body decay scheme, as expressed in Mev.

7) Quality

The general quality of the case is indicated in this column as follows:

A - excellent

B - good

C - average

D - poor

This classification is based solely upon the accuracy associated with the determination of the secondary masses and the Q-value. It is not based upon the numerical results obtained in these calculations.

Note: An absence of limits on any of the numerical values listed in the table indicates that these are merely approximate values. The angles, however, are an exception to this rule. These are accurate to at least a degree in most cases.

Case	θ_+	θ_-	θ_T	P_+	I_+	M_+	P_-	I_-	M_-	Decay	Q	Quality
06724			152	750±150	1.5-3.0	1400-2600	42±6	4-8	210-270	A	65±20	B
07800			39	125±25	10-20	800-1600	160±10	1.5-2.0	250-410	A	49±10	C
08796			43	530±75	1.1-1.6	570-1050	115±10	1.4-2.0	190-290	A	18±5	A
										B	106±20	A
09200	14	14	22									D
09489	13	42	55	355±20	1.5-3.0	600-1250	160±15	< 1.5	< 300	A	44±8	B
10065	1	2	3									D
10876	12	60	72	440±150	1.5-2.5	600-1800	93±5	1.5-2.5	170-300	A	28±7	A
11007	1.5	3.0	4.5									D
11326				1200±400	1.1-1.5	1300-2200	430±50	< 1.5	< 800	A	76±20	C
11373			132	350±75	4-8	1500-2200	68±10	2-4	165-290	A	37±10	B
12418	8	31	40	425	< 1.5	< 750	240±20	< 1.5	< 450	A	59±20	C
										B	80±30	C
12717			71	800±200	1.5-2.0	1500-2000	130±40	1.5-3	240-450	A	63±20	C
13231	7	35	42	740±150	1.5-3	1400-3000	160±30	1.1-2.0	170-400	A	33±10	C
14228			55	600	1.5	1200	350±30	< 1.5	< 500	A	145	C
14345			28	425±50	3-6	1300-2600	300±50	< 1.5	< 600	A	86±25	C
14538			11	800	< 1.5	< 1200	900	< 1.5	< 1700	A	237	C

Case	θ_+	θ_-	θ_T	P_+	I_+	M_+	P_-	I_-	M_-	Decay	Q	Quality
14539			45	390±50	3-4	1350-1650	150±10	< 2	< 370	A	33±5	A
15011			49	1000	< 1.5	< 1500	100±25	2-4	250-420	A	35±15	C
15181	3	12	15	1000	< 1.5	< 1850						D
15543			28	600±100	< 1.5	< 1200	350±50	< 1.5	< 600	A	91±25	C
										B	80±25	C
16631			49				120±40	1.5-3	220-410			D
17407			39	800±100	1.5-3	1600-2700	170±40	< 1.5	< 320	A	31±10	C
17582	6	22	26	700±100	< 2	< 1800	(200±30)	< 1.5	< 400	A	26±15	C
17596	9	24	25	1000±200	1.3-2.0	1550-2450	420±50	< 1.3	< 650	A	80±40	C
17685	4	18	22	740±150	1.5-3	1400-2600	(170±25)	< 1.5	< 320	A	14±7	C
19063 (1)			151	400±50	3-6	1400-2200	60±5	3-6	205-300	A	41±7	A
(2)	8	43	51	850±150	1.5-2	1600-2100	(180±20)	< 1.5	< 330	A	51±8	C
(3)	5	29	34	(1300±200)	< 1.5	< 2400	185±30	< 1.5	< 340	A	34±7	C
19286	2	14	16	1000	< 1.3	< 1500	250±50	< 2	< 600	A	18±10	C
19287	6	33	39	1350±200	< 1.5	< 2500	280±20	< 1.5	< 500	A	79±12	A
19796	23	51	74	294±50	< 1.5	< 550	(150±30)	< 1.5	< 280	B	110±25	B
19955			19	500±50	2-4	1300-2200	300±25	< 1.5	< 550	A	72±10	B

Case	θ_+	θ_-	θ_T	P_+	I_+	M_+	P_-	I_-	M_-	Decay	Q	Quality
20823	7	4	11									D
	3	5	8									D
21428	3	12	15									D
21578	1.5	2.5	4									D
21910	2	16	19	(1400)	< 1.5	< 2600	200±20	1.3-2	300-500	A	10±5	C
22578	9	33	42	(500±50)	2-4	1250-2100	(135±15)	1.3-2	210-330	A	25±10	C
22600	9	57	66	1000±200	1.3-2	1500-2500	135±10	1.5-2.5	240-380	A	72±15	B
22895	9	23	32	650±100	1.5-3	1200-2250	(260)	< 1.5	< 450	A	57±20	C
23159	12	25	37	700±50	1.5-2.5	1300-2100	210±10	< 1.5	< 390	A	42±6	B
23367	27	9	36	900	< 1.5	< 1600	750	< 1.5	< 1400	B	110	C
										A	285	C
23368				500±100	1.5-3	950-1700						D
23865	7	26	33	(1000)	< 1.5	< 1800	205±10	< 1.5	< 400	A	33±5	B
										B	134±10	B
23942			35	560±100	2-4	1400-2400						D
	23	43	65	220±20	5-9	1100-1600	(128±10)	1.5-2.0	240-320	A	37±5	B
24026	12	33	45	750±150	1.5-3	1400-2500	150±30	1.1-2	160-370	A	34±15	C

Case	θ_+	θ_-	θ_π	P_+	I_+	M_+	P_-	I_-	M_-	Decay	Q	Quality
24141	16	56	72	(360±50)	3-6	1200-2000	117±15	< 1.5	< 220	A	35±7	B
										D	43±5	B
24199			27	675±75	< 1.3	< 1000	1350±300	< 1.3	< 2100	B	250	C
										C	475	C
24358			31	1000±300	1.1-1.5	1200-1800	340±50	< 1.3	< 530	A	73±20	C
24390	4	25	29	900±300	< 1.5	< 1700	190±20	1.2-1.5	250-350	B	130±40	B
										A	22±5	B
24692			68	190±20	< 1.3	< 300	210±40	2-4	500-900	E	61±15	B
24876			47	(470±40)	< 1.3	< 650	(110)	2	275	B	98	C
24915			113				247±15	< 1.3	< 385			D
25504	4	38	42	690±150	1.1-2	750-1700	160±17	< 1.3	< 275	A	32±6	B
25587			43	735±100	1.5-2.5	1350-2200	150±30	1.3-2	230-370	A	31±10	C
25686			53	375±100	4-8	1600-2400	67±7	1.5-3	130-230	A	10±3	A
										D	11±3	A
25890			74	153±11	> 15	> 1500	122±4	1.2-1.5	170-230	A	36±5	C
26361	5	147	152	475±50	2-3	1200-1700	(60±19)	2.5-3.5	175-230	A	49±10	C
26585	4	34	37	900±300	< 1.3	< 2050	176±15	1.2-1.5	225-330	A	32±7	C
26769	8	16	24	400±50	2-4	1000-1700	236±20	< 1.3	< 370	A	50±10	B

Case	θ_+	θ_-	θ_T	P_+	I_+	M_+	P_-	I_-	M_-	Decay	Q	Quality
26867	13	39	52	(400±200)	> 1.3	> 600	140±50	< 1.3	< 200	A	32±20	C
										B	93	C
26912	2	9	11	(4600±1000)	< 1.2		1000±200	< 1.2	< 1300	A	29±10	C
27504	12	25	37	640±100	1.1-1.5	< 1200	465±40	< 1.3	< 700	A	150	C
										B	165	C
27529			62	590±75	1.5-2.0	1150-1500	180±15	< 1.3	< 275	A	60±12	B
27773	10	12	21	(970)	< 1.3	< 1500	(820)	< 1.3		A	154	C
										B	96	C
27796	5	3	7	567±30	2-3	1400-2000	198±15	< 1.3	< 310	A	21±6	B
27841			6	(1400)	> 1.0		750±100	< 1.3	< 1150	A	80±25	C
27875	5	74	79	(1000)			140±30	1.3-2	215-340	A	97±30	C
28167	10	104	114	800±150	1.5-2.0	1500-1900	77±7	3-4	265-310	A	79±15	A
28569			28	1800±300	< 1.5	< 2750	185±15	< 1.3	< 285	A	37±15	C
28738	30	11	40									D
29965			10	(1400)	< 1.3	< 2100	300±50	< 1.3	< 450	A	15	C
										B	107	C
30045	8	23	30	850±150	< 1.5	< 1600	290±50	< 1.5	< 550	A	59	C
30047	15	27	42	660±50	2-3	1650-2300	163±20	< 1.3	< 250	A	33±5	C

Case	θ_+	θ_-	θ_T	P_+	L_+	M_+	P_-	L_-	M_-	Decay	Q	Quality
30068	47	20	68	400	< 1.5	< 700	475	< 2	< 1200	B	282	C
										C	205	C
30095	6	39	45	1125±200	< 1.3	< 1800	170±5	< 1.3	<285	A	49±8	B
										B	205	B
30129	11	57	67	(500±35)	< 1.5	< 1000	110±5	< 1.5	< 200	A	34±5	C
										B	146	C
30266			48	395±40	< 1.5	< 700	280	2-4	600-1200	B	88	C
										C	155	C
30267	3	19	22	(2800±700)	< 1.3	< 3500	390±80	< 1.3	< 600	A	66±20	C
30334			14	(1400)	< 1.3	< 2100	(510)	< 1.3	< 750	A	67	C
30514	14	56	70	510±50	2.5-4	1500-2100	130±5	1.5-2.5	240-380	A	46±4	A
30586	6	36	42	1260±300	< 2	< 3000	117±5	1.5-2	215-290	A	39±15	C
30770	4	24	28	700±100	< 1.5	< 1300	200±20	1.2-1.7	265-420	A	28±7	C
30803	5	34	39	(1200±200)	< 1.5	< 2200	190±20	< 1.5	< 350	A	46±10	C
30843			28	600±100	1.3-1.8	1100-2400	340±20	< 1.5	< 600	A	87±15	C
30844	6	35	40	750±100	1.5-3	1400-2600	290±40	< 1.5	< 550	A	81±25	C
30925			90				55±5	4-6	230-300			D

Case	θ_+	θ_-	$\theta_\pm$	P_+	I_+	M_+	P_-	I_-	M_-	Decay	Q	Quality
30964	1	30	31	1400±500	< 1.5	< 2500	230±20	< 1.5	< 450	A	41±15	C
31044	8	24	32	660±100	1.5-3	1200-2300	205±10	< 1.5	< 380	A	36±5	A
31200			29	1000±300	< 1.5	< 1850	270±20	< 1.5	< 480	A	44±10	C
31251	5	5	10									D
31337	6	8	14									D
31341	40	10	50	380±50	< 1.3	< 600	(1400±250)	< 1.3	< 2100	B	411	C
										C	180±40	C
31476	5	25	30	(1350±200)	< 1.5	< 2500	275±20	< 1.5	< 500	A	48±10	C
31817			52	72±20	> 15	> 700	125±5	1.5-3	230-430	A	37±3	A

APPENDIX II

Charged V-Particles

In these experiments, a total of 18 charged V-particles were observed to decay, 7 positive and 11 negative. Inasmuch as these particles are to be analyzed as a separate research project, only a few observations will be presented at this time.

Nature of Charged Secondary Particle

A number of preliminary mass measurements have indicated that the charged secondary particle in the charged V-decay is a π- or μ-meson. In view of this fact, figure 36 is an especially interesting decay. In this figure, a negative V-particle decays in the upper chamber above the lead plate, the charged secondary penetrating the plate and traversing the lower chamber. Although the charged V-particle and its charged secondary are essentially at minimum ionization, this case is, nevertheless, of great interest because the secondary particle is scattered through an appreciable angle in the lead plate, thereby indicating a π-meson rather than a μ-meson.

Relationship of Charged and Neutral V-Particles

At the present time practically nothing is known concerning the identity of the neutral secondary particle (or particles) produced in the charged V-decay. Similarly, nothing is known concerning the possible relationship of charged and neutral V-particles. Is it possible that a neutral V-particle is produced in the decay of a charged V-particle? With this in mind, figure 37 is an especially interesting photograph. In this figure, a negative V-particle decays in the upper chamber above the lead plate, and a neutral V-particle decays in the lower chamber; these two V-decays are in exceptional

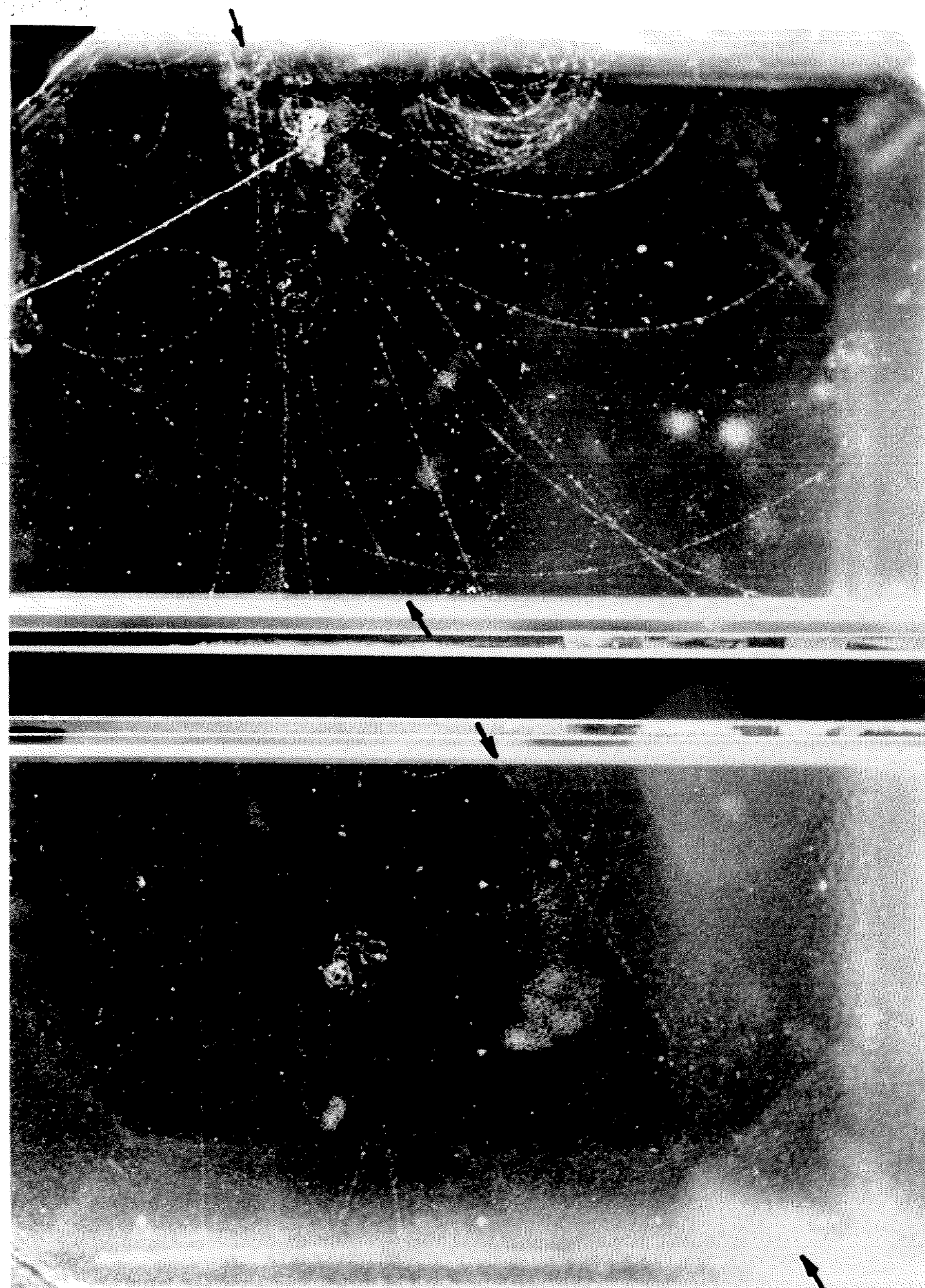

Fig. 36. (Case #16347) An example of a charged V-particle decay. The negative V-particle enters the upper chamber at the top, travels downward toward the right, and decays above the plate; the charged secondary particle continues downward and to the right (see arrows). This case is particularly interesting because the secondary particle undergoes a significant deflection in the plate.

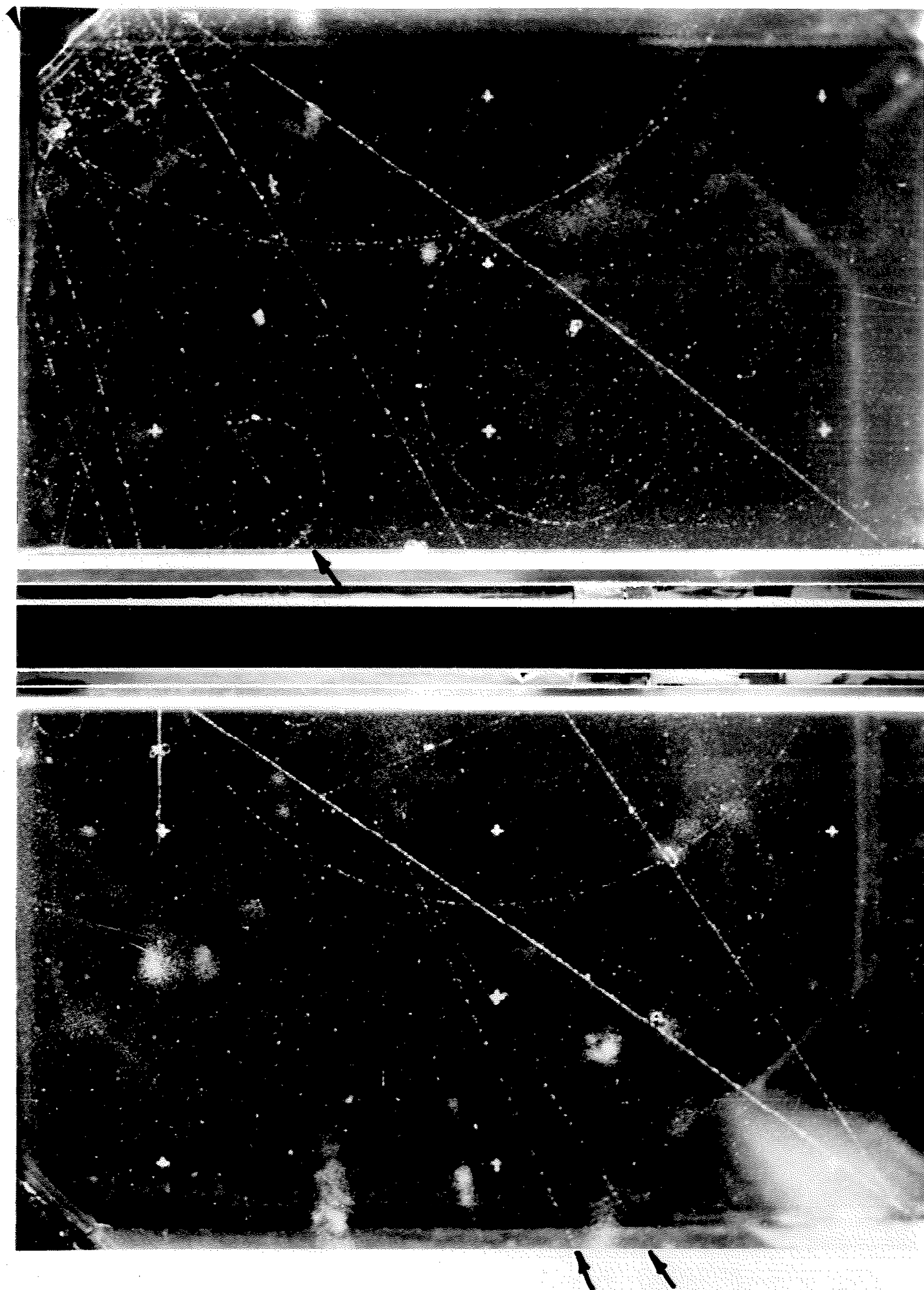

Fig. 37. (Case #26912) Example of the decay of a charged V-particle. This particle enters the upper chamber at the left, travels downward toward the right, and decays above the plate (see arrows). This case is of particular interest because of the existence of a neutral V-particle decay in the lower chamber. The general alignment of these two decays suggests that they may possibly be related.

alignment, as can be seen from the photograph. Is this a rare coincidence of two V-particles produced in the same event (above the chambers) and traveling in the same direction, or do cascade phenomena really exist?

APPENDIX III

Heavy Mesons

In the course of the present cloud-chamber study, a number of particles have been observed whose measured masses were heavier than π-mesons and yet lighter than protons[12]. Additional evidence for the existence of such a class of particles is available in the form of observed decay phenomena. These particles, which will be referred to as heavy mesons, will now be considered in some detail.

τ-Mesons

τ-meson is the name associated with an intermediate mass particle which decays into 3 π-mesons. Two events have been observed which probably represent the decay in flight of τ-mesons[14]. One of these decays is shown in figure 38. The τ-meson enters the chamber at the top, traverses the 2.5 cm lead plate with no detectable deflection, and decays in the lower section of the chamber into three charged particles. All of the tracks except that of the left-hand secondary are at, or very near, minimum ionization; the ionization of the left-hand secondary is estimated to be 1.4-2.2 times minimum. The momentum of the τ-meson, based upon its curvature in the 5000 gauss magnetic field, is 600$\pm$100 Mev/c, and the momenta of the three secondary particles are, from left to right, 155$\pm$30, 350$\pm$75, and 210$\pm$50 Mev/c. The masses of these secondaries are therefore 350$\pm$75 m_e, less than 600 m_e, and less than 300 m_e, respectively, and are thus all consistent with π-mesons, but none can be a proton. Charge is conserved, and the measured momenta are consistent with conservation of momentum in the decay. The mass of the τ-meson calculated from the above momenta, with the assumption that the decay products are π-mesons, is about

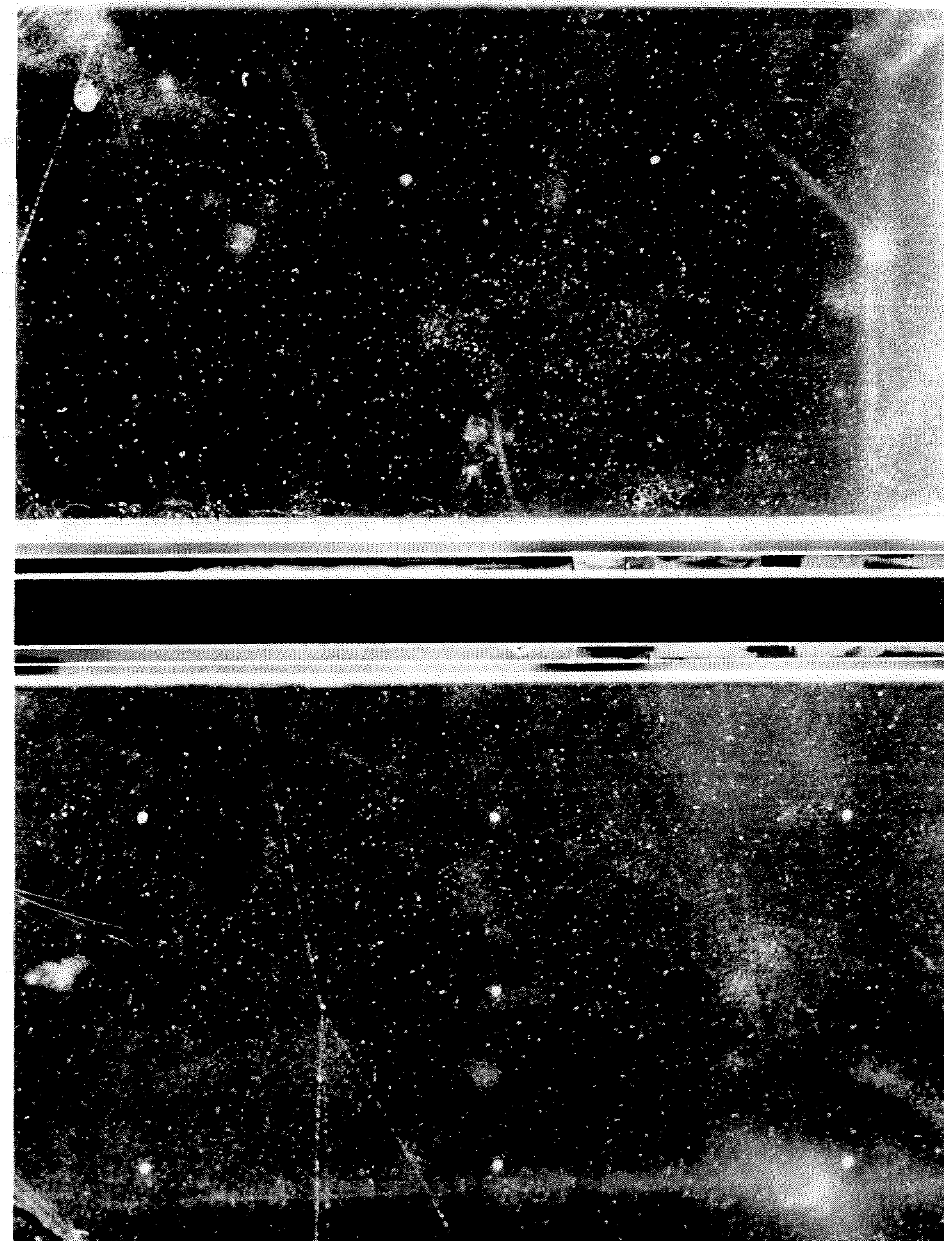

Fig. 38. (Case #18425) The decay in flight of a τ-meson. This meson traverses the upper chamber, passes through the lead absorber between the chambers, and finally decays in the lower chamber. The secondary particles produced are most likely π-mesons.

975 m_e, which corresponds to an energy release of about 75 Mev[14]. It would be extremely difficult to interpret this event as a collision phenomenon.

The second τ-meson decay is similar in appearance to the one above, but the momenta are higher, making the mass limits on the particles less sharp. Both of these τ-mesons travel much farther inside the chamber before decaying than do V-particles; this suggests that their mean life is considerably longer than that of V-particles --- perhaps 10^{-9} seconds or even longer.

κ-Mesons

A κ-meson[13] is likewise an intermediate mass particle, but in this case the only charged decay product is a μ-meson. An example of a κ-meson decay is shown in figure 39. The particle (heavily ionizing) enters the upper chamber from the right, proceeds downward toward the left, and decays above the lead plate, producing a single charged particle (which travels upward to the left) and presumably one or more neutral particles. The momentum of the κ-meson is 185 ± 20 Mev/c and its ionization is estimated to be 6-10 times minimum. Thus its mass is 1200 ± 300 m_e. The momentum of the secondary particle is 150 ± 15 Mev/c, and its ionization is estimated to be about 1.2-1.6 times minimum, indicating a mass of 250 ± 50 m_e, a value consistent with either a π- or μ-meson. The kinetic energy of the secondary particle (assumed to be a μ-meson) in the center-of-mass system is 82 Mev.

This event might alternatively be interpreted as the decay of a neutral or charged V-particle. However, the absence of a nearby origin from which either of these particles could have come suggests,

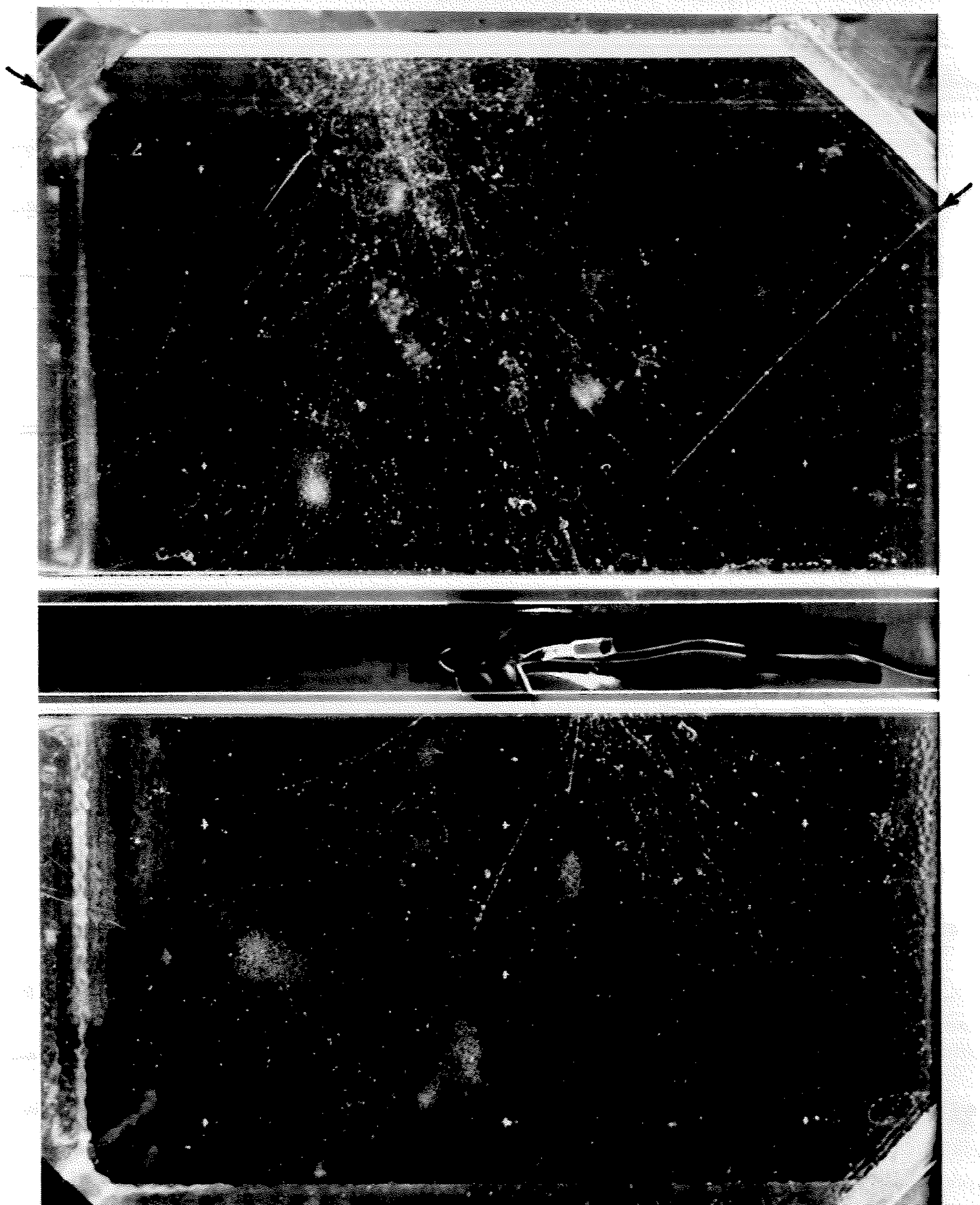

Fig. 39. (Case #13901) The decay of a K-meson. The K-meson enters the upper chamber from the right, proceeds downward toward the left, and decays above the plate. In the decay a single charged particle is produced; this particle travels upward toward the left (see arrows).

rather, a longer-lived particle which can decay at a great distance from its point of origin, even though it is moving slowly. Furthermore, if the event were to represent the decay of a neutral V-particle, the latter would have to be traveling upward, and would thus be the only such case ever observed.

Other Particles

In addition to τ- and κ-mesons, the present study has also yielded three cases which may indicate the existence of a particle whose mass lies in the range 400-650 m_e. The momenta of these particles are 100±15, 180±20, and 135±15 Mev/c, and their ionizations, estimated visually by comparing them with time-coincident protons, mesons, and electrons on the same photographs, are 3-6, 2-3, and 4-8 times minimum, respectively. These measurements indicate masses of 450±150 m_e, 550±150 m_e, and 750±150 m_e, respectively. (The first of these three cases is shown in figure 40.) Only with great difficulty can the first two tracks be reconciled with those of either π- or τ-mesons; the third cannot be a π-meson, but might conceivably be a τ-meson.

It should perhaps be mentioned that there are indications, mainly from the division of momentum between the neutral V-particle secondaries, that particles of mass 500-700 m_e are sometimes produced in neutral V-particle decays.

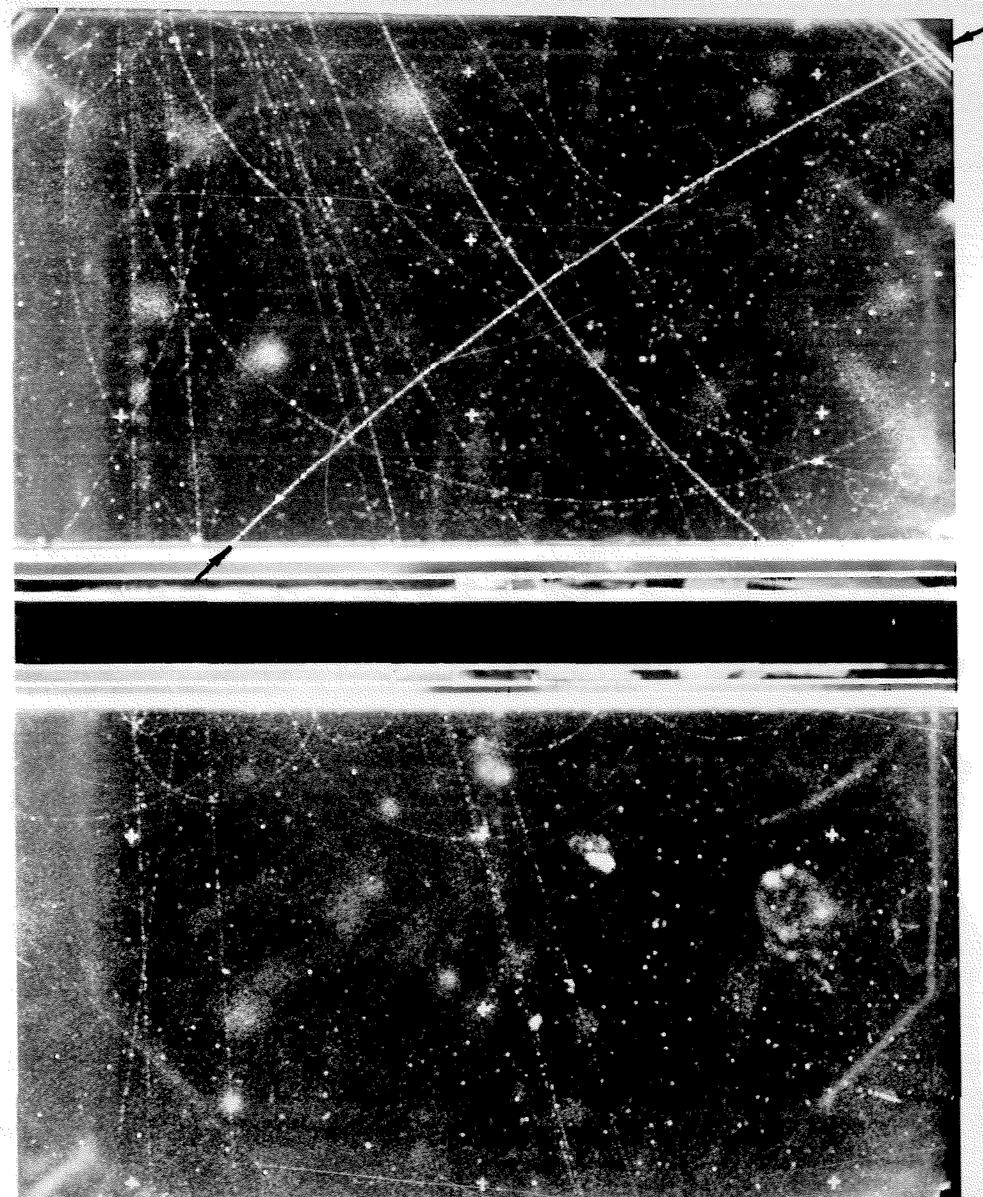

Fig. 40. (Case #30335) An example of a particle of intermediate mass. This particle (indicated by arrows) is one of a number of particles which have been observed whose measured mass lie in the range 400-650 electron masses.

References

1. G. D. Rochester and C. C. Butler, Nature 160, 855 (1947)
2. Seriff, Leighton, Hsiao, Cowan and Anderson, Phys. Rev. 78, 290 (1950)
3. Armenteros, Barker, Butler, Cachon and Chapman, Nature 167, 501 (1951)
4. Thompson, Cohn and Flum, Phys. Rev. 83, 175 (1951)
5. W. B. Fretter, Phys. Rev. 82, 294 (1951)
6. Leighton, Wanlass and Alford, Phys. Rev. 83, 843 (1951)
7. Armenteros, Barker, Butler and Cachon, Phil. Mag. 42, 113 (1951)
8. Camerini, Davies, Fowler, Franzinetti, Muirhead, Lock, Perkins and Yekutieli, Phil. Mag. 42, 1241 (1951)
9. Bristol Conference on V-particles and Heavy Mesons, December 1951
10. W. L. Alford, Ph.D. Thesis, (1953)
11. F. H. Shelton, Ph.D. Thesis, (1953)
12. R. B. Leighton and S. D. Wanlass, Phys. Rev. 86, 426 (1952)
13. C. O'Ceallaigh, Phil. Mag. 42, 1032 (1951)
14. Brown, Camerini, Fowler, Muirhead, Powell and Ritson, Nature 163, 82 (1949)